



UNIVERSIDADE DA BEIRA INTERIOR
Faculdade de Engenharia

Study of the Electromagnetic Properties of Textiles: Development of Textile Antennas for Energy Harvesting

Caroline Loss

Tese para a obtenção do Grau de Doutor em
Engenharia Têxtil
(3º ciclo de estudos)

Orientador: Prof. PhD. Luísa Rita Brites Sanches Salvado (Universidade da Beira Interior)

Co-orientador: Prof. PhD. Pedro Renato Tavares Pinho (Instituto Superior de Engenharia de Lisboa / Instituto de Telecomunicações - Aveiro)

Covilhã, Novembro de 2017

This PhD Thesis is funded by CAPES Foundation, Ministry of Education of Brazil, PhD Grant nº. 9371-13-3.

“Olhar para trás após uma longa caminhada pode fazer perder a noção da distância que percorremos, mas se nos detivermos em nossa imagem, quando a iniciamos e ao término, certamente nos lembraremos o quanto nos custou chegar até o ponto final, e hoje temos a impressão de que tudo começou ontem. Não somos os mesmos, mas sabemos mais uns dos outros. E é por esse motivo que dizer adeus se torna tão complicado! Digamos então que nada se perderá. Pelo menos dentro da gente...”

Guimarães Rosa

Acknowledgments

Thanks God for giving me strength and courage to not give up. I'm grateful for all people that was crossed my path during these years, helping me getting here. First of all, I would like to express my heartfelt gratitude to the three people that made this work possible. To my supervisor, Prof. PhD. Rita Salvado, for being an example of woman, researcher and mother. Thanks to help me during these years, not only for teaching me, but for supporting me on life, during my bad days. I really appreciate all your patience and kindness during these years of work. To my co-advisor, Prof. PhD. Pedro Pinho, for always being present, teaching me electromagnetism and antennas. Thanks for sharing your knowledge and to trust on my work, and especially for being always positive. And to PhD. Ricardo Gonçalves, thanks for your patience, to measure the prototypes, to be available any time for questions and to share your knowledge, combining skills to create the best results.

I would like to thank the CAPES Foundation, Ministry of Education of Brazil, for the financial support by the PhD Grant n°. 9371-13-3. To the Department of Textile Science and Technology and FibEnTech Research Unit at Universidade da Beira Interior (UBI), for hosting my research during all these years.

My appreciation to the Instituto de Telecomunicações - Aveiro, for hosting my research and support the measurements of the antennas. Also, I thank to the Project IC 1301 - Wireless Power Transmission for Sustainable Electronics (WIPE) in the framework of the European Cooperation in Science and Technology (COST), for supporting the Short Term Scientific Mission (STSM) COST IC 1301-18709.

Special thanks to the team of the Department of Information Technology at Ghent University. To Prof. PhD. Hendrik Rogier, for all exchanging of knowledge, for encouraging me to search new materials, solutions and scenarios of applications for the textile antennas. To PhD. Sam Agneessens, for the patience to teach me more about principles of the antennas, welding, use the anechoic chamber and Matlab. Also, PhD. Marco Rossi, for all support during the dielectric characterization of textiles, using the Resonator-Based Experimental Technique.

Thanks to the EURECAT Technologic Centre (Mataró, Spain), for the support on measurements of sheet resistance of the conductive fabrics, and the optical microscope images of the textiles materials. To Ana Paula Gomes from the Laboratory of Electron Microscopy (UBI), thank for all SEM images. Also, to the Department of Aeronautical Science of UBI, for the support on cutting all patch samples on the laser cut machine.

I am grateful to Prof. PhD. Fernando Velez and the colleges from the PROENERGY PROJECT - Prototypes for Efficient Energy Self-Sustainable Wireless Sensor Networks, reference PTDC/EEA-TEL/122681/2010, for introducing me the “world of antennas”. Also, thank for the

invitation to write the chapter for the book *Wearable Technologies and Wireless Body Sensor Networks for Healthcare*. To Isabel Cantista, for believe in this work and help disseminate the textile antennas, through the book *Fashion Spaces: Geographical, Physical and Virtual*. Also, to Sophia Cueto and Benilde Reis thank you for the photography of E-Caption. I would like to thank Prof. Paulo Moniz, Head of UBI Research Coordinating Institute, for believe in this work and help disseminate the textile antennas, through the television show called “Há Volta on RTP TV” in 02 of August of 2016.

Additionally, I wish to acknowledge the companies that provided the textiles materials studied on this thesis. To Manuel Barros from Leandro Manuel Araújo Lda., for the 3D samples used in this work, and to Marco Veras from Corticeira Amorim, for all cork samples used during the STSM COST IC 1301-18709. Also, to Borgstena Textile Portugal, in particularly Linda Costa, Odete Duarte and Fábio Pereira, to embrace this thesis, helping on the development and manufacturing of the Substrate Integrating the Ground Plane.

A big thank to Pedro Alves, for sharing the life with me, for all patience on this last months of work, for helping me every day at home, showing the best side of the life’s challenges. To Catarina Lopes, not only for helping me with the embroidered antennas, but to share with me the best and worst moments of my life. To my friends, Pedro Lindeza, João Barata, Lucas Naves, Julia Discacciati, Solange Fernandes, Liliana Ribeiro, Cristiana Costa, Jorge Antunes, Rui Lopes and David Resende, for being my Covilhã’s Family, supporting me no matter the situation. Also, to my Brazilian friends to standing with me, even on distance, during all these years.

Por último, o maior agradecimento é à minha família, que mesmo distante sempre esteve presente. Palavras nunca serão o suficiente para expressar o que sinto, mas fica o meu muito obrigada aos meus pais, que durante todos estes anos foram o meu porto seguro, deram-me forças e coragem todos os dias, e muitas vezes me mantiveram de pé quando fraquejei. Não há palavras para descrever o orgulho que sinto por ter vocês na minha vida. À minha irmã, por ser a minha melhor amiga, pelas horas de desabafo e pela partilha tanto dos momentos felizes, como dos de angústia. Ao Adriano e ao Miguel, por cuidarem tão bem dos meus pais e por serem a fortaleza da Franciele. Família, essa é uma conquista nossa, sem vocês nada disso teria sido possível. Gratidão eterna.

Abstract

The current socio-economic developments and lifestyle trends indicate an increasing consumption of technological products and processes, powered by emergent concepts, such as Internet of Things (IoT) and smart environments, where everything is connected in a single network. For this reason, wearable technology has been addressed to make the person, mainly through his clothes, able to communicate with and be part of this technological network.

Wireless communication systems are made up of several electronic components, which over the years have been miniaturized and made more flexible, such as batteries, sensors, actuators, data processing units, interconnectors and antennas. Turning these systems into wearable systems is a demanding research subject. Specifically, the development of wearable antennas has been challenging, because they are conventionally built on rigid substrates, hindering their integration into the garment. That is why, considering the flexibility and the dielectric properties of textile materials, making antennas in textile materials will allow expanding the interaction of the user with some electronic devices, by interacting through the clothes. The electronic devices may thus become less invasive and more discrete.

Textile antennas combine the traditional textile materials with new technologies. They emerge as a potential interface of the human-technology-environment relationship. They are becoming an active part in the wireless communication systems, aiming applications such as tracking and navigation, mobile computing, health monitoring and others. Moreover, wearable antennas have to be thin, lightweight, of easy maintenance, robust, and of low cost for mass production and commercialization.

In this way, planar antennas, the microstrip patch type, have been proposed for garment applications, because this type of antenna presents all these characteristics, and are also adaptable to any surface. Such antennas are usually formed by assembling conductive (patch and ground plane) and dielectric (substrate) layers. Furthermore, the microstrip patch antennas, radiate perpendicularly to a ground plane, which shields the antenna radiation, ensuring that the human body is exposed only to a very small fraction of the radiation.

To develop this type of antenna, the knowledge of the properties of textile materials is crucial as well as the knowledge of the manufacturing techniques for connecting the layers with glue, seam, adhesive sheets and others. Several properties of the materials influence the behaviour of the antenna. For instance, the bandwidth and the efficiency of a planar antenna are mainly determined by the permittivity and the thickness of the substrate. The use of textiles in wearable antennas requires thus the characterization of their properties. Specific electrical conductive textiles are available on the market and have been successfully used. Ordinary textile fabrics have been used as substrates.

In general, textiles present a very low dielectric constant, ϵ_r , that reduces the surface wave losses and increases the impedance bandwidth of the antenna. However, textile materials are constantly exchanging water molecules with the surroundings, which affects their electromagnetic properties. In addition, textile fabrics are porous, anisotropic and compressible materials whose thickness and density might change with low pressures. Therefore, it is important to know how these characteristics influence the behaviour of the antenna in order to minimize unwanted effects.

To explain some influences of the textile material on the performance of the wearable antennas, this PhD Thesis starts presenting a survey of the key points for the design and development of textile antennas, from the choice of the textile materials to the framing of the antenna. An analysis of the textile materials that have been used is also presented. Further, manufacturing techniques of the textile antennas are described.

The accurate characterization of textile materials to use as a dielectric substrate in wearable systems is fundamental. However, little information can be found on the electromagnetic properties of the regular textiles. Woven, knits and nonwovens are inhomogeneous, highly porous, compressible and easily influenced by the environmental hygrometric conditions, making their electromagnetic characterization difficult. Despite there are no standard methods, several authors have been adapting techniques for the dielectric characterization of textiles. This PhD Thesis focuses on the dielectric characterization of the textile materials, surveying the resonant and non-resonant methods that have been proposed to characterize the textile and leather materials. Also, this PhD Thesis summarizes the characterization of textile materials made through these methods, which were validated by testing antennas that performed well.

Further a Resonant-Based Experimental Technique is presented. This new method is based on the theory of resonance-perturbation, extracting the permittivity and loss tangent values based on the shifts caused by the introduction of a superstrate on the patch of a microstrip antenna. The results obtained using this method have shown that when positioning the roughest face of the material under test (MUT) in contact with the resonator board, the extracted dielectric constant value is lower than the one extracted with this face positioned upside-down. Based on this observation, superficial properties of textiles were investigated and their influence on the performance of antennas was analysed.

Thus, this PhD Thesis relates the results of the dielectric characterization to some structural parameters of textiles, such as surface roughness, superficial and bulk porosities. The results show that both roughness and superficial porosity of the samples influence the measurements, through the positioning of the probes. Further, the influence of the positioning of the dielectric material on the performance of textile microstrip antennas was analysed. For this, twelve prototypes of microstrip patch antennas were developed and tested. The results show that, despite the differences obtained on the characterization when placing the face or reverse-sides

of the MUT in contact with the resonator board, the obtained average result of ϵ_r is well suited to design antennas ensuring a good performance.

According to the European Commission Report in 2009, “Internet of Things – An action plan for Europe”, in the next years, the IoT will be able to improve the quality of life, especially in the health monitoring field. In the Wireless Body Sensor Network (WBSN) context, the integration of textile antennas for energy harvesting into smart clothing is a particularly interesting solution for a continuous wirelessly feed of the devices. Indeed, in the context of wearable devices the replacement of batteries is not easy to practice. A specific goal of this PhD Thesis is thus to describe the concept of the energy harvesting and then presents a survey of textile antennas for RF energy harvesting. Further, a dual-band printed monopole textile antenna for electromagnetic energy harvesting, operating at GSM 900 and DCS 1800 bands, is also proposed. The antenna aims to harvest energy to feed sensor nodes of a wearable health monitoring system. The gains of the antenna are around 1.8 dBi and 2.06 dBi allied with a radiation efficiency of 82% and 77.6% for the lowest and highest frequency bands, respectively.

To understand and improve the performance of the proposed printed monopole textile antenna, several manufacturing techniques are tested through preliminary tests, to identify promising techniques and to discard inefficient ones, such as the gluing technique. Then, the influence of several parameters of the manufacturing techniques on the performance of the antenna are analysed, such as the use of steam during lamination, the type of adhesive sheet, the orientation of the conductive elements and others. For this, seven prototypes of the printed monopole textile antenna were manufactured by laminating and embroidering techniques.

The measurement of the electrical surface resistance, R_s , has shown that the presence of the adhesive sheet used on the laminating process may reduce the conductivity of the conductive materials. Despite that, when measuring the return loss of printed monopole antennas produced by lamination, the results show the antennas have a good performance. The results also show that the orientation of the conductive fabric does not influence the performance of the antennas. However, when testing embroidered antennas, the results show that the direction and number of the stitches in the embroidery may influence the performance of the antenna and should thus be considered during manufacturing.

The textile antennas perform well and their results support and give rise to the new concept of a continuous substrate to improve the integration of textile antennas into clothing, in a more comfortable and pleasure way. A demonstrating prototype, the E-Caption: Smart and Sustainable Coat, is thus presented. In this prototype of smart coat, the printed antenna is fully integrated, as its dielectric is the textile material composing the coat itself. The E-Caption illustrates the innovative concept of textile antennas that can be manipulated as simple emblems. The results obtained testing the antenna before and after its integration into cloth, show that the integration does not affect the behaviour of the antenna. Even on the presence of the human body the antenna is able to cover the proposed resonance frequencies (GSM 900 and DCS 1800 bands) with the radiation pattern still being omnidirectional.

At last, the exponential growth in the wearable market boost the industrialization process of manufacturing textile antennas. As this research shows, the patch of the antennas can be easily and efficiently cut, embroidered or screen printed by industrial machines. However, the conception of a good industrial substrate that meets all the mechanical and electromagnetic requirements of textile antennas is still a challenge. Following the continuous substrate concept presented and demonstrated through the E-Caption, a new concept is proposed: the continuous Substrate Integrating the Ground Plane (SIGP). The SIGP is a novel textile material that integrates the dielectric substrate and the conductive ground plane in a single material, eliminating one laminating process. Three SIGP, that are weft knitted spacer fabrics having one conductive face, were developed in partnership with the Borgstena Textile Portugal Lda, creating synergy between research in the academy and industry. The results of testing the performance of the SIGP materials show that the integration of the ground plane on the substrate changes the dielectric constant of the material, as a consequence of varying the thickness. Despite this, after the accurate dielectric and electrical characterization, the SIGP I material has shown a good performance as dielectric substrate of a microstrip patch antenna for RF energy harvesting. This result is very promising for boosting the industrial fabrication of microstrip patch textile antennas and their mass production and dissemination into the IoT network, guiding future developments of smart clothing and wearables.

Keywords

Textile antenna, electromagnetic properties, electromagnetic characterization, energy harvesting, smart clothing and wearable systems.

Resumo

Os atuais desenvolvimentos socioeconômicos e tendências de estilo de vida apontam para um crescimento do consumo de produtos e processos tecnológicos, impulsionado por conceitos emergentes como a Internet das Coisas, onde tudo está conectado em uma única rede. Por esta razão, as tecnologias usáveis (*wearable*) estão a afirmar-se propondo soluções que tornam o utilizador possivelmente através das suas roupas, capaz de comunicar com e fazer parte desta rede.

Os sistemas de comunicações sem fios são constituídos por diversos componentes eletrónicos, que com o passar dos anos foram sendo miniaturizados e fabricados em materiais flexíveis, tais como as baterias, os sensores, as unidades de processamento de dados, as interconexões e as antenas. Tornar os sistemas de comunicações sem fios em sistemas usáveis requer trabalho de investigação exigente. Nomeadamente, o desenvolvimento de antenas usáveis tem sido um desafio, devido às antenas serem tradicionalmente desenvolvidas em substratos rígidos, que dificultam a sua integração no vestuário. Dessa forma, considerando a flexibilidade e as propriedades dielétricas dos materiais têxteis, as antenas têxteis trazem a promessa de permitir a interação dos utilizadores com os dispositivos eletrónicos através da roupa, tornando os dispositivos menos invasivos e mais discretos.

As antenas têxteis combinam os materiais têxteis tradicionais com novas tecnologias e emergem assim como uma potencial interface de fronteira entre seres humanos-tecnologias-ambientes. Expandindo assim a interação entre o utilizador e os dispositivos eletrónicos ao recurso do vestuário. Assim, através das antenas têxteis, o vestuário torna-se uma parte ativa nos sistemas de comunicação sem fios, visando aplicações como rastreamento e navegação, computação móvel, monitorização de saúde, entre outros. Para isto, as antenas para vestir devem ser finas, leves, de fácil manutenção, robustas e de baixo custo para produção em massa e comercialização.

Desta forma, as antenas planares do tipo *patch microstrip* têm sido propostas para aplicações em vestuário, pois apresentam todas estas características e também são adaptáveis a qualquer superfície. Estas antenas são geralmente formadas pela sobreposição de camadas condutoras (elemento radiante e plano de massa) e dielétricas (substrato). Além disso, as antenas *patch microstrip* irradiam perpendicularmente ao plano de massa, que bloqueia a radiação da antena, garantindo que o corpo humano é exposto apenas a uma fração muito pequena da radiação.

Para desenvolver este tipo de antena, é crucial conhecer as propriedades dos materiais têxteis, bem como as técnicas de fabricação para conectar as camadas, com cola, costuras, folhas adesivas, entre outros. Diversas propriedades dos materiais influenciam o comportamento da antena. Por exemplo, a permissividade e a espessura do substrato determinam a largura de

banda e a eficiência de uma antena planar. O uso de têxteis em antenas usáveis requer assim uma caracterização precisa das suas propriedades. Os têxteis condutores elétricos são materiais específicos que estão disponíveis comercialmente em diversas formas e têm sido utilizados com sucesso para fabricar o elemento radiante e o plano de massa das antenas. Para fabricar o substrato dielétrico têm sido utilizados materiais têxteis convencionais.

Geralmente, os materiais têxteis apresentam uma constante dielétrica (ϵ_r) muito baixa, o que reduz as perdas de ondas superficiais e aumenta a largura de banda da antena. No entanto, os materiais têxteis estão constantemente a trocar moléculas de água com o ambiente em que estão inseridos, o que afeta as suas propriedades eletromagnéticas. Além disso, os tecidos e os outros materiais têxteis planares são materiais porosos, anisotrópicos e compressíveis, cuja espessura e densidade variam sob muito baixas pressões. Portanto, é importante saber como estas grandezas e características estruturais influenciam o comportamento da antena, de forma a minimizar os efeitos indesejáveis.

Para explicar algumas das influências do material têxtil no desempenho das antenas usáveis, esta Tese de Doutoramento começa por fazer o estado da arte sobre os pontos-chave para o desenvolvimento de antenas têxteis, desde a escolha dos materiais têxteis até ao processo de fabrico da antena. Além disso, a tese identifica e apresenta uma análise dos materiais têxteis e técnicas de fabricação que têm sido utilizados e referidos na literatura.

A caracterização rigorosa dos materiais têxteis para usar como substrato dielétrico em sistemas usáveis é fundamental. No entanto, pouca informação existe sobre a caracterização das propriedades eletromagnéticas dos têxteis vulgares. Como já referido, os tecidos, malhas e não-tecidos são materiais heterogêneos, altamente porosos, compressíveis e facilmente influenciados pelas condições higrométricas ambientais, dificultando a sua caracterização eletromagnética. Não havendo nenhum método padrão, vários autores têm vindo a adaptar algumas técnicas para a caracterização dielétrica dos materiais têxteis. Esta Tese de Doutoramento foca a caracterização dielétrica dos materiais têxteis, revendo os métodos ressonantes e não ressonantes que foram propostos para caracterizar os materiais têxteis e o couro. Além disso, esta Tese de Doutoramento resume a caracterização de dielétricos têxteis feita através dos métodos revistos e que foi validada testando antenas que apresentaram um bom desempenho.

No seguimento da revisão, apresenta-se uma Técnica Experimental Baseada em Ressonância. Esta nova técnica baseia-se na teoria da perturbação de ressonância, sendo a permitividade e tangente de perda extraídas com base nas mudanças de frequência causadas pela introdução de um superstrato no elemento radiante de uma antena *patch microstrip*. Os resultados de caracterização obtidos através deste método revelam que, ao posicionar a face mais rugosa do material em teste em contato com a placa de ressonância, o valor da constante dielétrica extraída é inferior ao valor extraído quando esta face é colocada ao contrário. Com base nesta observação, as propriedades estruturais da superfície dos materiais têxteis foram investigadas e a sua influência no desempenho das antenas foi analisada.

Assim, esta Tese de Doutorado relaciona os resultados da caracterização dielétrica com alguns parâmetros estruturais dos materiais, como rugosidade da superfície, porosidades superficial e total. Os resultados mostram que tanto a rugosidade como a porosidade superficial das amostras influenciam os resultados, que dependem assim do posicionamento do material que está a ser testado. Também foi analisada a influência do posicionamento do material dielétrico na performance das antenas têxteis tipo *patch microstrip*. Para isso, foram desenvolvidos e testados doze protótipos de antenas *patch microstrip*. Os resultados mostram que, apesar das diferenças observadas durante o processo de caracterização, o valor médio da permissividade é adequado para a modelação das antenas, garantindo um bom desempenho.

De acordo com o relatório da Comissão Europeia, “Internet das Coisas - Um plano de ação para a Europa”, emitido em 2009, nos próximos anos a Internet das Coisas poderá melhorar a qualidade de vida das pessoas, nomeadamente pela monitorização da saúde. No contexto das Redes de Sensores Sem Fios do Corpo Humano, a integração de antenas têxteis para recolha de energia em roupas inteligentes é uma solução particularmente interessante, pois permite uma alimentação sem fios e contínua dos dispositivos. De fato, nos dispositivos usáveis a substituição de baterias não é fácil de praticar. Um dos objetivos específicos desta Tese de Doutorado é, portanto, descrever o conceito de recolha de energia e apresentar o estado da arte sobre antenas têxteis para recolha de energia proveniente da Rádio Frequência (RF). Nesta tese, é também proposta uma antena impressa do tipo monopolo de dupla banda, fabricada em substrato têxtil, para recolha de energia eletromagnética, operando nas bandas GSM 900 e DCS 1800. A antena visa recolher energia para alimentar os nós de sensores de um sistema usável para monitorização da saúde. Os ganhos da antena apresentada foram cerca de 1.8 dBi e 2.06 dBi, aliados a uma eficiência de radiação de 82% e 77.6% para as faixas de frequência mais baixa e alta, respetivamente.

Para entender e melhorar o desempenho da antena impressa tipo monopolo de dupla banda em substrato têxtil, várias técnicas de fabrico foram testadas através de testes preliminares, de forma a identificar as técnicas promissoras e a descartar as ineficientes, como é o caso da técnica de colagem. De seguida, analisou-se a influência de vários parâmetros das técnicas de fabrico sobre o desempenho da antena, como o uso de vapor durante a laminação, o tipo de folha adesiva, a orientação dos elementos irradiantes e outros. Para isto, sete protótipos da antena têxtil monopolar impressa foram fabricados por técnicas de laminação e bordado.

As medições da resistência elétrica superficial, R_s , mostrou que a presença da folha adesiva usada no processo de laminação pode reduzir a condutividade dos materiais condutores. Apesar disso, ao medir o S_{11} das antenas impressas tipo monopolo produzidas por laminação, os resultados mostram que as antenas têm uma boa adaptação da impedância. Os resultados também mostram que a orientação do tecido condutor, neste caso um tafetá, não influencia o desempenho das antenas. No entanto, ao testar antenas bordadas, os resultados mostram que a direção e o número de pontos no bordado podem influenciar o desempenho da antena e, portanto, estas são características que devem ser consideradas durante a fabricação.

De um modo geral, as antenas têxteis funcionam bem e seus resultados suportam e dão origem ao um novo conceito de substrato contínuo para melhorar a integração de antenas têxteis no vestuário, de maneira mais confortável e elegante. A tese apresenta um protótipo demonstrador deste conceito, o *E-Caption: A Smart and Sustainable Coat*. Neste protótipo de casaco inteligente, a antena impressa está totalmente integrada, pois o seu substrato dielétrico é o próprio material têxtil no qual é feito o casaco. O *E-Caption* ilustra um conceito inovador de antenas têxteis que podem ser manipuladas como simples emblemas. Os resultados obtidos testando a antena antes e depois da integração no casaco mostram que a integração não afeta o comportamento da antena. Mesmo na presença do corpo humano, a antena têxtil é capaz de cobrir as frequências de ressonância propostas (bandas GSM 900 e DCS 1800), e de assegurar um padrão de radiação omnidirecional.

Por fim, o crescimento exponencial do mercado de dispositivos usáveis impulsiona o processo de industrialização do fabrico de antenas têxteis. Como mostrado ao longo desta investigação, os elementos radiantes das antenas podem ser cortados, bordados ou serigrafados por máquinas industriais de forma fácil e eficiente. No entanto, a conceção de um bom substrato industrial, que satisfaça todos os requisitos mecânicos e eletromagnéticos das antenas têxteis, ainda é um desafio. Seguindo o conceito do substrato contínuo apresentado e demonstrado através do *E-Caption*, propõe-se um novo conceito: o desenvolvimento de um Substrato contínuo Integrando o Plano de Massa (SIGP). O SIGP é um material têxtil inovador que integra o substrato dielétrico e o plano de massa em um único material, eliminando assim uma das fases do processo de laminagem.

Três SIGP, que são malhas 3D com uma face condutora, foram desenvolvidos em parceria com a Borgstena Textile Portugal Lda, criando assim uma sinergia entre academia e indústria. Os resultados dos testes de desempenho dos SIGP mostram que a integração do plano de massa no substrato dielétrico altera a constante dielétrica do material, devido à variação da espessura ocasionada pela integração do plano de massa. Apesar disso, após a caracterização eletromagnética do material, o material SIGP I mostrou um bom desempenho quando aplicado como substrato dielétrico de uma antena tipo *patch microstrip* para recolha de energia eletromagnética. Este resultado é muito promissor para impulsionar a fabricação industrial de antenas têxteis do tipo *patch microstrip*, e a sua produção em massa e disseminação na rede da Internet das Coisas, orientando futuros desenvolvimentos de tecnologias usáveis e vestuário inteligente¹.

Palavras-chave

Antenas têxteis, propriedades eletromagnéticas, caracterização eletromagnética, recolha de energia, vestuário inteligente e sistemas usáveis.

¹ Resumo redigido ao abrigo do Novo Acordo Ortográfico da Língua Portuguesa.

Index

Acknowledgments.....	V
Abstract.....	VII
Resumo.....	XI
List of Figures	XIX
List of Tables	XXIII
List of Symbols	XXV
List of Acronyms	XXVII
Chapter 1 - Introduction	1
1.1 Motivation.....	3
1.2 Objectives.....	4
1.3 Outline.....	5
1.4 Original Contributions	6
Chapter 2 - Materials and Processes for Textile Antennas	9
2.1 Introduction.....	9
2.2 Electromagnetic Properties of Textiles.....	10
2.2.1 Dielectric Textiles.....	11
2.2.1.1 Influence of the Thickness of Dielectric Textiles	12
2.2.1.2 Influence of the Moisture Content	13
2.2.2 Conductive Textiles	14
2.3 Influence of Mechanical Deformation of Conductive and Dielectric Textiles	16
2.4 Brief Survey on Textile Materials Used in Wearable Antennas.....	17
2.5 Manufacturing Techniques of Textile Antennas	20
2.6 Conclusions	23
Chapter 3 - Dielectric Characterization Methods Applied to Textile Materials: A Survey .	25
3.1 Introduction.....	25
3.2 Non-resonant Methods	26
3.2.1 Parallel Plate Method	26
3.2.2 Planar Transmission Lines Methods	27
3.2.3 Free Space Methods	29
3.3 Resonant Methods.....	30
3.3.1 Cavity Perturbation Methods	31
3.3.2 Microstrip Resonator Ring Method	32
3.3.3 Microstrip Patch Sensor.....	33
3.3.4 Microstrip Resonator Patch Method.....	34
3.3.5 Agilent 85070E Dielectric Measurement Probe Kit	34
3.4 Conclusions	36

Chapter 4 - Resonator-Based Experimental Technique: Method and Analysis	39
4.1 Introduction.....	40
4.1.1 Experimental Procedure.....	42
4.1.2 Results.....	43
4.2 Surface Characterization Method.....	45
4.2.1 Surface Roughness.....	45
4.2.2 Superficial Porosity.....	46
4.2.3 Results.....	47
4.3 Structural Parameters Characterization.....	50
4.3.1 Bulk Porosity	50
4.4 Significance of the Dielectric Results on the Design of Microstrip Patch Antennas ..	51
4.5 Conclusions	54
Chapter 5 - Textile Antenna for RF Energy Harvesting	57
5.1 Introduction.....	57
5.2 Review of Textile Antennas for RF Energy Harvesting	59
5.3 Spectrum Opportunities.....	62
5.4 Printed Monopole Textile Antenna	64
5.5 Conclusions	67
Chapter 6 - Influence of the Manufacturing Techniques on the S_{11} Parameter of Printed Textile Antennas	69
6.1 Introduction.....	69
6.2 Preliminary Results: Miscellaneous Techniques	70
6.3 Laminating Manufacturing Technique	74
6.3.1 Influence of using Thermal Adhesive Sheet on the Sheet Resistance of Conductive Fabrics	74
6.3.2 Laminated Printed Monopole Antenna	78
6.3.3 Influence of the Cutting Direction of the Conductive Fabrics	80
6.4 Embroidery Manufacturing Technique	81
6.5 Conclusions	84
Chapter 7 - Smart Coat With a Fully Embedded Antenna for RF Energy Harvesting	87
7.1 Introduction.....	87
7.2 Integration into Clothing.....	88
7.3 E-Caption: Smart and Sustainable Coat	89
7.4 Influence of the Human Body on the Performance of E-Caption	91
7.5 Conclusions	93
Chapter 8 - Development of a Continuous Substrate Integrating the Ground Plane	95
8.1 Introduction.....	95
8.2 Method and Materials	96
8.3 Structural Parameters.....	98
8.4 Characterization of the Electromagnetic Properties	99

8.4.1	Dielectric Constant.....	99
8.4.2	Surface Resistance	102
8.5	Validation of the Performance of SIGP	104
8.6	Conclusions	105
Chapter 9	- Final Remarks	107
9.1	General Conclusions	107
9.2	Future Works	110
References	113
Appendix A	- Fundamental Parameters of Antennas	125
A.1	Evaluation of Antennas	125
A.2	Parameters of antennas	126
Appendix B	- Measurements of the Permittivity of Textiles	129
Appendix C	- Experiments with Cork	133
C.1	Dielectric Characterization	133
C.2	Validation	133
C.3	Experiments at 5 GHz.....	134
Appendix D	- Preliminary Tests of Integration of Textile Antenna on Cloth.....	137
Appendix E	- E-Caption on Television Show	141
Appendix F	- E-Caption 2.0 - A Smart and Safety Coat.....	143
Appendix G	- Awards & Honours	145

List of Figures

Figure 1-1 Growing of IoT, based on Cisco data [5]	1
Figure 1-2 Layout of microstrip patch antenna (a) Front view and (b) cross section	2
Figure 1-3 Schematic of the interdependence between fields to the development of technical textile for ICT, based on [9]	3
Table 2-1 Relative permittivity of different type of materials	12
Figure 2-1 Basic setup for surface resistance and surface resistivity measurement	15
Figure 2-2 Schema of textile directions in (a) example of Jersey knit - wales and courses and in (b) example of plain weave - warp and weft.....	16
Figure 3-1 Parallel plate method	27
Figure 3-2 Types of transmission lines: (a) microstrip, (b) coplanar waveguide, (c) coplanar waveguide with ground plane and (d) stripline. Where: h and t are the thickness of the dielectric and conductive materials, respectively; w is the length of the line and g is the gap between the line and the ground plane in coplanar lines; W_{gnd} is the length of the ground plane, respectively	27
Figure 3-3 Free-space measurement system	29
Figure 3-4 Cavity perturbation (a) original cavity (b) perturbed cavity after the material insertion. E_1 and H_1 are the electric and magnetic fields, respectively; ϵ_1 and μ_1 are the permittivity and permeability of the cavity; V_c is the volume of the cavity; ϵ_2 and μ_2 are the permittivity and permeability of the material; and V_s is the volume of the sample.....	31
Figure 3-6 Types of microstrip resonators: (a) straight ribbon resonator (b) ring resonator and (c) circular resonator. Where: l is the length of straight ribbon resonator; r_1 and r_2 are the inner and outer radius of the resonator ring, respectively; and r is the radius of the circular resonator	33
Figure 3-7 Setup up of dielectric material covering a patch antenna	34
Figure 3-8 Schematic of the coaxial probe by Agilent Measurement Kit	35
Figure 4-1 Measurement results from the patch antenna stand-alone and after the introduction of superstrate	40
Figure 4-2 Design of microstrip patch antenna resonating at 2.25 GHz (a) front and (b) rear	41
Figure 4-3 Setup of resonator-based experimental technique.....	41
Figure 4-4 Scheme to cut and prepare the textile samples	42

Figure 4-5 KES-F - 3 Compressional Tester of Kawabata's Evaluation System for Textiles (Laboratory of Physical Tests - DCTT, UBI)	43
Figure 4-6 Results of the dielectric constant of textile materials when positioning face- and reverse-sides in contact with the resonator board	45
Figure 4-7 KES-F - 4 Surface Tester of Kawabata's Evaluation System for Fabrics Laboratory of Physical Tests - DCTT, UBI).....	46
Figure 4-8 Process of the image analysis.....	47
Figure 4-9 Relative dielectric constant vs Pores per cm ² (logarithmical regression).....	49
Figure 4-10 Relative difference of dielectric constant vs relative difference of superficial porosity (linear regression).....	49
Figure 4-11 Relative dielectric constant vs bulk porosity (linear regression)	50
Figure 4-12 3D II textile antenna patch placed on (a) face side and (b) on reverse side of the fabric, and (c) rear of the antenna	51
Figure 4-13 Simulated and measured S_{11} of textile antennas, (a) antenna 1 (b) antenna 2 (c) antenna 3 (d) antenna 4 (e) antenna 5 and (f) antenna 6	52
Figure 5-1 Measurements locations in Covilhã	63
Figure 5-2 Average received power for all measurements	63
Figure 5-3 Design of dual-band printed monopole textile antenna	64
Figure 5-4 Simulated radiation pattern for the proposed printed monopole, YZ plane (dashed) and XZ plane (solid), for (a) 900 MHz and for (b)1800 MHz	65
Figure 5-5 Dual-band printed monopole after assembly (a) front (b) rear	66
Figure 5-6 Simulated and measured S_{11} of the dual-band printed monopole.....	66
Figure 5-7 Printed monopole textile antenna connected to a 5-stage Dickson voltage multiplier	67
Figure 6-1 Design of the microtip patch antenna used to test several manufacturing techniques	70
Figure 6-2 S_{11} of the microstrip patch antennas	73
Figure 6-3 Set-up of resistance measurement test	75
Figure 6-4 Example of the group D of probes, for 3D I substrate.	76
Figure 6-5 Results of sheet resistance measurements ($[\Omega/\square]$, $n = 9$)	77
Figure 6-6 SEM image of the surface of Zelt [®] after applying in the other face, in (a) the adhesive sheet I and in (b) the adhesive sheet II	78

Figure 6-7 Comparison between ironing processes with and without steam	79
Figure 6-8 SEM images: cross-section of the antenna assembled (a) without steam and (b) with steam	80
Figure 6-9 Simulated and measured return loss of laminated antennas	81
Figure 6-10 SWF MA-6 automatic embroidering machine	82
Figure 6-11 Embroidered patches of printed monopole textile antenna	83
Figure 6-12 Simulated and measured return loss of embroidered antennas	84
Figure 7-1 Comparison of techniques of integration of antennas into cloth (a) typical integration and (b) “emblem” approach	88
Figure 7-2 Unobtrusive areas to integrate wearable devices, according to [143]	89
Figure 7-3 E-Caption: Smart and Sustainable Coat (Credits: Sophia Cueto Photography and Make Up Artist, Model: Benilde Reis)	90
Figure 7-4 Logotype of E-Caption: Smart and Sustainable Coat	90
Figure 7-5 Textile printed monopole antenna integrated on clothing. (a) 5-stage Dickson voltage multiplier integrated on lining of E-Caption to harvest the RF energy and (b) the in-situ antenna harvesting	91
Figure 7-6 Performance of the antenna in the anechoic chamber (a) in free space and (b,c) on-body measurements	91
Figure 7-7 Simulated and measured return loss, before/after dressing the coat	92
Figure 7-8 Measured radiation pattern of the textile antenna into the coat, free-space and on-body measurements at (a) 900 MHz and (b) 1800 MHz	93
Figure 8-1 Continuous Substrate Integrating the Ground Plane - 3D Weft knitted spacer fabric (white) with an integrated conductive layer (gold)	96
Figure 8-2 V-LEC6BS Knitting Machine by Monarch Knitting Machinery Ltd. (Courtesy Borgstena Textile Portugal)	97
Figure 8-3 Scheme of the Substrate Integrating the Ground Plane. (a) knitting structure diagram, being the green, orange and purple yarns correspondent to the conductive, dielectric and spacer yarns, respectively, based on [151]; (b) SEM image of the SIGP I, with 35X amplification	97
Figure 8-4 Microstrip patch antenna designed for the dielectric characterization, dimensions in mm	100
Figure 8-5 Measured S_{11} of the microstrip patch antenna designed for the dielectric characterization	101

Figure 8-6 Plot of the previously measured S_{11} and of the new simulation of the prototype 1	102
Figure 8-7 SEM images of the conductive side of the Substrate Integrating the Ground Plane (a) SIGP I, (b) SIGP II and (c) SIGP III	104
Figure 8-8 Microstrip patch antenna for energy harvesting at ISM band, dimensions in mm .	104
Figure 8-9 S_{11} of the microstrip patch antenna for energy harvesting at ISM band	105
Figure A-1 Vector Network Analyser - Department of Technology Information at Ghent University	126
Figure A-2 Anechoic chamber at Instituto de Telecomunicações - Aveiro	126
Figure C-1 Design and dimensions of coaxial cork antenna for 2.45 GHz	134
Figure C-2 Measured S_{11} of coaxial cork antenna	134
Figure C-3 Design and dimensions of coaxial cork antenna for 5 GHz (a) front (b) rear.....	135
Figure C-4 Measured return loss of coaxial cork antennas (prototype 1 - red line and prototype 2, blue line).....	135
Figure D-1 Quarter-Mode SIW textile antenna.....	137
Figure D-2 Styrofoam support to stabilise the glove during the measurements. In (a) antenna stand-alone (b) on the glove	138
Figure D-3 Measured S_{11} of Quarter-Mode SIW textile antenna (a) stand-alone - red line, and (b) on glove - blue line	138
Figure D-4 3D radiation pattern of Quarter-Mode SIW textile antenna (a) stand-alone and (b) on glove	139
Figure E-1 The RTP TV presenter, Mário Augusto, using the E-Caption Coat during the TV show Há Volta (Courtesy RTP TV)	141
Figure F-1 Logotype of E-Caption 2.0.....	143
Figure F-2 E-Caption 2.0 under construction (a) front and (b) rear	143

List of Tables

Table 2-1 Relative permittivity of different type of materials	12
Table 2-2 Summary of the textile materials that have been used on the design of wearable antennas.....	20
Table 3-1 Summary of non-resonant methods to characterize textile materials and leather .	29
Table 3-2 Summary of resonant methods to characterize textile materials and leather.....	35
Table 3-3 Summary of the advantages and drawbacks of resonant and non-resonant methods	37
Table 4-2 Characterized materials using the Resonator-Based Experimental Technique	44
Table 4-3 Average values obtained with the Resonator-Based Experimental Technique at 2.25 GHz, and their standard deviation (SD)	44
Table 4-4 Results of surface characterization.....	47
Table 4-5 Results of bulk porosity.....	50
Table 4-6 Dimensions of the textile antennas.....	52
Table 4-7 Simulated and measured resonant frequencies.....	53
Table 5-1 Wireless energy transfer techniques and applications.....	59
Table 5-2 Index terms and results of the search.....	60
Table 5-3 Textile materials used in the development of printed monopole	64
Table 5-4 Dimensions of the textile antenna.....	65
Table 6-1 Dimensions of the microstrip patch antenna.....	70
Table 6-2 Description of the manufacturing techniques used to produce the microstrip patch antennas.....	71
Table 6-3 Conductive materials under test	75
Table 6-4 Characteristics of the thermal adhesive sheets used on the lamination process....	75
Table 6-5 Results of sheet resistance measurements of laminated probes [Ω/\square]	77
Table 6-6 Ironing conditions	79
Table 6-7 Characteristics of the materials used to develop embroidered printed monopoles	82
Table 6-8 Parameters of the embroidered antennas	83

Table 8-1 Summary of structural parameters of the produced SIGP	99
Table 8-2 Structural parameters of the reference spacer knit	99
Table 8-3 Electrical properties of the SIGP	102
Table B-1 Compilation of permittivity measurements	129
Table C-1 Description of cork materials characterized at 2.25 GHz	133

List of Symbols

ε	Permittivity
ε_r	Relative Permittivity or Dielectric Constant
ε_0	Permittivity of Vacuum
ε'_r	Dielectric Constant
μ	Permeability
σ	Conductivity
R_s	Surface Resistance or Sheet Resistance
ρ_s	Surface Resistivity or Sheet Resistivity
U	DC Voltage
I_s	Surface Current
\square	Square Area
$\tan\delta$	Loss Tangent
D_f	Dissipation Factor
Q	Quality Factor
Q_{rad}	Space Waves Losses on Quality Factor
Q_c	Conductive Ohmic Losses on Quality Factor
Q_{sw}	Surface Waves on Quality Factor
Q_d	Dielectric Loss on Quality Factor
Q_e	Electric Quality Factor
Q_m	Magnetic Quality Factor
λ	Wavelength
®	Registered Mark
S_{11}	Return Loss Parameter
%	Percentage
f	Frequency
\emptyset	Bulk Porosity
\emptyset_{sup}	Superficial Porosity
\bar{X}	Average
R^2	R-Squared, Coefficient of Determination
Δ	Relative Difference
ρ	Density
ρ_f	Nominal Density

List of Acronyms

3D	Three-Dimensional
AC	Alternating Current
AATCC	American Association of Textile Chemists and Colorists
ATP	Associação Têxtil e Vestuário de Portugal - in English, Textile and Garment Association of Portugal
ASTM	American Society for Testing and Materials
BAN	Body Area Networks
BW	Bandwidth
CO	Cotton
COST	European Cooperation in Science and Technology
DC	Direct Current
DCTT	Department of Textile Science and Technology
DSC	Digital Selective Calling
EEH	Electromagnetic Energy Harvesting
EGB	Electromagnetic Band Gap
GSM	Global System for Mobile
GPS	Global Positioning System
<i>h</i>	Height of the Material (Thickness)
ICT	Information and Communication Technologies
IEEE	Institute of Electrical and Electronics Engineers
IET	Institute of Engineering Technology
IoT	Internet of Things
ISM	Industrial, Scientific and Medical
KES	Kawabata Evaluation System for Fabrics
<i>L</i>	Length
LCP	Liquid Crystal Polymer
LCR	Inductance, Capacitance and Resistance
LMF	Low Melting Fibre
LNA	Low-Noise Amplifier
LTE	Long-Term Evolution
<i>m</i>	Mass per Unit of Surface
MIMO	Multiple-Input Multiple Output
MUT	Material Under Test
NFC	Near Field Communication
PA	Polyamide
PANs	Personal Area Networks
PAN	Polyacrylic
PES	Polyester
PET	Polyethylene Terephthalate
PHEV	Plug-in Hybrid Electric Vehicle
PIFA	Planar Inverted F Antenna
PPE	Personal Protective Equipment
PU	Polyurethane
R	Circumference Radius
RF	Radio Frequency
RFID	Radio Frequency Identification

S-	Scattering Parameters
RH	Relative Permittivity
SAB	Services Ancillary to Programme
SAP	Services Ancillary to Broadcast
SEM	Scanner Electronic Microscopy
SIGP	Substrate Integrated on Ground Plane
SIW	Substrate Integrate Waveguides
SMA	Sub Miniature Version A Connector
SMD	Superficial Geometric Roughness
STSM	Short Term Scientific Mission
TPU	Thermoplastic Polyurethane
TUM	University of Mississippi
TUT	Tampere University of Technology
UBI	Universidade da Beira Interior
UMTS	Universal Mobile Telecommunication System
USA	United States of America
UWB	Ultra-Wideband
VNA	Vector Network Analyser
W	Width
WIPE	Wireless Power Transmission for Sustainable Electronics
WBAN	Wireless Body Area Network
WBSN	Wireless Body Sensor Network
WLAN	Wireless Local Area Network
WPT	Wireless Power Transmission
WSN	Wireless Sensor Network

1 Chapter

Introduction

Nowadays, the socio-economic development and lifestyle trends indicate an increasing consumption of technological products and processes, powered by emergent concepts such as Internet of Things (IoT), where everything is connected in a single network [1]. According to Cisco, IoT describes a system where items in the physical world, and sensors within or attached to these items, are connected to the Internet via wireless and wired Internet connections. These sensors can use various types of local area connections such as Radio Frequency Identification (RFID), Near Field Communication (NFC), Wi-Fi, Bluetooth, and Zigbee. Sensors can also have wide area connectivity such as Global System for Mobile Communication (GSM), Global Positioning System (GPS), 3G, and Long-Term Evolution (LTE) [2].

Following the European Commission Report [3], in the next years, the IoT will be able to improve the quality of life, especially in the health monitoring field. The development of smart objects for IoT applications, include the capacity of this objects to be identifiable, to communicate and to Interact [4]. In this context, wearable technology has been addressed to make the person, mainly through his clothes, able to communicate with and be part of this technological network. Figure 1-1 illustrated the growing of the IoT in the last decades.

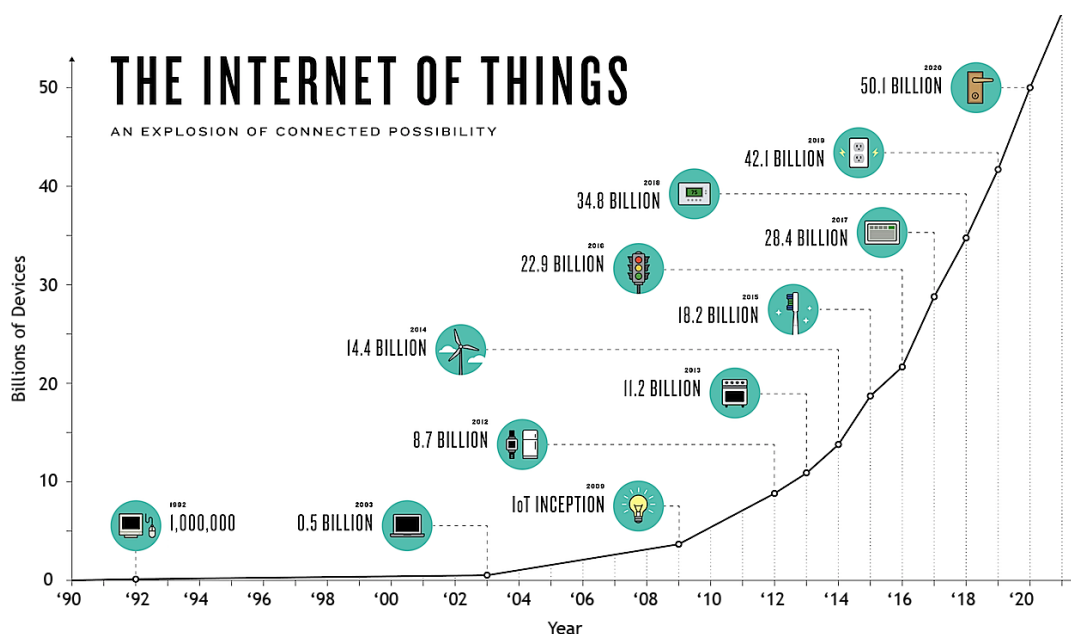


Figure 1-1 Growing of IoT, based on Cisco data [5]

Wireless communication systems are made up of several electronic components, which over the years have been miniaturized and made more flexible, such as batteries, sensors, actuators, data processing units, interconnectors and antennas [6]. In the systems for on-body applications, the antennas have been challenging, because they are conventionally built on rigid substrates, hindering their efficient and comfortable integration into the garment. However, embedding antennas into clothing allows expanding the interaction of the user with some electronic devices, making them less invasive and more discrete. Since 2001, when P. Salonen *et al.* [7] proposed the first prototype of flexible antenna made of fabrics, the use of textile materials to develop wearable antennas has increased exponentially.

The integration of electronics into textiles has started a new era for the apparel industry. In a near future, wearable antennas will be part of everyday clothing, transforming the garment in an interface for wireless communication actions. Thus, textile antennas that are designed combining the traditional textile materials with new technologies emerge as a potential interface of the human-technology-environment relationship, aiming applications such as tracking and navigation, mobile computing and others.

To achieve a low profile and unobtrusive integration of the antenna into the garment, antennas have to be thin, lightweight, robust and easy to maintain. Moreover, they must be low cost for manufacturing and commercializing. In this way, planar antennas have been proposed for wearable applications, because this type of antenna topology combines all these characteristics, and is also adaptable to any surface. Such antennas are usually formed by assembling conductive (patch and ground plane) and dielectric (substrate) layers [8], as shown on Figure 1-2. Furthermore, planar antennas, such as the microstrip patch antenna, radiate perpendicularly to a ground plane, which shields the antenna radiation, ensuring that the human body is exposed only to a very small fraction of the radiation.

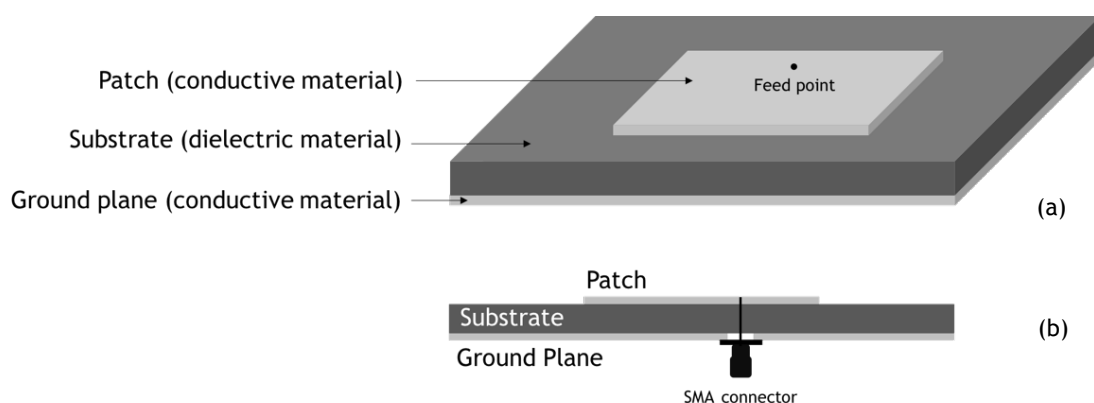


Figure 1-2 Layout of microstrip patch antenna (a) Front view and (b) cross section

To develop planar textile antennas, the knowledge of the properties of textile materials is crucial as well as insight into the manufacturing techniques for assembling the layers, such as laminating with glue, seam and adhesive sheets. Fabrics are planar fibrous materials whose

properties are mainly determined by the properties of the component fibres and the structure of the yarns and/or of the fabric. They are porous materials, in which the density of the fibres, air volume and size of the pores determine general behaviour, for instance, air permeability and thermal insulation. Moreover, as these features are somehow difficult to control in real applications of textiles, it would be very important to study how they influence the behaviour of the antenna in order to minimize any unwanted effects².

1.1 Motivation

Besides IoT being a hot current research topic challenging textile engineers to develop novel materials, processes and products for wearable electronics, according to the ATP - Associação Têxtil e Vestuário de Portugal (in English, Textile and Garment Association of Portugal) the technical textiles applied to Information and Communication Technologies (ICT), are pointed as one of the ten macro trends for the textile market until 2020 [9].

Based on the ATP study [9], the growing market of technical textiles for ICT means an interdependence between research fields. The studies that combine intersections of science, technology, materials engineering, business and fashion, emerge in Europe and will lead the R&D strategies, on the next decades, following the diagram presented on Figure 1-3.

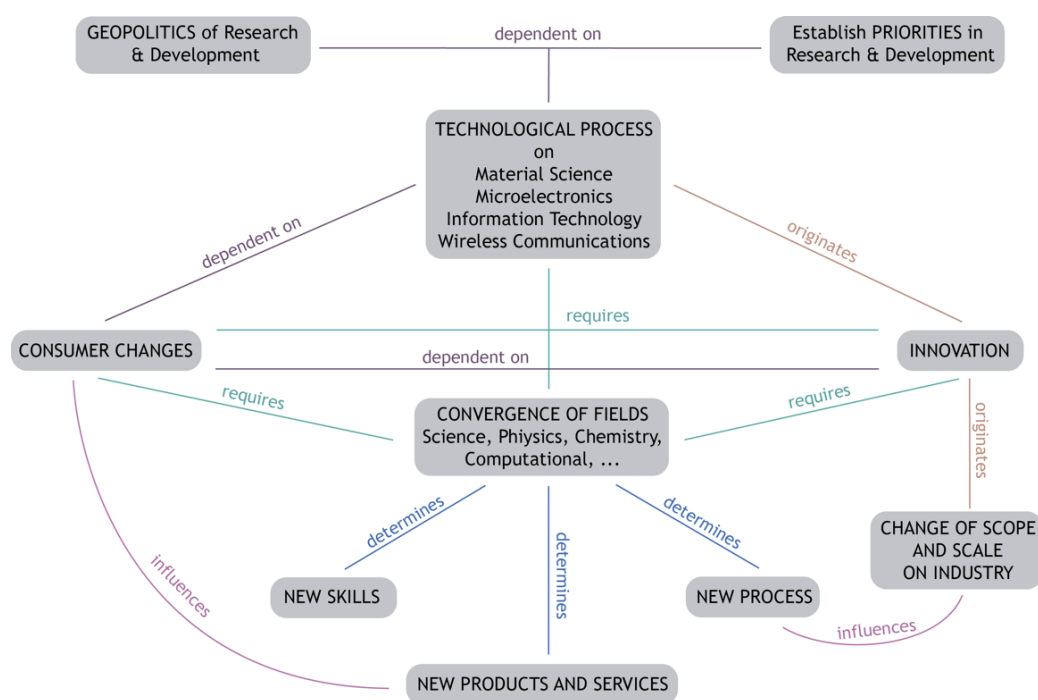


Figure 1-3 Schematic of the interdependence between fields to the development of technical textile for ICT, based on [9]

² In this PhD Thesis on Textile Engineering some fundamental parameters of antennas will be discussed, in order to relate the performance of the antennas with the applied textile materials and manufacturing techniques. The fundamental parameters of antennas are described on Appendix A.

The integration of wearable technologies and wireless communications into textile materials and products still is in an emerging phase. The majority of the studies found in the state of the art of textile antennas, were made by electrical engineers, only a few works presented the point of view of textile engineering. For this reason, the main motivation of this work is to contribute for the expansion of the textile presence in IoT, through advancing on the integration of wearable devices and systems for IoT into textiles, covering some gaps on the state of the art, fully described in the following Chapters. Four main gaps have been lead to this study:

- Despite the growing study of textile antennas in the past decades, the electromagnetic characterization of dielectric textile materials, to use as dielectric substrate, is still a challenge. Until now, none work has analysed the influence of the structural parameters of textiles on their dielectric behaviour;
- Also, so far, all textile antennas have been built stand-alone and are further glued into clothing to measure the performance when close to human body. No one has so far fully integrated a textile antenna on clothing, consequently there are no studies about the influence of the human body on the integrated antenna;
- Several manufacturing techniques of textile antennas are presented in the state of the art, but no industrial solution was found;
- At last, the integration of wearable devices raises the question about how to feed them. The textile antennas for energy harvesting emerge as a particularly interesting solution when the replacement of batteries is not easy to practice, such as in embedded wearable systems. Despite the growth in rigid antennas for energy harvesting and wireless power transmission, only few works have been presented using textile antennas.

1.2 Objectives

The general objective of this PhD Thesis is to characterize the dielectric properties of the textile materials, in order to select and develop a group of industrial textile materials, well suited to apply as dielectric substrates for textile antennas for energy harvesting. To achieve this goal, six specific objectives were considered:

1. Characterize the dielectric properties of textile materials, studying the influence of some structural properties of textiles on their electromagnetic behaviour;
2. Test several manufacturing processes to produce textile antennas, analysing the influence of the manufacturing technique on the performance of the antenna;
3. Develop, produce and test a textile antenna for RF energy harvesting;
4. Analyse the integration of antenna on clothing, and the influence of the human body on its performance;
5. Create a prototype of a smart garment, demonstrating the concept of energy harvesting through textile antennas on cloth;

6. At last, develop a new textile structure that reduces hand-made manufacturing effects, and improves the integration of industrial textile antennas on cloth.

1.3 Outline

This PhD Thesis is organized in nine Chapters. This first one presents the motivation to study textile antennas and the objectives of this work. Chapter 2 describes the electromagnetic properties of the textile materials used to manufacturing textile antennas. Also, presents a survey of the key points for the design and development of textile antennas, from the choice of the textile materials to the framing of the antenna. Still, manufacturing techniques of the textile antennas are described.

Chapter 3 gives an overview about the resonant and non-resonant methods to characterize the dielectric properties of textile materials. Moreover, it presents and compares the obtained results in the dielectric characterization to the performance of textile antennas. Chapter 4 presents the Resonator-Based Experimental Technique. This new method to characterize the dielectric properties of textiles is based on the theory of resonance-perturbation. It aims extracting the permittivity and loss tangent values based on the shifts caused by the introduction of a superstrate on the patch of a microstrip antenna. Also, this Chapter correlates the results obtained on the dielectric characterization with some structural parameters of textiles, such as surface roughness and superficial and bulk porosities.

Chapter 5 describes the concept of the energy harvesting and presents a survey of textile antennas for RF energy harvesting. A dual-band printed monopole textile antenna for electromagnetic energy harvesting, operating at GSM 900 and DCS 1800 bands is also proposed in this Chapter. In order to improve the performance of this printed monopole textile antenna, Chapter 6 then tests several manufacturing techniques by evaluating the S_{11} parameter of a patch microstrip textile antenna. Also, the electrical resistance sheet of two conductive fabrics was characterized and analysed. Further, seven prototypes of the printed monopole textile antennas were manufactured by laminating and embroidering techniques and were tested.

Chapter 7 presents the first prototype with a fully integrated textile antenna, named E-Caption: Smart and Sustainable Coat. It has an embedded dual-band printed monopole textile antenna for RF energy harvesting. This printed antenna is fully integrated, as its dielectric is the textile material composing the coat itself. The E-Caption illustrates the innovative concept of textile antennas that can be manipulated as simple emblems. Furthermore, this Chapter analyses the results obtained, before and after the integration of the antenna into cloth.

Finally, Chapter 8 ends the experimental work presenting the first continuous Substrate Integrating the Ground Plane (SIGP). The SIGP is a novel textile material that integrates the dielectric substrate and the conductive ground plane in a single textile fabric. The manufacturing and electromagnetic characterization processes are described. Also, to validate this new substrate, a microstrip patch antenna for energy harvesting was developed and tested.

To sum up, Chapter 9 gives a final remark, summarizing the main conclusions and presenting the future works.

1.4 Original Contributions

During these years, part of this study has been presented and recognized by the scientific community, through the following listed original contributions in international journals, conferences and books.

Articles in Scientific International Journals

- C. Loss, R. Gonçalves, P. Pinho and R. Salvado, “Influence of the Structural Parameters of Textiles on their Dielectric Behaviour”, Submitted to Textile Research Journal in 28/06/2017.
- C. Loss, R. Gonçalves, C. Lopes, P. Pinho and R. Salvado, “Smart Coat with a Fully-Embedded Textile Antenna for IoT Applications”, in *Sensors*, Vol. 16, No. 6, 938, 2016.
- O. Caytan, S. Lemey, S. Agneessens, D. V. Ginste, P. Demeester, C. Loss, R. Salvado, and Hendrik Rogier, “Half-Mode Substrate-Integrated-Waveguide Cavity-Backed Slot Antenna on Cork Substrate,” in *IEEE Antennas and Wireless Propagation Letters*, vol. 15, pp. 162-165, 2016.
- R. Salvado, C. Loss, R. Gonçalves and P. Pinho, “Textile materials for the design of wearable antennas: a survey”, in *Sensors*, Vol. 12, No. 11, pp. 15841-15857, 2012.

Articles in the Proceedings of International Conferences

- C. Loss, R. Gonçalves, P. Pinho and R. Salvado, “Influence of the Laminating Manufacturing Technique on the S_{11} Parameter of Printed Textile Antennas” in *IEEE International Microwave Workshop Series on Advanced Materials and Processes (IEEE-MTTS)*, Pavia, pp. 1-3, 2017.
- C. Loss, R. Gonçalves, R. Salvado and P. Pinho, “Textile Antenna for RF Energy Harvesting Fully Embedded in Clothing”, in *European Conference on Antennas and Propagation (EUCAP)*, Davos, pp. 1-4, 2016.
- C. Loss, R. Gonçalves, S. Agneessens, P. Pinho, H. Rogier and R. Salvado, “Electromagnetic Characterization of Textile Materials for the Design of Wearable Antennas”, in *The Fiber Society Conference*, Mulhouse, pp. 108-109, 2016.
- C. Loss, C. Lopes, R. Gonçalves, P. Pinho and R. Salvado, “Smart Coat with a Textile Antenna for Electromagnetic Energy Harvesting” in *2nd International Electronic Conference on Sensors and Applications*, vol.2, S3006, 2015.
- C. Loss, R. Salvado, C. Lopes, P. Pinho, R. Gonçalves, F. Velez, J. Tavares, H. Saraiva and N. Barroca and L. M. Borges, “Developing Sustainable Communication Interfaces Through Fashion Design”, in *5th STS Italia Conference - A Matter of Design: Making Society Through Science and Technology*, Milan, pp. 1-15, 2014.

- H. M. Saraiva, L. M. Borges, N. Barroca, J. Tavares, P. Gouveia, F. Velez, C. Loss, R. Salvado, P. Pinho, R. Gonçalves, N. B. Carvalho, R. Chavéz-Santiago and I. Balasingham, “Experimental Characterization of Wearable Antennas and Circuits for RF Energy Harvesting in WBANs”, in *79th IEEE Vehicular Technology Conference (VTC)*, Seoul, pp.1-5, 2014.
- L. M. Borges, N. Barroca, H. M. Saraiva, J. Tavares, P. Gouveia, F. Velez, C. Loss, R. Salvado, P. Pinho, R. Gonçalves, N. B. Carvalho, R. Chavéz-Santiago and I. Balasingham, “Design and Evaluation of Multi-Band RF Energy Harvesting Circuits and Antennas for WSNs”, in *21st International Conference on Telecommunications (ICT)*, Lisbon, pp. 308 - 312, 2014.
- C. Lopes, C. Loss, R. Salvado, P. Pinho, R. Gonçalves, F. Velez, J. Tavares, H. Saraiva and N. Barroca, “Conductive textiles: Emerging interface between the individual and the environment”, in *Proceedings of DESIGNA 2013 - International Conference on Design Research*, Covilhã, pp. 291-298, 2013.
- N. Barroca, H. M. Saraiva, P. Gouveia, J. Tavares, L. M. Borges, F. Velez, C. Loss, R. Salvado, P. Pinho, R. Gonçalves, N. B. Carvalho, R. Chavéz-Santiago and I. Balasingham, “Antennas and Circuits for Ambient RF Energy Harvesting in Wireless Body Area Networks,” in *24th IEEE International Symposium on Personal, Indoor and Mobile Radio Communication (PIMRC)*, London, pp. 532-537, 2013.
- R. Gonçalves, N. B. Carvalho, P. Pinho, C. Loss and R. Salvado, “Textile Antenna for Electromagnetic Energy Harvesting for GSM 900 and DCS 1800 Bands”, in *IEEE International Symposium on Antennas and Propagation and Radio Science Meeting (APS/URSI 2013)*, Florida, pp. 1206-1207, 2013.
- J. Tavares, N. Barroca, H. M. Saraiva, L. M. Borges, F. Velez, C. Loss, R. Salvado, P. Pinho, R. Gonçalves and N. B. Carvalho, “Spectrum Opportunities for Electromagnetic Energy Harvesting from 350 MHz to 3 GHz,” in *7th International Symposium on Medical Information and Communication Technology (ISMICT)*, Tokyo, pp. 126-130, 2013.

Chapter in Books

- C. Loss, R. Gonçalves, S. Agneessens, M. Rossi, P. Pinho, H. Rogier and R. Salvado, “Electromagnetic Characterization of Textile Materials for the Design of Wearable Systems”, in *Wearable Technologies and Wireless Body Sensor Networks for Healthcare*, IET: Stevenage, pp. 1-31, to appear in 2017.
- C. Loss, C. Lopes, P. Pinho, and R. Salvado, “Electromagnetic Pollution and the New Challenges in Fashion: Antenna in Clothing as a Space for Fashion”, in *Fashion Spaces - Geographical, Physical and Virtual*, Actual: Coimbra, pp. 119-146, 2016.
- C. Loss, C. Lopes, P. Pinho, and R. Salvado, “Poluição Eletromagnética e os Novos Desafios em Moda: Antenas no Vestuário”, in *Espaços de Moda - Geográficos, Físicos e Virtuais*, Actual: Coimbra, pp. 119-146, 2016.
- C. Loss, R. Salvado, P. Pinho, S. Agneessens, and H. Rogier, “Wearable Technologies: Dielectric Materials for Textile Antennas”, in *Pesquisa em Design, Gestão e Tecnologia de Têxtil e Moda*, São Paulo: Escola de Artes, Ciências e Humanidades, pp.107-114, 2014.

2 Chapter

Materials and Processes for Textile Antennas

The content of this chapter was partially published on Sensors Journal (2012), and as chapter on the books Fashion Spaces: Geographical, Physical and Virtual (2016), and Wearable Technologies and Wireless Body Sensor Networks for Healthcare (2017).

In the context of IoT, textile antennas offer the possibility of ubiquitous monitoring, communication and energy harvesting and storage. Several properties of the materials influence the behaviour of the antenna. For instance, the bandwidth and the efficiency of a planar antenna are mainly determined by the permittivity and the thickness of the substrate. The use of textiles in wearable antennas requires the characterization of their properties. Specific electrical conductive textiles are available on the market and have been successfully used. Ordinary textile fabrics have been used as substrates. In general, textiles present a very low dielectric constant that reduces the surface wave losses and increases the impedance bandwidth of the antenna. However, textile materials are constantly exchanging water molecules with the surroundings, which affects their electromagnetic properties. In addition, textile fabrics are porous, anisotropic and compressible materials whose thickness and density might change with low pressures. Therefore, it is important to know how these characteristics influence the behaviour of the antenna in order to minimize unwanted effects. This Chapter presents a survey of the key points for the design and development of textile antennas, from the choice of the textile materials to the framing of the antenna. An analysis of the textile materials that have been used is also presented. Further, manufacturing techniques of the textile antennas are described.

2.1 Introduction

Body worn systems endowed with sensing, processing, actuation, communication and energy harvesting and storage abilities are emerging as a solution to the challenges of ubiquitous monitoring of people in applications such as healthcare, lifestyle, protection and safety [10], [11]. Accordingly, the new generation of clothing will be able to sense, communicate data and harvest energy in a nonintrusive way. The wearable antenna is thus the bond that integrates cloth into the communication system, making electronic devices less obtrusive. To achieve good

results, wearable antennas have to be thin, lightweight, low maintenance, robust, inexpensive and easily integrated in radio frequency (RF) circuits. Thus, planar antennas are the preferred type of antenna as, despite the fact their maximum attainable bandwidth-efficiency is significantly lower than the theoretical limit for electrically small antennas, they allow an excellent integration of the antenna with the RF circuits, feeding lines and matching circuits on a standard multilayer board material [8]. Specific requirements for the design of wearable antennas are thus: planar structure; flexible conductive materials in the patch and ground plane; and flexible dielectric materials. The characteristics of the materials are crucial for the behaviour of the antenna. For instance, the permittivity and the thickness of the dielectric substrate mainly determine the bandwidth and the efficiency performance of the planar antenna [8]. Also, the conductivity of the ground plane and of the patch is an important factor in the efficiency of the antenna and must be the highest possible.

Textile materials, being universally used and easily available, are possible materials to design wearable antennas. Therefore, specific conductive textiles, sometimes designated electrotiles, that are commercially available have been successfully used in antennas. Ordinary textile fabrics have been used as dielectric substrates. However, little information is found on the electromagnetic properties of regular commercialized textiles.

Fabrics are flexible and compressible materials which thickness and density might change with low pressures. Moreover, the main orientation of the fibres and/or yarns introduces an intrinsic planar anisotropy of general properties. Plus, fibres are constantly exchanging water molecules with the surroundings, which affects their morphology and properties. All these features are somehow difficult to control in real applications of textiles. This Chapter presents the state of art reviewing the characteristics of textiles that influences the performance of the antennas.

2.2 Electromagnetic Properties of Textiles

As explained on Chapter 1, planar antennas, such as microstrip patch type, have been proposed for wearable applications. These antennas are usually formed by assembling conductive and dielectric layers, as previously presented on Figure 1-2. Their dimensions are directly related to the desired resonance frequency which are defined as portions of the wavelength of propagation [8]. The wavelength is dependent on the permittivity and permeability of the propagation medium (e.g. the dielectric substrate). For this reason, the knowledge of the electromagnetic properties of the textile materials is crucial to design wearable antennas [12].

The response of the material to the electromagnetic fields is described by the constitutive parameters of the material: permittivity (ϵ), permeability (μ) and conductivity (σ). These parameters also determine the spatial extent to which the electromagnetic field can penetrate the material at a given frequency. The relationship between these constitutive parameters and the electromagnetic fields is described through the Maxwell's equations [13]. For the design of antennas, the permittivity is the key parameter to characterise the substrate material and the

conductivity characterises the conductive components. The next subsections will present the definition and physical significance of the main variables. The conductive and dielectric textile materials, that have been used to develop wearable antennas, will also be described and discussed.

2.2.1 Dielectric Textiles

In the dielectric materials, the conductivity is very small or null ($\sigma \ll 1$). Thus, their electromagnetic behaviour is mainly determined by the permittivity and the permeability. Permittivity describes the interaction of the material with the electric field applied on it, whereas permeability describes the interaction of the material with the magnetic field applied on it.

Permittivity is a complex value that generally depends on frequency, temperature and moisture [13]-[15]. Furthermore, permittivity is usually expressed as a relative value (ϵ_r), given by (2-1), where ϵ_0 is the permittivity of vacuum, equal to 8.854×10^{-12} F/m.

$$\epsilon = \epsilon_0 \epsilon_r = \epsilon_0 (\epsilon'_r - j \epsilon''_r) \quad (2-1)$$

The relative permittivity is often called dielectric constant. The real part of the relative permittivity (ϵ'_r) is a measure of how much energy from an external electric field is stored in the material. The imaginary part of the relative permittivity (ϵ''_r), or loss factor, is a measure of how dissipative a material is to an external electric field.

The ratio between the imaginary and the real part of the relative permittivity is the loss tangent ($\tan \delta$) - often called the material dissipation factor (D_f), expressed by (2-2). In the ideal scenario, the perfect dielectric material has $\tan \delta = 0$.

$$\tan \delta = \frac{\epsilon''_r}{\epsilon'_r} \quad (2-2)$$

When designing antennas, the key parameter for the performance of the dielectric substrate is the relative permittivity as well as the loss tangent.

As textile materials are anisotropic materials, their characterization also depends on the electric field's orientation. This anisotropy is fully described by a permittivity tensor, although in most practical applications like the ones herein surveyed, one specific component of this tensor is enough to characterize the behaviour of the textile material for a specific application.

Besides the dielectric behaviour of textile materials being dependent on frequency, temperature and humidity [16]-[19], it also depends on the properties of the component fibres and the structure of the yarns and/or of the fabrics, and on the fibre packing density in the fibrous material [16], [20]-[22]. Also, textile materials incorporate some intrinsic singularities difficulties due to their inhomogeneity and instability, being a challenge in terms of accurate characterization, as will be discussed on Chapters 3 and 4.

In general, textiles present a very low dielectric constant as they are very porous materials and the presence of air approaches the relative permittivity to one. As reference, Table 2-1 shows the dielectric constant of different materials.

Table 2-1 Relative permittivity of different type of materials

Reference	Material	ϵ_r
[23]	Alumina	10.1
[24]	FR-4	4.50
[25]	Paper	7
	Glass	5 - 10
[26]	Quartzel [®] Fabric	1.95
	100% cotton fabric	1.60

For the development of wearable antennas, several conventional textile fabrics have been applied as dielectric substrate, exhibiting very low ϵ_r and $\tan\delta$, which reduce the surface wave losses and improve the impedance bandwidth of the antenna. Surface waves are connected to the guided wave propagation within the substrate. Hence, by reducing the dielectric constant, the contribution of the spatial waves increases, and consequently the impedance bandwidth of the antenna increases, allowing the development of antennas with higher gain and acceptable efficiency [27]-[30]. A sufficiently wideband and efficient planar textile antenna is realized by selecting a substrate with a low dielectric constant (preferably ≤ 4) and a low loss tangent ($<10^{-2}$) [31].

2.2.1.1 Influence of the Thickness of Dielectric Textiles

The thickness of the substrate is critical in the design of the antenna. As textile materials present a quite narrow range of relative permittivity values, it is therefore their thickness, which values may present much larger variations, that will mainly determine the bandwidth as well the input impedance of the antenna and so its resonance frequency [8], [32].

For a fixed relative permittivity, the substrate thickness may be chosen to maximize the bandwidth of the planar antenna. Therefore, the choice of the thickness of the dielectric material is a compromise between efficiency and bandwidth of the antenna [32]. The influence of the thickness on the bandwidth (BW) of the antenna may be explained by Equation (2-3), where Q is the antenna quality factor:

$$BW \sim 1/Q \quad (2-3)$$

The Q factor is influenced by the space wave (Q_{rad}) losses, the conduction Ohmic (Q_c) losses, the surface waves (Q_{sw}) and dielectric (Q_d) losses as shown in Equation 2-4 [8]:

$$\frac{1}{Q} = \frac{1}{Q_{rad}} + \frac{1}{Q_c} + \frac{1}{Q_d} + \frac{1}{Q_{sw}} \quad (2-4)$$

For thin substrates ($h \ll \lambda$), where h is the thickness of the material and λ is the wavelength of the frequency), the quality factor associated with radiation (Q_{rad}) is usually the dominant factor and is inversely proportional to the height of the substrate [8], [32]. Therefore, increasing the height of the substrate lowers the Q factor (Q_t). As the Q -factor decreases with an increased spacing between the patch and the ground planes of the antenna, a thicker substrate yields a larger antenna bandwidth [31].

Moreover, the thickness of the substrate also influences the geometric sizing of the antenna. This means that a thick substrate with low dielectric constant (value between 1 and 2) results in a large patch and a thin substrate with the same dielectric constant results in a smaller patch [33]. There are commercially available fabrics with a very large range of thickness values. Plus, nominal thickness values are given in any technical data sheet, allowing a careful choice of the material based on the required thickness. Moreover, accurate values of the thickness of fabrics under specific pressure are easily obtained by simple standard methods, such as ISO 5084:1996 [34] or with the Kawabata's Evaluation System for Fabrics [35]. Therefore, the thickness of the fabrics is a feature that may guide the search for suitable textile dielectrics.

2.2.1.2 Influence of the Moisture Content

Textiles always establish a dynamic equilibrium with the temperature and humidity of the air surrounding they are in contact with, as the fibres are constantly exchanging water molecules with the air. However, the amount of water that a material takes until reaching this equilibrium depends on the type of material. The extent to which a material is sensitive to moisture is described by its regain, which is defined, by the ratio of the mass of absorbed water in specimen to the mass of dry specimen, expressed as a percentage [16]. In [16], page 169 shows the relation between regain and relative humidity of the air (RH), for various textile fibres, compiling studies made by several authors. Indeed, for the same RH conditions, there are textile fibres with largely different moisture contents. For instance, at 65% RH, wool fibre might present a regain of 14.5%, cotton might present a regain of 7.5% and polyester fibre might present a regain of 0.2%.

In general, the moisture absorption changes the properties of the fabrics. Because of this, textile metrology is performed always in a conditioned environment (20°C and 65% RH). Also, for commercial transactions there are national legislations setting nominal values of moisture content that are values close to the regain obtained at 65% RH.

Water has a dielectric constant of $\epsilon_r = 78$ at 2.45 GHz and 25°C [18]. Although this value depends on the salinity, temperature and frequency, water has a much higher and more stable dielectric constant than textile fabrics, whose dielectric constant is generally in the range $\epsilon_r = 1 - 2$ because of their high porosity, as previously presented. Therefore, when water is absorbed by the textile fibres or is trapped into the fabric structure, it changes the electromagnetic properties of the fabric, increasing its dielectric constant and loss [16]-[18], [22], [36]. Charts presenting the relationship between the RH of the air or the moisture content of various fibres

and their dielectric properties can be found in [16]. Additionally, several authors have been correlating the electromagnetic properties of fabrics to their absorption properties [17], [18], [37], [38].

Likewise, the absorbed water by or trapped into the textile components of the antenna dramatically changes the behaviour of the antenna. The higher permittivity of the water drives the performance of the antenna, reducing its resonance frequency and bandwidth [18], [29], [36], [37].

Beyond these effects, when textile fibres absorb water they swell transversely and axially, causing tightening of the fabrics [16]. This tightness affects the dimensional stability of the fabrics and therefore affects the dimensional stability of the antenna, influencing its behaviour [36]. In general, the characteristics of antennas based on textile materials with small moisture absorption values (regain less than 3%) are more stable [18]. Therefore, materials with low regain are preferable for use as substrates and the same conclusion applies to the textile conductive components of the antenna.

2.2.2 Conductive Textiles

Generally, the fabrics are insulating materials. However, there are materials with high electrical conductivity, which incorporate fibres, filaments or coatings of metals or conductive polymers [39]-[44]. There is a large range of commercially available electrotexiles (e.g., Less EMF Inc. at <http://www.lessemf.com> or Shieldex Trading at <http://www.shieldextrading.net>) with high conductivity, enabling the development of antennas with acceptable performance.

Fabrics are planar materials and, therefore, their electrical behaviour may be quantified by the surface (or sheet) resistance (R_s) and characterized by the surface (or sheet) resistivity (ρ_s). The resistance, which unit is $[\Omega]$, is the ratio of a DC voltage (U) to the current flowing between electrodes that are in contact with the same face of the material under test in a specific configuration, as shown on Figure 2-1. In a conductivity measuring apparatus, the resistance may be dependent on the geometry of the electrodes used for measurement. Nevertheless, resistance can be related to the sheet resistance, which is independent of the geometry of the conductor. The sheet resistance is the ratio of the DC voltage drop per unit length (L) to the surface current (I_s) per unit width (D). It is thus a property of the material, not depending on the configuration of the electrodes used for the measurement [45]. The results of sheet resistance (R_s) are given in $[\Omega/\square]$ [46]. The sheet resistivity is then determined by multiplying the sheet resistance by the thickness of the material.

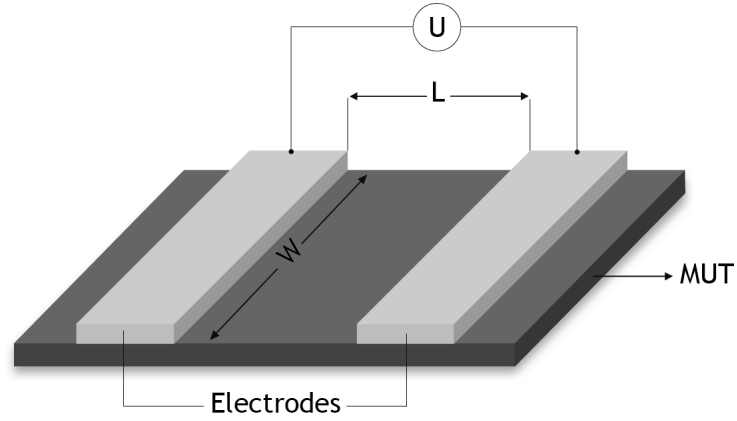


Figure 2-1 Basic setup for surface resistance and surface resistivity measurement

The conductivity of the fabric, which unit is Siemens per meter [S/m], is related to the sheet resistance by Equation (2-5), where h is the thickness of the fabric:

$$\sigma = \frac{1}{(R_s \cdot h)} \quad (2-5)$$

The sheet resistance is usually given by the manufacturer and may be measured by standard methods, such as, ASTM Standard D 257-99 Standard Test Method for DC Resistance or Conductance of Moderately Conductive Materials [46], ASTM Standard F 1896 - Test Method for Determine the Electrical Resistivity of a Printed Conductive Material [47], AATCC Test Method 76-2011: Electrical Surface Resistivity of Fabrics [48], among others [49], [50]. Despite the existence of several standard methods, an accurate characterization of highly conductive fabrics demands specific techniques, such as for instance the ones based on transmission lines and waveguide cavities [26], [51]-[53].

Besides the dielectric constant of the substrate, the choice of the conductive fabric for the patch and the ground planes is also very important to assure a good performance of the antenna. In general, the conductive fabrics must have a very low electrical sheet resistance, $\leq 1 \Omega/\square$, in order to minimize the electric losses and thus increase the antenna efficiency.

Despite the fact that the surface resistance value should be constant over the area of the antenna [36], the fabric may present some heterogeneities, such as for instance some discontinuities in the electric current. If these discontinuities are parallel to the surface current they will not interfere with the electromagnetic fields [54], but if discontinuities prevents the flow of the electrical current, the fabric resistance will increase [36].

Other factors, as for instance the float, which is the length of the conductive yarns laying on the surface of the woven, also influence the electrical behaviour of the material. The side with the longest floats of conductive electric wires exhibit lower sheet resistance than the other side [36]. Likewise, a higher density of conductive wires also cause lower sheet resistance [51]. Furthermore, the humidity content in the material is also an important factor to consider when

determining the electrical resistivity of textile materials, because the presence of moisture in the fibres significantly decreases the electrical resistivity [16], [38], [52], [55].

2.3 Influence of Mechanical Deformation of Conductive and Dielectric Textiles

Flexibility and elasticity are other requirements of the textile materials used to develop wearable antennas, in order to withstand the deformations caused by the bending angles of the human body. However, when the textile fabric adapts to the surface topology it bends and deforms, causing changes to its electromagnetic properties and thus influencing the antenna performance [29], [56]-[59]. Indeed, the bending and the elongation of the dielectric fabric change the geometric precision of the shape of the antenna, influencing its permittivity and its thickness, which affects the resonance frequency of the antenna and especially the bandwidth, as previously explained.

Moreover, knits may present higher anisotropy than woven, showing different electric surface resistance along the longitudinal and the transversal directions and this anisotropy may increase with the knit deformation. According to Locher *et al.* [36], for the studied knit material that is composed of silver plated polyamide fibres, deformations under 8% of elongation along the direction of the wales (see on Figure 2-2) slightly change the surface resistivity. However, when elongating the knitted fabric along the direction of the courses the electric surface resistivity results stable up to 3% of elongation but then increases and at 8% of elongation it reaches the triple of the initial value.

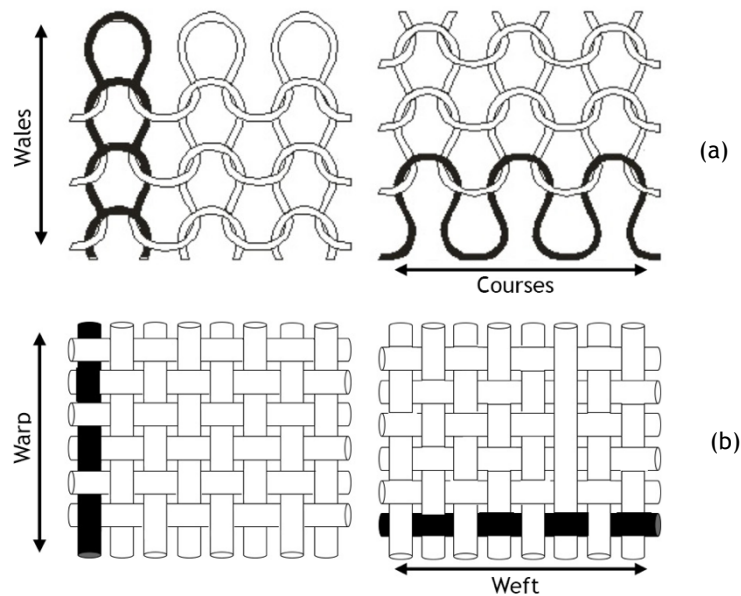


Figure 2-2 Schema of textile directions in (a) example of Jersey knit - wales and courses and in (b) example of plain weave - warp and weft

In addition, from the point of view of manufacturing antennas, the elasticity of the fabrics is an inconvenience as it makes difficult the precise definition and cut of the shape of the components and also makes difficult the superposition of the several materials without folds. Woven and nonwovens, being more stable fabrics than knits, allow higher geometrical accuracies of the frame of the antenna. In general, the accuracy depends on the thickness of the component yarns or fibres. For instance, conductive woven may allow an accuracy of about ± 0.15 mm [36].

2.4 Brief Survey on Textile Materials Used in Wearable Antennas

Wearable antennas are a recent research subject [27]. One of the first proposals on the subject was a Planar Inverted F Antenna (PIFA) for dual-band operation, built on a flexible unspecified substrate, presented in 2001 by Salonen *et al.* [7]. It was intended to be placed in the sleeve of clothing and operate at Global System for Mobile (GSM) (900 MHz) and Bluetooth (2.4 GHz) frequency, although the lower band was not achieved, the antenna still showed good performance, even in human-body presence, around the 2.4 GHz band. Later in 2003, they presented an antenna built on a textile substrate intended for Wireless Local Area Network (WLAN) applications [60], where results are claimed to be acceptable. Furthermore, in 2004 Salonen *et al.* [28] proposed a Global Positioning System (GPS) antenna with circular polarization, in which they have experimented with five different synthetic fabric materials as dielectric substrates. The conductive parts were made of copper tape. The dielectric synthetic materials used were: (1) Vellux[®], which is a 5 mm thick fabric covered on both surfaces with thin layers of plastic foam; (2) synthetic felt, which is a 4 mm thick nonwoven in which fibres are looser on the surface than in the centre; (3) Delinova 200[®], which is a strong fabric made of polyamide Cordura[®] fibres laminated with Gore-Tex membrane, weighing about 370 g/m² and having a thickness of 0.5 mm; (4) fleece, which is a very soft polyester fabric with 4 mm thickness, commonly used in sportswear; (5) upholstery fabric, which is composed of three fabric layers bound together resulting in a thin (1.1 mm) fabric of polyester and acrylic that has firmness. The ϵ_r of the five fabrics was measured by a cavity perturbation method, at 1.575 GHz, and the values ranged between 1.1 and 1.7. Among the studied fabrics, the one made of high tenacity polyamide fibres (Cordura[®]) was pointed out as the more interesting fabric for the development of a flexible antenna, because of its constant thickness and its high resistance. These properties yield more stable geometric dimensions of the antenna.

More recent demonstrations on wearable antennas for personal area networks (PANs) to operate in the 2.45 GHz industrial, scientific and medical (ISM) band and for GPS applications are presented in [33], [61]. In these examples, antennas for wearable protective clothing intended for professional use under rough conditions are presented and their behaviour in various practical scenarios is discussed. High performance aramid fabric that can withstand high

temperatures is applied as substrate while conductive textiles, like Shieldit® and Electron®, are used for the antenna patch and ground planes. These antennas have shown acceptable performance, even in a real environment with human-body presence and when subjected to bending and deformations.

In 2006, Locher *et al.* [36] have built four purely textile wearable patch antennas for Bluetooth applications. They have used three electrical conductive fabrics: (1) a nickel-plated woven fabric (with plating thickness about 250 nm applied on the fabric surface); (2) a silver-plated knitted fabric; (3) a silver-copper-nickel-plated woven fabric. Fabric (3) is the one preferred for building textile antennas with geometric precision, as it is woven and not knitted and its electric surface resistance was more homogeneous than the one of fabric (1). For the dielectric substrate, they used two types of fabrics: (1) woollen felt of 1.050 g/m² with a thickness of 3.5 mm and (2) polyamide spacer fabric, of 530 g/m², with a thickness of 6 mm. The felt was dimensionally more stable and harder to bend, whereas the spacer fabric was lighter and more elastic owing to its knitting-based structure. The dielectric properties were measured by a transmission line method, at a frequency of 2.4 GHz, obtaining as results for the felt: $\epsilon_r = 1.45$ and $\tan\delta = 0.02$, and for the spacer fabric: $\epsilon_r = 1.14$ and the loss tangent was negligible. The four different antennas produced have shown good performance and could satisfy the Bluetooth specifications, even when subjected to bending effects. However, the antennas lose their circular polarization when subject to bending.

In the same year, Tronquo *et al.* [29] presented rectangular-ring textile antennas for body area networks (BAN) that are circularly polarized, covering a bandwidth of more than 190 MHz. For the conductive antenna patch and ground plane they applied Electron®, which is a thin copper plated fabric with low sheet resistance, lesser than 0.1 Ω/\square . For the dielectric substrate they relied on a fleece fabric of 2.56 mm thickness. Its dielectric properties were measured by testing antennas and they obtained a dielectric constant of $\epsilon_r = 1.25$.

In 2007, Zhu and Langley [62] developed a dual-band coplanar patch antenna integrating electromagnetic band gap material (EGB), to operate at the 2.45 and 5.8 GHz wireless bands. The conductive parts were made of Zelt® fabric whereas the dielectric substrate was a thin felt, with 1.1 mm thickness, and with $\epsilon_r = 1.30$ and $\tan\delta = 0.02$.

The performance of the textile antennas presented earlier can be improved with integrated solutions, if diverse techniques such as for instance Multiple-Input-Multiple-Output (MIMO) are considered [63], or, as shown in [64], by introducing a low-noise amplifier (LNA) in a garment to achieve an active integrated antenna, increasing the sensitivity and the gain of the overall system.

Declercq *et al.* [65] showed another integrated solution consisting of an aperture-coupled antenna on a textile and foam substrate, with a flexible solar cell for tracking and monitoring solutions. Instead of integrating a LNA to increase the wearable antenna performance, Zhu and Langley [62], [66] developed a dual-band coplanar patch antenna, to operate in the 2.45 and

5.8 GHz wireless bands, in which they integrated an electromagnetic bandgap (EBG) to reduce body-presence effects and increase antenna gain. As shown in Table 1, the conductive parts were made of Zelt[®] fabric while the dielectric substrate was a thin felt with $\epsilon_r = 1.30$ and $\tan\delta = 0.02$. They proved that the introduction of the 3x3 arrays EBG with the coplanar patch could reduce the radiation towards the body by 10 dB, while increasing the antenna gain in 3 dB.

In order to improve flexibility in the antenna design and to achieve compact dimensions for easier antenna integration into clothing, in 2015 [67] S. Agneessens *et al.* designed and manufactured a circular quarter-mode textile antenna, using Substrate Integrate Waveguides (SIW) technology, operating in the ISM band. The patch and ground planes were made of conductive e-textile copper-plated polyester plain woven fabric, with low sheet resistance $0.18 \Omega/\square$ at 2.45 GHz, whereas the dielectric substrate was a flexible closed-cell expanded rubber protective foam, with 3.7 mm thickness, $\epsilon_r = 1.495$ and $\tan\delta = 0.016$. Furthermore, this paper studies the influence of the human body on the antenna behaviour, obtaining gains equals 3.8 and 4.2 dBi in an on-body and free space scenario, respectively. Previously, in 2014 [68], these authors had already proposed another antenna design, a dual-band antenna for body-worn application operating in the ISM frequency bands 2.4 and 5.8 GHz, using the same materials described above. In this SIW technology, several wearable antennas were implemented with conductive fabrics and diverse flexible substrates, including 3D knit and cork [69]-[71].

In the Radio Frequency Identification (RFID) context, the miniaturization of the tag technology brought significant advances in this field, improving their functionality and applicability. Nowadays, the size of the RFID tag depends on the constraints of the antenna. For this reason, the design of suitable antennas continues to be challenging. Based on this framework, some authors have been investigating textile antennas for commercial advertisement proposes, such as brand names and logotypes. Elmahgoub *et al.* [72] in 2010 proposed two RFID tags based on the merge of logos from The University of Mississippi (TUM) and Tampere University of Technology (TUT). The authors applied four different substrates, (1) PET - Polyethylene Terephthalate film, (2) thin film, (3) paper and (4) fabric, and applied three manufacturing techniques: (A) manual cutting, (B) stitching and (C) screen print, in order to verify the efficiency of the designed logo. In the textile fabric case, despite the woven fabric used as dielectric substrate remains unspecified, the most promising results in terms of conductivity and performance by screen printing with silver ink. Using the materials described above (3 and C), two tags have been proposed: one operating at 866 MHz and another at 915 MHz. Both tags performed well when compared with simulation, and long read distances of 11.2 and 7 meters, were achieved respectively.

Not only limited to RFID tags, Tak and Choi in 2015 [73], developed a Luis Vuitton logo antenna for integration into a handbag. This dual-band antenna, for ISM 2.45GHz and 4.5 GHz, was designed and fabricated using five layers of sheepskin-leather substrate with 0.7 mm thickness for each layer (3.5 mm in total), $\epsilon_r = 2.5$ and $\tan\delta = 0.035$. For the conductive parts, Zell[®] fabric

(Shieldex Trading, Palmyra, USA), with $R_s = 0.02 \Omega/\square$ and 0.1 mm thickness was used. The antenna is essentially a microstrip patch antenna, in which the patch assumes the form of the Louis Vuitton logo. It achieves dual band operation due to its characteristic structure. The size of the logo was obtained through optimization in order to match its input impedance in the ISM bands. The radiation pattern is expected to be directive. However, due to the large losses of the dielectric, the efficiencies fall short at 15.2% at 2.49 GHz, and at 41.4% at 4.52 GHz, yielding gains of -0.29 dBi and 3.05 dBi, respectively. Nevertheless, it is reasonable to consider this antenna for IoT applications, which usually comprises short distances of communication. Table 2-2 summarizes the several textile materials that have been applied to develop wearable antennas.

Table 2-2 Summary of the textile materials that have been used on the design of wearable antennas

Ref.	Application	Dielectric material				Conductive material
		Material	Thickness (mm)	ϵ_r	$\tan\delta$	
[7]	GSM (900 MHz) and Bluetooth (2.4 GHz)	Unspecified textile fabric	0.236	3.29	0.0004	-
[60]	WLAN (2.4 GHz)	Fleece fabric	3	1.04	-	Knitted copper fabric
[28]	GPS (1,5 GHz)	Cordura®	0.5	Between 1.1 and 1.7	-	Copper tape
[36]	Bluetooth (2.4 GHz)	Polyamide spacer fabric	6	1.14	Negligible	Silver-copper-nickel plated woven fabric
[36]	Bluetooth (2.4 GHz)	Woollen felt	3.5	1.45	0.02	Silver-copper-nickel plated woven fabric
[29]	190 MHz	Fleece fabric	2.56	1.25	-	Flectron®
[62], [66]	WLAN (2,45 and 5,8 GHz)	Felt	1.1	1.30	0.02	Zelt®
[65]	ISM (900 MHz)	Polyurethane protective foam	11	1.16	0.01	Flectron®
[67]	2.45 GHz	Closed-cell expanded rubber protective foam	3.7	1.49	0.016	Flectron®
[73]	ISM (2.45 GHz and 4.5 GHz)	Sheepskin leather	0.7	2.5	0.035	Zell
[74]	ISM (2,4 GHz)	Cotton/Polyester	2.808	1.6	0.02	Flectron® / Conductive ink

2.5 Manufacturing Techniques of Textile Antennas

In the printed antennas developed by Hertleer *et al.* [18] an alteration of no more than 0.5 mm on the length or the width of the patch influenced the performance of the antenna by causing a slight shift of the antenna characteristics. For this reason, woven fabrics, being more stable, are preferred to make the patches. However, the antenna geometrical stability can be achieved if at least one component is less deformable. For example, bonding using an adhesive sheet with a deformable patch, such as a conductive knit, with a less deformable substrate, such a

woven dielectric, results in a stable frame [28], [36].

The techniques used to connect the various layers must not affect the electrical properties of the patch, such as its surface resistivity, nor the permittivity of the substrate. Connections using adhesive sheets or conductive fabrics with a thermal adhesive face have shown good results [33], [36], [37], [73], [75]. This process of attachment of the superposed layers is very simple to perform by a simple ironing operation. However, attention should be made to the ironing process, in special if the patch is made of a fabric with metallic components. Indeed, the oxidation of the metallic component, due to the hot moistening of the fabric, may increase the surface resistance of the fabric and so decrease the efficiency of the textile antenna [51], [76].

Connection with seams is an alternative technique [28], [29], [36], [58] but it presents some difficulties. Firstly, the seam must be plane, without wrinkling, what might be difficult to achieve with deformable materials. Secondly, the stitch passes through all materials: the patch, then the substrate and further the ground plane of the antenna, which may cause electrical shorts between them. In Locher *et al.* [36] report that the sewing needle has pulled conductive fibres from the patch through the substrate, shorting the patch with the ground plane.

Another technique is connecting with liquid adhesives. However, it is difficult to apply a thin layer of glue. This difficulty introduces heterogeneity and in the zones where there are accumulations the glue may play the role of insulator between the conductive yarns of the patch. Furthermore, these adhesives are usually stiff and brittle, and so they cannot be applied in an area-wide manner on textiles as they will interfere in their flexibility [36]. In order to obtain a uniform thickness of the attachment of the several layers, Tronquo *et al.* [29], [30] perform an additional stitch, in addition to the glue. Also, in [33] a smooth fabric was added to both faces of the substrate to optimise the attachment of the conductive components.

The positioning of the textile components must consider the differences between right and back faces, in terms of roughness and of density of conductive elements [51], [52], [77]. In [51], [77], a satin 5 woven was tested in a microstrip resonator, placing it in two positions: (1) with the right face against the dielectric substrate and (2) with the back face, the conductive one, against the dielectric substrate. It was observed that when the conductive face is placed on the top of the substrate and so underneath the nonconductive yarns of the nonconductive face, most of the electrical field is contained in the substrate. Thus, the dielectric loss in the nonconductive yarns is minimized.

Besides the use of conductive fabrics, several other ways to manufacture the conductive parts of the antenna have been explored, such as embroidering and screen printing. Matthews and Pettit presented in [78] three types of antennas, which are integrated into clothing: a broadband wire dipole, a bowtie and a spiral antenna, operating in frequencies from 100 MHz to 1 GHz. They have tested different materials (textiles and others), different frames and

manufacturing techniques. Among the tested conductive materials there are conductive ribbon, conductive paint and ink, conductive nylon fabric (that is also adhesive on the back face), phosphor bronze mesh fabric (also adhesive on the back face), conductive thread, liquid crystal polymer (LCP) and copper coated fabric. The phosphor bronze mesh, LCP and copper coated fabric have the advantage that the antennas can be directly soldered onto. In some antennas, a conducting epoxy was used to bond the materials, but this results in some lack of robustness. In terms of radio frequency (RF) performance of the designed antennas, the spiral antenna, where the spiral is embroidered with conductive thread, performed worse than any other antenna and was clearly lossy. Overall, based on RF performance, they concluded the most attractive materials to design wearable antennas were the textile fabrics: the conductive nylon and the copper coated fabrics.

In [74] the stability and efficiency of wearable and washable antennas are discussed for textile antennas in which the conductive parts were screen printed with conductive ink. These antennas have shown acceptable performance. The combination of screen-printing with a breathable thermoplastic polyurethane (TPU) coating ensured that performance was maintained even after several wash cycles. Also in [79] the authors were used screen printing technique to manufacture a rectenna for 2.45 GHz for RF power transfer and harvesting. In this work, to reduce the surface roughness insuring the continuous conductivity of the conductive layer, an interface ink layer was applied between the textile substrate and the conductive ink. Besides the interface layer increase the losses on the dielectric substrate, the measured and the simulated S_{11} of antenna³, agree very well.

An embroidered technique was applied in [62], [66] to sew conductive fibres into polymer and fabric substrates. It was proved that by increasing the density of the embroidering stitching, the conductivity of the conductive section increases as well as the accuracy of the fabricated prototypes, yielding better agreement with the simulations. Dipole, spiral and microstrip patch antennas were fabricated with this technique. They yielded very good RF performance when compared to the corresponding rigid copper structures.

Finally, the connections at the antenna terminals may also be critical as in wearable and flexible antennas these connections have to be mechanically robust. In general, textile fabrics cannot be directly soldered to (an exception is Flectron[®] that already showed good resistance to soldering [33]). Therefore, conductive epoxy has been used, but some concerns remain as this connection is not very resistant [78].

A promising way to produce conductive elements is integrating conductive wires into the textiles through the three-dimensional (3D) weaving technique. This technique may contribute to improving the mechanical robustness and to eliminating the influence of the glue and/or seam [80].

³ see the S_{11} (return loss) definition on Appendix A.

2.6 Conclusions

The developed wearable antennas are mainly planar ones, specifically microstrip patch antennas, because they mainly radiate perpendicularly to the planar structure and also their ground plane efficiently shields the human body. The bandwidth and efficiency performance of a planar microstrip antenna is mainly determined by the substrate dielectric constant and its thickness.

In general, textiles present a very low dielectric constant, between 1 and 2, as they are very porous materials and the presence of air approaches the relative permittivity to one. The low dielectric constant reduces the surface wave losses that are tied to guided wave propagation within the substrates. Therefore, lowering the dielectric constant increases spatial waves and hence increases the impedance bandwidth of the antenna. However, lowering the substrate permittivity can also increase the resonance frequency of the antenna, allowing the development of antennas with acceptable efficiency and high gain.

In addition, the ability of the fibres to absorb moisture must also be considered in the characterization of the dielectric behaviour of textiles. Water has a much higher and more stable dielectric constant than textile fabrics. Therefore, when water is absorbed by the textile fibres or is trapped in the fabric structure, it changes the electromagnetic properties of the fabric, increasing its dielectric constant and loss tangent. Likewise, the absorbed water by or trapped into the textile substrate reduces the resonance frequency and bandwidth of the antenna. In general, the characteristics of antennas based on textile materials with small moisture absorption (regain less than 3%) are more stable. Therefore, materials with such low regain values are preferable for use as substrates and as conductive components of the antenna.

The thickness of the dielectric material is also crucial in the design of antennas. For a fixed relative permittivity, the substrate thickness may be chosen to maximize the bandwidth of the planar antenna. However, this value may not optimize the antenna efficiency. Therefore, the choice of the thickness of the dielectric material is a compromise between efficiency and bandwidth of the antenna. Moreover, the thickness of the substrate also influences the geometric sizing of the antenna.

The conductive fabrics for the patch and the ground planes must have a very low electrical sheet resistance in order to minimize the electric losses and so increase the antenna efficiency. There are several conductive textile fabrics, and also yarns, available on the market that have been successfully used in planar antennas. Coated fabrics might perform worse than the fabrics having conductive fibres, because of discontinuities that may increase the surface resistivity. Woven and nonwovens, being more stable fabrics than knits, allow higher geometrical accuracies of the frame of the antenna and thus may be preferred to make the patch. In general, the sizing accuracy of the patch made of woven fabric depends on the thickness of the component yarns.

Finally, after choosing the textile materials, their assemblage may also be critical, as the elongation and bending causes mechanical deformations that interfere with the antenna behaviour. The presence of at least one textile material presenting high tensile strength, high bending rigidity and stable geometry stabilizes the frame of the antenna. When connecting the various layers making up the antenna, the positioning of the textile fabrics must consider differences between right and back faces in terms of roughness and of density of conductive elements, in order to minimize losses.

3 Chapter

Dielectric Characterization Methods Applied to Textiles Materials: A Survey

The content of this Chapter was partially published as Chapter on the Book Wearable Technologies and Wireless Body Sensor Networks for Healthcare (2017).

The accurate characterization of conventional textile materials to use as dielectric substrates in wearable systems is fundamental. However, little information can be found on the electromagnetic properties of regular textiles. Woven, knits and nonwovens are inhomogeneous, highly porous, compressible and easily influenced by the environmental hygrometric conditions, making their electromagnetic characterization difficult. Despite there is no standard method, several authors have been adapting techniques for the dielectric characterization of textiles. This survey gives an overview of the resonant and non-resonant methods to characterize the textile materials and leather, to be used as dielectric substrate on wearable antennas. Also, this Chapter summarizes the characterization of textile materials made through these methods and that were validated by testing antennas which perform well.

3.1 Introduction

The knowledge of the electromagnetic properties of the materials is essential to a good design of the antenna. As reviewed on Chapter 2, many criteria should be considered, as several characteristics of the textile materials directly affect the behaviour of the antenna. Specific electrically-conductive textiles are available on the market and have been successfully used in the radiating components. Conventional textile fabrics have been used as substrates. However, little information can be found on the electromagnetic properties of these regular textiles.

Since [81], during the past century, several textile engineers have studied the dielectric properties of single fibres [16]. The main challenge founded on these works was the heterogeneity of air and fibres. Lather, in 2010, Bal and Kothari have reported a comparison of formulas for the air fibre mixture, used in the dielectric characterization [21]. Besides the large reports on the fibre context, only few researches on the characterization of fabrics were founded.

The dielectric behaviour of textiles depends on the properties of the component fibres and the structure of the yarns and/or of the fabrics, and on the fibre packing density in the fibrous material [16], [22]. Also, being textiles highly porous materials, the presence of air and moisture influences their dielectric characterization.

Despite the growth of research studies on textile antennas, the accurate characterization of the dielectric properties of the textile materials is still a challenge due to the intrinsic inhomogeneity and deformability of textiles [82]. Up today there is no standard method to measure the dielectric properties of textiles.

The main objective of the methods for the electromagnetic characterization of dielectric materials is to measure the relative permittivity of the specimen for a specific frequency, or bandwidth frequency, and field orientation [15]. The methods for the characterization of the dielectric properties that have been used are generally subdivided into two main categories: resonant and non-resonant methods [13]. Each of these categories includes several procedures. The following Subsections describe the ones that have already been proposed and applied to characterize textile materials.

3.2 Non-resonant Methods

The non-resonant methods mainly include procedures based on reflection and transmission/reflection measurements. As the reflection-based techniques, the dielectric properties of the Material Under Test (MUT) are extracted based on the reflection of the electromagnetic waves in free space by the sample [13]. In transmission/reflection methods, the dielectric properties are calculated based on the reflection from and transmission through the sample [13]. For the characterization of textile materials, several non-resonant methods have been tested, such as transmission lines [12], [76], [83]-[85], metallic and dielectric waveguides [26] and free space [11], [62]-[63].

3.2.1 Parallel Plate Method

The parallel plate method is the oldest way to measure the dielectric properties in fibre materials [81]. In this method, the material under test is placed between two parallel plates, as shown on Figure 3-1. In this case, the structure creates a capacitor whose capacity is measured by a LCR meter⁴. Owing to the simplicity of the procedure and the power measured by the LCR, this method is limited to the maximum 1 MHz frequency. Details about the theoretical equations can be found in [12]-[13]. In [89], nine textile fabrics were characterized at 200 kHz, under controlled ambient conditions to avoid the influence of moisture. The obtained results are summarized in following Table 3-1.

⁴LCR meter is an electronic equipment used to measure the inductance (L), capacitance (C) and resistance (R) of an electronic component.

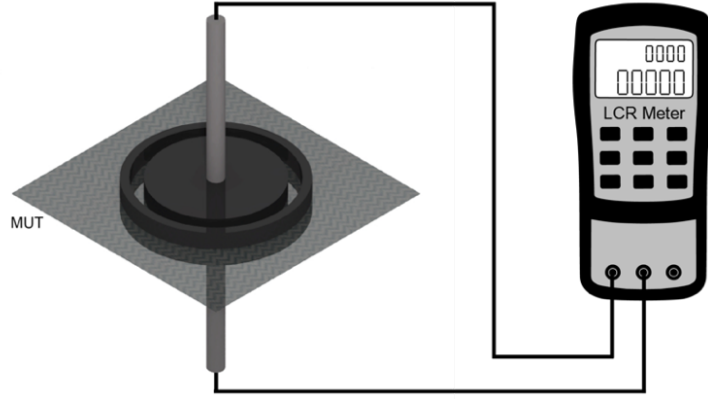


Figure 3-1 Parallel plate method

3.2.2 Planar Transmission Lines Methods

Planar transmission lines methods are the most common methods applied to characterize textile materials. Based on the scattering (S-) parameters, the advantage of this method is that it can also be applied to determine conductive properties, as presented in [14]-[15]. The planar transmission lines are subdivided into three types: microstrip, coplanar and stripline ones, as illustrated on Figure 3-2.

As shown on Figure 3-2 (d), the stripline consists of upper and lower grounding planes, and a central conductive line. The dielectric material under test is placed between the grounding planes and the central line. The advantage of this structure of transmission line is that the radiation losses are negligible. In [83], a stripline prototype was built to characterize a denim fabric, 100% cotton, at 2.45 GHz. For the conductive parts Electron[®] fabric was applied and to design the transmission line they used an estimated $\epsilon_r = 1.2$. As this stripline required $h = 2.45$ mm, five layers of denim fabric were superposed. The measurements with the VNA yielded $\epsilon_r = 2.117$ and $\tan\delta = 0.01$. To validate this method, a microstrip patch antenna for 2.45 GHz was designed and manufactured using the same materials. The antenna has shown good performance and 6.1594 dBi of gain was obtained.

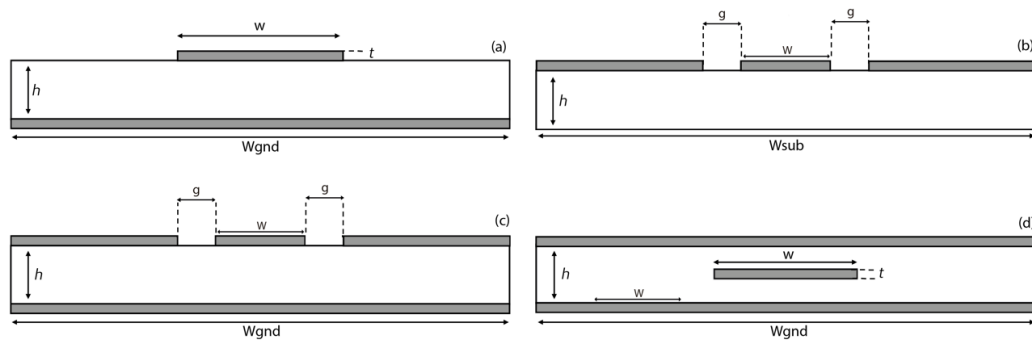


Figure 3-2 Types of transmission lines: (a) microstrip, (b) coplanar waveguide, (c) coplanar waveguide with ground plane and (d) stripline. Where: h and t are the thickness of the dielectric and conductive materials, respectively; w is the length of the line and g is the gap between the line and the ground plane in coplanar lines; W_{gnd} is the length of the ground plane, respectively

In [84], Mantash *et al.* propose a comparison between a stripline and an open stub resonator, described in [91], to characterize felt and denim fabric. For the stub resonator, a copper tape was used for the conductive parts. Measuring at a non-specified single frequency, for the denim they extract $\epsilon_r = 1.6$ and $\tan\delta = 0.05$, and for felt $\epsilon_r = 1.22$ and $\tan\delta = 0.016$. As to the broadband measurements, the authors have used a stripline fixture resonator for the dielectric material. The results between 1 GHz and 6 GHz have shown a range of values from $\epsilon_r = 1.215$ to $\epsilon_r = 1.225$ for the felt material, and from $\epsilon_r = 1.6$ to $\epsilon_r = 1.65$ for the denim fabric. Comparing the obtained results from the two methods, both are acceptable. In order to validate the results, two patch antennas for 2.45 GHz were proposed, using the permittivity value extracted at single frequency, and Shieldit[®] Super fabric ($R_s = <0.5 \Omega/\square$) for the conductive parts. These antennas have shown a good agreement between the results and the simulated parameters.

The propagation characteristics of two microstrip transmission lines with different lengths were measured in [85]. The lines were made using Nora[®] fabric, with $R_s = 0.03 \Omega/\square$, for the conductive parts, and an acrylic fabric with 0.5 mm of thickness for the dielectric substrate. Knowing the length difference and measuring the S-parameters between 3 and 10 GHz, the permittivity value for the acrylic fabric was calculated: $\epsilon_r = 2.6$. In order to validate the method, two Ultra Wide-Band (UWB) (3.1 - 10.6 GHz) wearable antennas were designed. The measured antenna parameters have shown to be in agreement with simulation estimations. Besides, the antennas have been tested for transmission of UWB pulses into the human body in order to evaluate reflectivity, which can be used in diagnosis applications. Moreover, they have proven to be reliable when in close contact with the human body, proving the usefulness of the development of such antennas in textiles.

In [79] the authors have used the two-lines technique as well. They characterize a fabric, whose fibrous composition is 65% PES and 35% CO, to use as a dielectric substrate of patch antenna for 2.45 GHz RF power transfer and harvesting. The fabric showed $\epsilon_r = 3.23$ and $\tan\delta = 0.06$. The measurement of the S_{11} of screen printed antenna shows an excellent agreement with the simulated results.

In [76], the authors have combined the two-lines method for microstrip lines with the matrix-pencil technique, in order to reduce the perturbations in the parameters of the transmission lines. They have characterized four different materials: (1) woven fabric, 98% aramid and 2% carbon, with $h = 0.60$ mm and $\epsilon_r = 1.57$; (2) woven fabric, 98% aramid and 2% carbon, with $h = 0.40$ mm and $\epsilon_r = 1.91$; (3) nonwoven polypropylene fabric with $h = 3.60$ mm and $\epsilon_r = 1.18$; (4) fleece with $h = 2.56$ mm and $\epsilon_r = 1.25$. For the conductive parts, copper sheet and Electron[®] fabric were used to manufacture the transmission lines. The authors concluded that the lines using copper sheet enabled to estimate the loss tangent of the substrates under test, given that the losses in copper sheet are much smaller than in the Electron[®]. To validate this method, the authors designed three textile antennas for 2.45 GHz, using the tested materials (1, 2 and 3)

as dielectric substrate. For the conductive parts, copper sheets and Flectron[®] fabric were used, and both copper and Flectron[®] based antennas exhibited good results.

3.2.3 Free Space Methods

This method typically consists in placing the material under test between two horn antennas, as show on Figure 3-3. By measuring the S-parameters - transmission (S_{11}) and reflection (S_{21}) coefficients - of the antennas with a VNA, the dielectric constant is estimated. The main advantage of the free space method is that it is contactless and non-destructive. The main drawback of this method is the required precise calibration of the horn antennas.

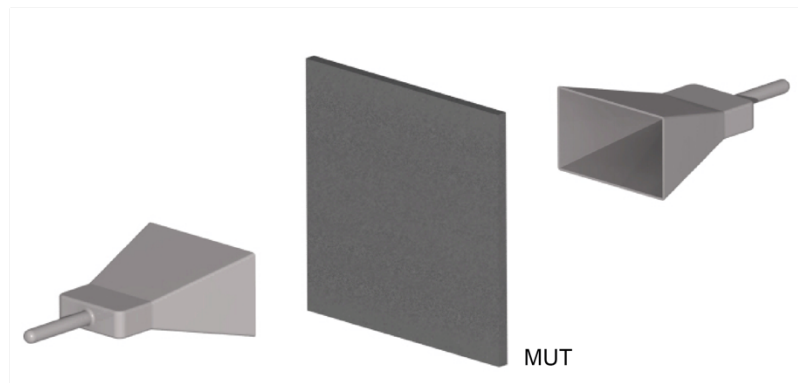


Figure 3-3 Free-space measurement system

In [86], this method was used to measure the dielectric properties of textile composites. The results of these characterizations can be found on Table 3-1. Furthermore, in [88] the authors present a variation of this method, based on an angular-invariant approach. Due the typical non-regular surface of the textiles and leathers, in this angular-invariant approach based on Rayleigh scattering, the authors have measured the scattering parameters of the antenna by varying the angle of the material under the test. All materials tested in this work have shown variations in the complex permittivity as a function of the different incidence angles, due to irregular thickness, surface roughness and texture of the materials. Also, the free-space method can be used to characterize the conductive textiles [87].

Table 3-1 Summary of non-resonant methods to characterize textile materials and leather

Ref.	Frequency application	Material	Thickness (mm)	ϵ_r	$\tan\delta$	Method
[89]	200 kHz	100% Cotton, twill weave	0.62	2.23	0.0366	Parallel Plate
		100% Cotton, plain weave	0.48	2.07	0.0314	
		100% Wool plain weave	0.42	1.86	0.0079	
		Wool, twill weave fabric	0.64	2.05	0.0076	
		Wool, plain weave fabric	1.26	1.67	0.0073	
		Wool + Polyamide, twill weave	1.47	1.53	0.0053	

Ref.	Frequency application	Material	Thickness (mm)	ϵ_r	$\tan\delta$	Method
[89]	200 kHz	100% Polyester (PES) plain weave	0.36	1.74	0.0044	Parallel Plate
		Viscose + PES twill weave	0.52	1.70	0.0079	
		100% Polyester plain weave	0.08	2.12	0.0035	
[83]	2.45 GHz	100% Cotton, Denim by Santista	0.49	2.11	0.01	Transmission line
[84]	Non-specified single frequency	Felt fabric	4.0	1.22	0.016	Stub resonator
		Denim woven	-	1.6	0.05	
	1 GHz - 6 GHz	Felt fabric	4.0	1.215 - 1.225	0.016	Stripline
		Denim woven	-	1.6 - 1.65	0.05	
[85]	UWB (3.1-10.6 GHz)	100% PAN fabric	0.5	2.6	-	Two-lines method
[79]	2.45 GHz	65% PES 35% CO	-	3.23	0.06	
[76]	2.45 GHz	98% PAR 2% Carbon Woven 1	0.6	1.57	0.007	Matrix-Pencil Two-line method
		98% PAR 2% Carbon Woven 2	0.4	1.91	0.015	
		100% PP Nonwoven	3.60	1.18	0.025	
		Fleece fabric	2.56	1.25	0.007	
[86]	8 - 11 GHz	E-Glass G7628	0.210	4.8 - 5.0	0.003 - 0.11	Free space
		E-Glass G880	0.152	3.84 - 4.0	0.003 - 0.11	
		Kevlar K141	0.254	3.97 - 4.05	0.003 - 0.11	
		Kevlar K151	0.254	3.88 - 3.04	0.003 - 0.11	
[88]	330 GHz	Denim woven	0.8	2.73	0.073	Free space: Angular-invariant approach
		Textile 1	0.45	2.74	0.031	
		Textile 2	0.25	2.72	0.068	
		Textile 3	0.7	3.66	0.042	
		Textile 4	0.25	2.54	0.066	
		Wool fabric from scarf	1.6	3.18	0.15	
		Stockinet fabric	0.65	3.22	0.08	
		Satin fabric	0.2	2.74	0.075	
		Natural leather	1.15	3.4	0.127	
		Artificial leather	0.95	3.104	0.079	
		Artificial leather	1	3.008	0.08	
		Artificial leather	0.6	2.17	0.066	
		Artificial leather	0.8	3.02	0.084	
		Artificial leather	0.6	2.49	0.085	

3.3 Resonant Methods

Resonant methods usually provide higher accuracy and sensitivity than non-resonant methods for low-loss materials [14], even though they only allow material characterization for a single frequency. They include the resonator method and the resonance-perturbation method. The

resonator method is based on the fact that the resonant frequency and quality factor of a dielectric resonator with given dimensions are determined by its permittivity and permeability. These methods are usually applied to measure low-loss dielectric materials. The resonance-perturbation method is based on resonant perturbation theory. For a resonator with given electromagnetic boundaries, when part of the electromagnetic boundary condition is changed by introducing a sample, its resonant frequency and quality factor (Q -factor) will also change. Measuring these shifts in the frequency and in the Q -factor is possible to extract the permittivity value, as presented in [13]. The Q -factor [13] is a parameter often used to describe an electromagnetic material, according to equations (3-1), (3-2) and (3-3):

$$Q_e = \frac{\epsilon'_r}{\epsilon''_r} = \frac{1}{\tan \delta_e} \quad (3-1)$$

$$Q_m = \frac{\mu'_r}{\mu''_r} = \frac{1}{\tan \delta_m} \quad (3-2)$$

where Q_e is the electric quality factor and Q_m is the magnetic quality factor. Based on this, it is possible to calculate the total quality factor (Q) of the material:

$$\frac{1}{Q} = \frac{1}{Q_e} + \frac{1}{Q_m} \quad (3-3)$$

3.3.1 Cavity Perturbation Methods

The most common resonance techniques are those based on resonant cavities formed by a rectangular or circular waveguide. The material under test is inserted into the resonant cavity and their electromagnetic properties are calculated from the changes in the resonant frequency and in the quality factor of the cavity caused by the introduction of the material [13], [92]-[94]. This phenomenon is illustrated on Figure 3-4 and the theoretical equations can be found in [13].

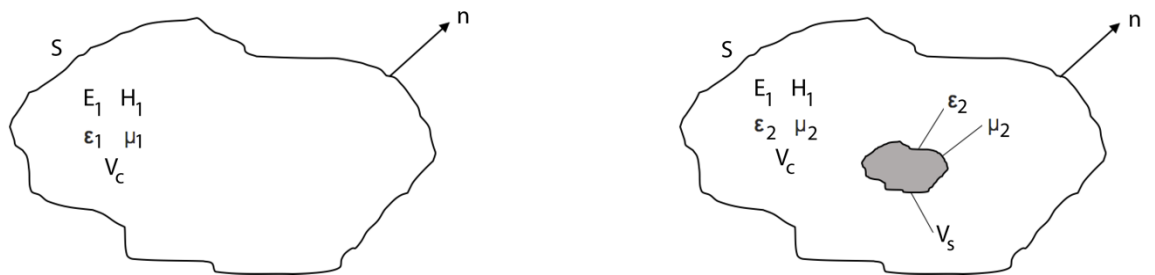


Figure 3-4 Cavity perturbation (a) original cavity (b) perturbed cavity after the material insertion. E_1 and H_1 are the electric and magnetic fields, respectively; ϵ_1 and μ_1 are the permittivity and permeability of the cavity; V_c is the volume of the cavity; ϵ_2 and μ_2 are the permittivity and permeability of the material; and V_s is the volume of the sample

These methods are difficult to apply as in every measurement the sample has to be placed in the same position. Figure 3-5 shows some examples of resonant cavities. Also, the cavity needs to be dismantled and reassembled every time a new sample is tested [13], consuming time and maybe introducing errors on the measurements. Moreover, the cavity resonator methods measure the permittivity in the plane of the sample and, therefore, cannot determine any anisotropy in the measured plane [14].

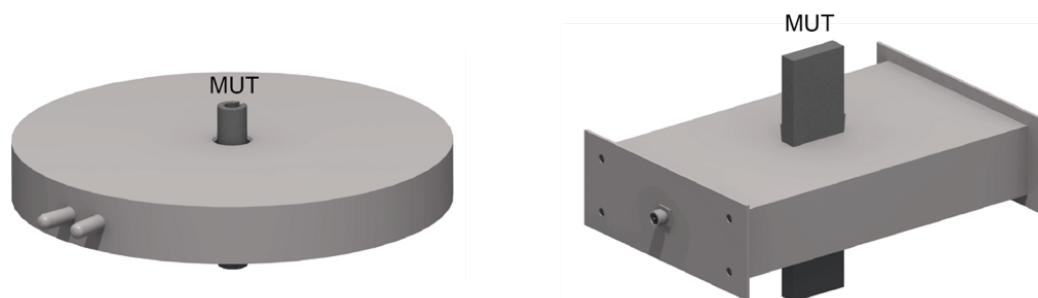


Figure 3-5 Examples of resonant cavities: (a) circular resonator cavity (b) rectangular resonator cavity

In [94], Kumar and Smith present the electromagnetic characterization of yarns and fabrics using a cylindrical split cavity resonator. In this work, the averaged result obtained for five yarns with different diameters, $\epsilon_r = 3.1141$, is compared to the averaged result for three fabrics made with these yarns $\epsilon_r = 2.7851$. As the textile materials are a mixture of nylon fibres and air, the authors concluded that fabrics exhibit higher porosity and, for this reason, a lower permittivity value than the yarns measured stand-alone.

Furthermore, [90] presents the dielectric characterization of nine textiles, using a closed cavity resonator. The authors have measured the textiles in all planes (x, y and z). The obtained results showed the influence of different alignments of the material with the electromagnetic field. The anisotropy caused by the different density of yarns in the warp and weft directions is clearly seen.

3.3.2 Microstrip Resonator Ring Method

The microstrip resonator methods are based in the resonance-perturbation method. The sample of the material under test is placed over the microstrip resonator affecting its resonant frequency and quality factor. Measuring the shift in the frequency and in the Q -factor enables to extract the permittivity values [13]. The microstrip resonator methods are subdivided into three types: straight ribbon resonator, ring resonator and circular resonator, as shown on Figure 3-6.

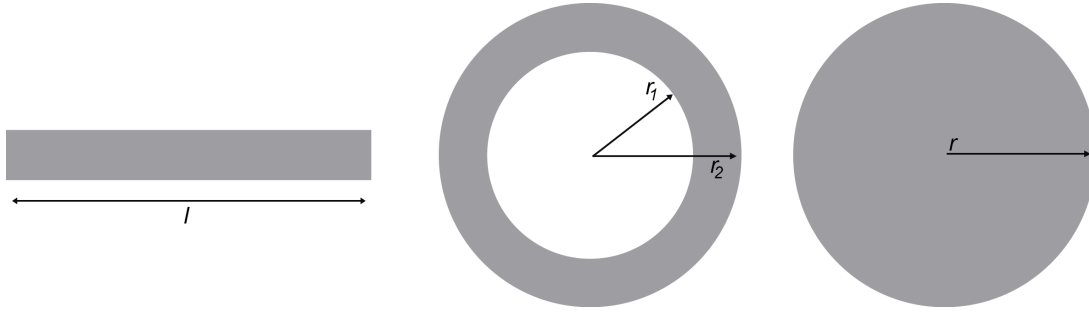


Figure 3-6 Types of microstrip resonators: (a) straight ribbon resonator (b) ring resonator and (c) circular resonator. Where: l is the length of straight ribbon resonator; r_1 and r_2 are the inner and outer radius of the resonator ring, respectively; and r is the radius of the circular resonator

The microstrip ring resonator does not have open ends, decreasing the radiation loss and consequently increasing the quality factor. For this reason, the ring resonator is more accurate and sensitive than the straight and circular resonators. Details about the theoretical equations of microstrip resonator can be found in [13]. For the characterization of the textile materials, the procedure of the microstrip ring resonator method only involves attach the conductive parts, made of copper foil, to the textile dielectric probe under test. In [95], the characterization of a “Bakhram” textile fabric at two different frequencies (831.940 MHz and 1.6890 MHz) is presented. After the measurements, the permittivity and loss tangent extracted values were $\epsilon_r = 2.031$ and $\tan\delta = 0.0038$, and $\epsilon_r = 1.965$ and $\tan\delta = 0.0024$, respectively. To validate the method, the authors designed a textile patch antenna to resonate at 831.940 MHz, also made of copper foil in the conductive parts. Despite the deviation in the measured frequency, the authors considered the characterization method well suited for the characterization of textile materials, considering this deviation as part of the design and manufacturing process of the antenna.

3.3.3 Microstrip Patch Sensor

The microstrip patch sensor consists of a patch antenna covered with the dielectric material under test, called superstrate, as shown on Figure 3-7. As for the microstrip ring resonator method, this technique relies on the resonance-perturbation method, where the calculation of the permittivity value is based on the shift in frequency caused by the introduction of the superstrate. More information about theoretical equations can be found in [96]-[98].

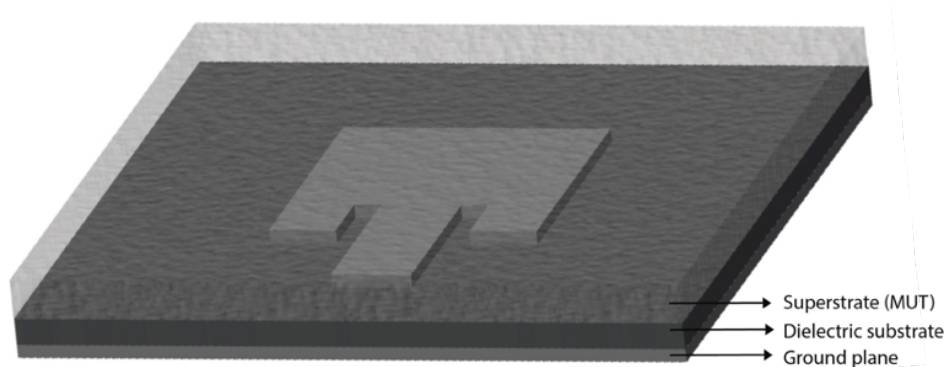


Figure 3-7 Setup up of dielectric material covering a patch antenna

In [97], this method is presented to measure solids and liquids. In [98], the method is used to test six nonwoven materials at 1.9 GHz. All tested nonwoven materials were manufactured by the stitching method and the results of their electromagnetic characterization are presented in Table 3-2. This non-destructive method can be a solution for a quick, easy and low-cost characterization procedure.

3.3.4 Microstrip Resonator Patch Method

In [20], Sankaralingam and Bhaskar proposed a novel microstrip patch radiator method, that consists in designing a patch antenna using an estimated permittivity value found by literature review. After manufacturing the antenna and measuring its S_{11} , the real value of the dielectric constant is calculated based on the shift of the resonant frequency. Six different textile materials were characterized and the extracted values can be found in Table 3-2. To validate this method, the authors designed some textile antennas for 2.45 GHz, using three tested materials as a dielectric substrate, and copper sheets for the conductive parts. Despite that these antennas exhibit good results, confirming the suitability of this method, the results can be influenced by the manufacturing technique. Indeed, the use of an interface to assembly the layers, such as glue or an adhesive sheet, and the inaccuracies when soldering the SMA connector to the microstrip patch radiator, can introduce errors in the final values.

3.3.5 Agilent 85070E Dielectric Measurement Probe Kit

The Agilent 85070E Dielectric Measurement Probe Kit, is an equipment by Agilent Technologies, available on the market to measure the dielectric properties of several types of materials [99]. In [73], the characterisation of textile and leather was performed using the open-ended coaxial probe method. In this method, the permittivity value is calculated only from the S_{11} parameter from the coaxial probe, measured with the VNA or impedance analyser, as illustrated on Figure 3-8. On the one side, the advantages of this method are: non-destructive technique, quick and easy to perform. On the other side, this method is very expensive (price of probe kit + software) and a complex calibration of the probe is required, using standard materials such as distilled water or methanol.

Five types of leather were characterized at 2.45 GHz: (1) original cowhide, $\epsilon_r = 1.76$ and $\tan\delta = 0.0009$, (2) original sheepskin $\epsilon_r = 2.5$ and $\tan\delta = 0.035$, (3) oiled sheepskin $\epsilon_r = 2.66$ and $\tan\delta = 0.085$, (4) scratched cowhide $\epsilon_r = 3.13$ and $\tan\delta = 0.15$, and (5) oiled cowhide $\epsilon_r = 2.3$ and $\tan\delta = 0.04$. Among the characterized leathers, considering the operating frequency, leather (2) was chosen to develop a dual-band wearable antenna for 2.45 GHz and 4.5 GHz applications. Due to the structure of five-layered substrate, the simulated and measured results deviate. For this reason, the authors included a new simulation using four air gaps of 0.0875 mm thickness to correct the results. The size of the air gaps was obtained through the difference between the simulated substrate thickness (3.5 mm) and the measured thickness of the final substrate (3.85 mm). The gain and the radiation efficiency at the lower frequency (2.49 GHz) are -0.29 dBi and 15.2%, respectively; and at the higher frequency (4.52 GHz) 3.05 dBi and 41.4%, respectively.

In [100] a denim fabric was characterized using the open-ended coaxial probe method, as well. The denim fabric, with 1.6 mm of thickness, was show $\epsilon_r = 1.7$ and $\tan\delta = 0.085$; and was used as dielectric substrate for a slotted antenna for RF energy harvesting between 2.22 - 2.59 GHz.

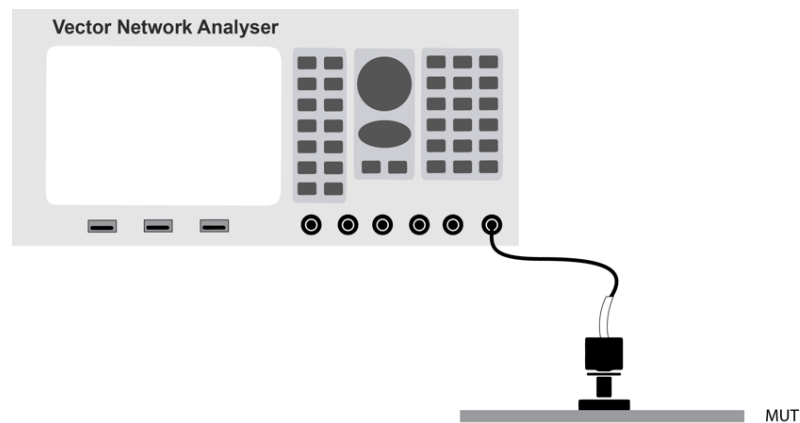


Figure 3-8 Schematic of the coaxial probe by Agilent Measurement Kit

Table 3-2 Summary of resonant methods to characterize textile materials and leather

Ref.	Frequency application	Material	Thickness (mm)	ϵ_r	$\tan\delta$	Method
[94]	9.8 GHz	100% Nylon 6.6 fabric	-	2.82	0.02681	Resonant microwave cavity
			-	2.75	0.02420	
			-	2.78	0.02831	
[28]	GPS (1.5 GHz)	100% PA, Cordura® fabric	0.5	Between 1.1 and 1.7	-	Cavity perturbation technique
[60]	WLAN (2.4 GHz)	Fleece fabric	3	1.04	-	
[95]	831. 940 MHz	“Bakhram” fabric	0.37	2.031	0.00038	Microstrip ring resonator method
	1.6890 GHz			1.965	0.0024	
[20]	2.45 GHz	100% washed cotton fabric	3.0	1.51	-	Microstrip patch radiator

Ref.	Frequency application	Material	Thickness (mm)	ϵ_r	$\tan\delta$	Method
[20]	2.45 GHz	100% cotton, denim	2.84	1.67	-	Microstrip patch radiator
		65% PES 35% CO fabric	3.0	1.56	-	
		100% CO, fabric for Curtain	3.0	1.47	-	
		100% Polyester (PES)	2.85	1.44	-	
		100% CO, Bed sheet/ floor spread fabric	3.0	1.46	-	
[73]	ISM (2.45 GHz) and 4.5 GHz	Original cowhide leather	0.7	1.76	0.0009	Agilent 85070E Dielectric Measurement Probe Kit
		Original sheepskin leather	0.7	2.5	0.0035	
		Original oiled sheepskin leather	0.7	2.66	0.085	
		Original scratched cowhide leather	0.7	3.13	0.15	
		Original oiled cowhide leather	0.7	2.3	0.04	
[100]	2.22 - 2.59 GHz	Denim fabric	1.6	1.7	0.085	
[98]	1.9 GHz	PES + (LMF-PES), Stitched nonwoven	10	1.013	-	Microstrip patch sensor
		P84® + (LMF-PES), stitched Nonwoven	8	1.012	-	
		Kermel® + (LMF-PES), stitched Nonwoven	8	1.014	-	
		(PES+ LMF-PES)/T, stitched Nonwoven, Thermal processed	1.4	1.175	-	
		(P84®+ LMF-PES)/T, stitched Nonwoven, Thermal processed	4	1.036	-	
		(Kermel® + LMF-PES)/T, stitched Nonwoven, Thermal processed	4	1.050	-	

3.4 Conclusions

This Chapter has presented a review of the methods to characterize the dielectric properties of textile materials, to be used as dielectric substrates of wearable antennas and systems. Also, this Chapter summarizes the characterization of textile materials made through these methods and that were validated by testing antennas which perform well.

The resonant and non-resonant techniques were presented. Despite the resonant techniques only characterize the material in a single frequency, generally, the resonant methods provide higher accuracy and sensitivity than non-resonant methods for low-loss materials. In this review all methods have shown good results and have characterized textile materials, which are summarized on Table 3-1 and Table 3-2, that are suitable for use as dielectric substrate in antennas. Table 3-3 summarizes the presented methods and describes their advantages and drawbacks.

Table 3-3 Summary of the advantages and drawbacks of resonant and non-resonant methods

Method	Measured planes	Required equipment	Advantages	Drawbacks
Parallel Plate	Z plane	Parallel plates and LCR	Non-destructive method	Maximum frequency of measurements: 1 MHz
Transmission lines	Z plane	VNA	Quick to perform	Requires a complex sample preparation, due to the mechanical instability of the fabrics, such as fraying and deformation in/after the cut process. The measured values are influenced by the conditions of some variables, as for example, the type of e-textile or conductive metal that is used, the glue/adhesive sheet, the connector and the manufacturing technique to make the probe, which can lead to non-repeatability of the measurements and introduce errors in the final values
Free-space	Z plane	Anechoic chamber	Non-destructive method	Requires a precise calibration of the horn antennas
Resonance cavities	X, Y and Z plane	Resonance cavities and VNA	Non-destructive method and possibility to measure the dielectric properties on several planes	In every measurement the sample has to be placed in the same position. Also, the cavity needs to be dismantled and reassembled every time a new sample is tested
Microstrip Resonator Ring and Microstrip Patch Sensor	Z plane	Resonator antenna and VNA	Non-destructive method, easy and quick to perform. Also no need sample preparation	Require a precise calibration of the VNA
Microstrip Patch Radiator	Z plane	VNA	Not require a sophisticated equipment	Complex sample preparation and estimation of an initial permittivity value. Also, the results are influence by the inaccuracies of manufacture process of the antenna
Agilent 85070E Dielectric Measurement Probe Kit	Z plane	Agilent 85070E Dielectric Measurement Probe Kit and VNA or impedance analyser	Easy and quick to perform	Very expensive equipment and a complex calibration of the probe is required

4 Chapter

Resonator-Based Experimental Technique: Method and Analysis

The content of this Chapter was partially submitted to the Textile Research Journal (June of 2017) and published on the IEEE International Microwave Workshop Series on Advanced Materials and Process (2017), and as Chapter of the Book Wearable Technologies and Wireless Body Sensor Networks for Healthcare (2017). Also, was presented in The Fiber Society Conference (2016 and 2017) - the paper presented in 2017, received the 3rd place in The Fiber Society Graduate Student Paper Competition. The experimental research presented in this Chapter was developed during the Short Term Scientific Mission (STSM), in the framework of the European Cooperation in Science and Technology (COST) - Project IC 1301 - Wireless Power Transmission for Sustainable Electronics (WIPE), held on the Department of Information Technology of Ghent University (Belgium), under the supervision of Prof. PhD. Hendrik Rogier.

The knowledge of the electromagnetic properties of the textile materials is crucial to design wearable antennas. Despite the increase of research studies on textile antennas, the accurate characterization of the dielectric properties of textile materials is still a challenge due to the intrinsic inhomogeneity and deformability of textiles. In this Chapter, the Resonator-Based Experimental Technique is presented. This method is based on the theory of resonance-perturbation, extracting the permittivity and loss tangent values based on the shifts caused by the introduction of a superstrate on the patch of a microstrip antenna. The results obtained using this method have shown that when positioning the roughest face of the MUT in contact with the resonator board, the extracted dielectric constant value is lower than the one extracted with this face positioned upside-down. Based on this observation, superficial properties of textiles were investigated. Thus, this paper relates the results of the dielectric characterization to some structural parameters of textiles, such as surface roughness, superficial and bulk porosities. The results show that both roughness and superficial porosity of the samples influence the measurements, through the positioning of the probes. Further, the influence of the positioning of the dielectric material on the performance of textile microstrip antennas was analysed. For this, twelve prototypes of microstrip patch antennas were developed and tested. The results show that, despite the differences obtained on the characterization when placing the face or reverse-sides of the MUT in contact with the

resonator board, the obtained average result of ϵ_r is well suited to design antennas ensuring a good performance.

4.1 Introduction

To alleviate the problems and complexity of the sample preparation, the influence of the conductive material and the expensive equipment required in the methods described on Chapter 3, an experimental resonator-based technique was developed. It is based on the resonance-perturbation theory, based on similar principles as the microstrip patch sensor technique presented in 3.3.3. However, the method outlined on this Section relies on full-wave simulators rather than approximating formulas for the extraction of the electromagnetic properties of the MUT, thus yielding an overall higher accuracy. More specifically, it consists in computing the electromagnetic parameters of the MUT by comparing the simulated and measured shifts in the resonance frequency and in the value of Q -factor of a microstrip patch antenna. These shifts are caused by the introduction of a superstrate on the patch that is the material under study, MUT.

Indeed, the presence of the superstrate will change the characteristics of the antenna, such as resonance frequency, as shown on Figure 4-1. This shift in the frequency ($f_{r1} - f_{r2}$) is caused by the difference of the electromagnetic wavelength of the uncovered antenna, simulated during the design process, and the measured antenna covered by a dielectric material of unknown ϵ_r . The amplitude of the frequency shift depends on the ϵ_r and on the thickness of the covering material.

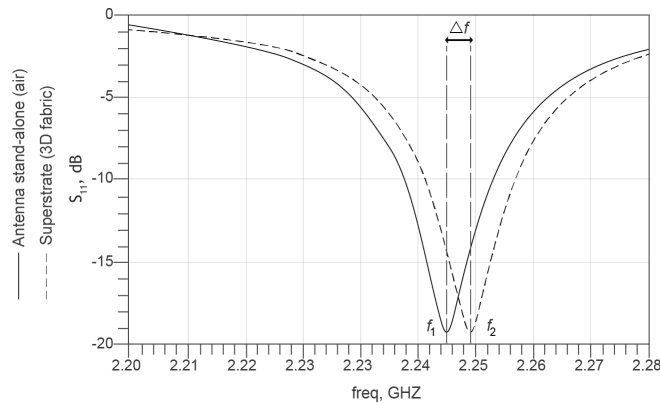


Figure 4-1 Measurement results from the patch antenna stand-alone and after the introduction of superstrate

The test equipment consists of a board on which a microstrip patch antenna is implemented and in a vector network analyser to perform the measurements. The antenna is designed to operate at 2.25 GHz, thus in the proximity of the 2.45 GHz, ISM frequency band, which is paramount for wearable systems. The antenna is realized on a rigid I-Tera MT40 high-frequency

laminates, with $\epsilon_r = 3.56$, $\tan\delta = 0.0035$ and thickness $h = 0.508$ mm, whereas the patch is etched in a copper layer with a thickness of $35\text{ }\mu\text{m}$. It is fed by a coaxial line through the SMA connector, with 50Ω of impedance. The designed antenna is shown on Figure 4-2 and its dimensions are given on Table 4-1. Also, the measurement set-up of the resonator-based experimental technique is illustrated on Figure 4-3. To stabilise the planar geometry of the MUT and avoid large air gaps between the MUT and the microstrip patch antenna of the resonator board, a block of Styrofoam was placed over the MUT. All dielectric measurements were performed in Department of Technology Information at Ghent University.

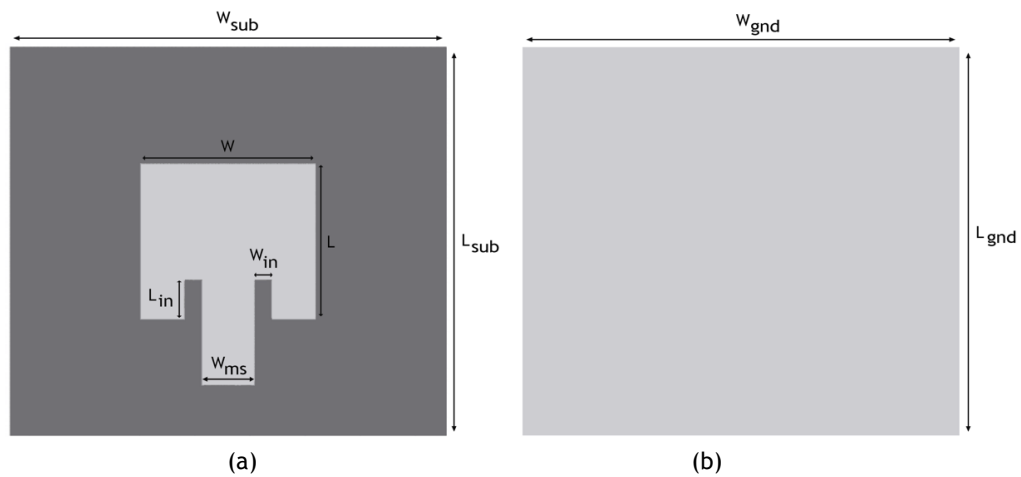


Figure 4-2 Design of microstrip patch antenna resonating at 2.25 GHz (a) front and (b) rear

Table 4-1 Dimensions of microstrip patch antenna used on Resonator-Based Experimental Technique

Parameter	Dimensions (mm)
W_{sub}, L_{sub}	100, 100
W, L	36.5, 36
W_{in}, L_{in}, W_{ms}	3, 10, 1.2
W_{gnd}, L_{gnd}	100, 100

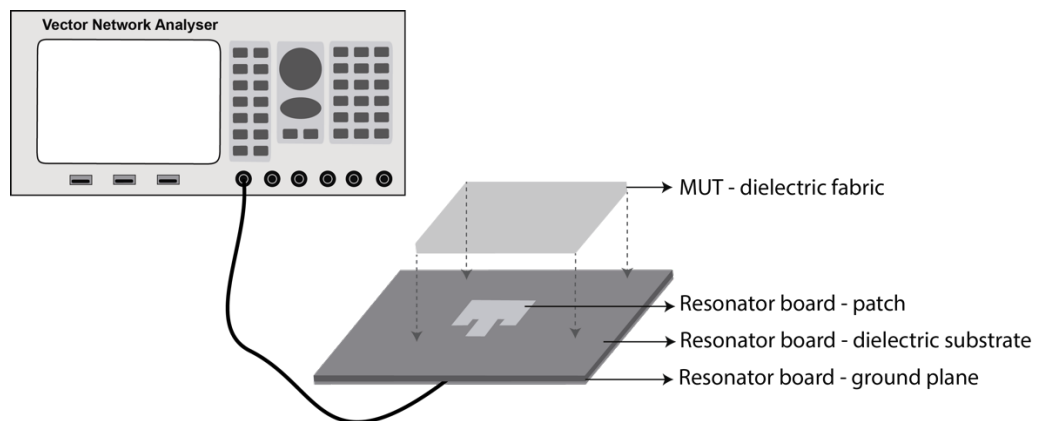


Figure 4-3 Setup of resonator-based experimental technique

4.1.1 Experimental Procedure

In order to extract the ϵ_r and $\tan\delta$ of the textile fabric under test, the following procedure is carried out:

1. Prepare the textile samples, cutting a square $10 \times 10 \text{ cm}^2$ (or sized enough to cover all the patch of the antenna) from the selvedge of the fabric and numerating its sides clockwise, as shown on Figure 4-4;
2. Calibrate the VNA in the frequency range of interest by using the electronic calibration module;
3. Connect the microstrip patch antenna to the VNA;
4. Measure the S_{11} parameter of the antenna;
5. Save the data;
6. Put the textile sample on the resonator board and mark the board in order to place future samples in the exact same place;
7. Measure again the S_{11} parameter of the antenna, this time with the textile sample on the patch;
8. Save the data;
9. Repeat the previous steps (6, 7 and 8) four times by positioning the substrate sample such that each time one different side is aligned with the microstrip feed of the antenna. Then, repeat the complete procedure by turning the sample upside-down. As a result, a total number of 8 measurements is acquired (2 faces x 4 positions);
10. Finally, by leveraging full-wave simulations of the antenna, extract the ϵ_r and $\tan\delta$ of the material under test by fitting the measured shift ($f_{r1} - f_{r2}$) in the antenna's resonance frequency and the measured variation in the Q -factor to the simulated ones, respectively.

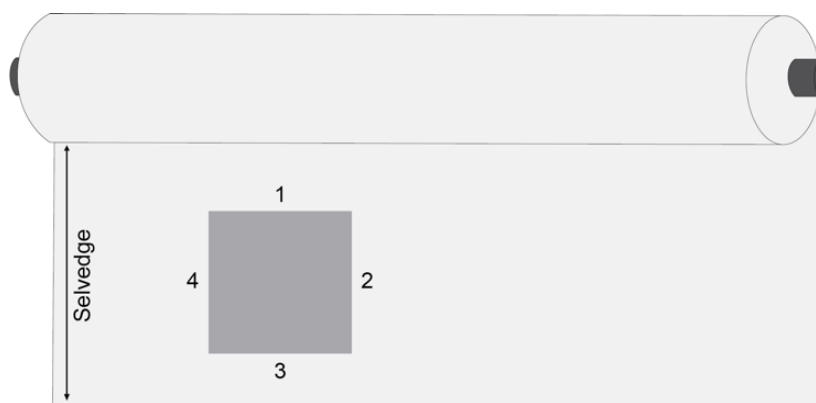


Figure 4-4 Scheme to cut and prepare the textile samples

The most advantageous feature of this experimental method is that it does not require sophisticated equipment, so it is fast and simple to apply. Moreover, in contrast to some of the aforementioned techniques, this method is non-destructive. As such, the MUT is not modified during the characterization process, thus yielding values of the permittivity and loss tangent

that are not influenced by the glue, the conductive material or the manufacturing of the measured structures.

4.1.2 Results

In order to study general relationships between the structure and the dielectric properties, eleven fabrics which vary in terms of composition, porosity and structure were analysed. More specifically, two samples of each material were characterized according to the procedure outlined in 4.1.1. All these fabrics are deliberately composed of synthetic fibres, aiming a low interaction with moisture, minimizing its effect on the electromagnetic performance of the materials. Table 4-2 presents the structural features of the studied fabrics.

The thickness of the samples was measured using the KES-F - 3 Compressional Tester of Kawabata's Evaluation System for Fabrics, presented on Figure 4-5, under controlled environment conditions of 25°C and 65% of RH, on Department of Textile Science and Technology (DCTT) at Universidade da Beira Interior. In this method the specimen is compressed by two circular-plates of steel having 2 cm² area. The velocity of the compression is 50 sec/mm and when the pressure attains 50 g/cm², the recovery process proceeds at the same velocity [35].



Figure 4-5 KES-F - 3 Compressional Tester of Kawabata's Evaluation System for Textiles (Laboratory of Physical Tests - DCTT, UBI)

Table 4-2 Characterized materials using the Resonator-Based Experimental Technique

Sample	Manufacturer	Manufacturer reference	Composition	Thickness (mm)
3D fabric I	LMA - Leandro Manuel Araújo Ltda. (Matosinhos, Portugal)	3003	100% Polyester	2.650
3D fabric II		3013		3.068
3D fabric III		3037		2.821
3D fabric IV		3006		2.410
3D fabric V		3015		4.140
Cordura I	B. W. Wernerfelt Group (Søborg, Denmark)	LTE1N184	Plain weave 100% PA 6.6, PU coated	0.503
Cordura II		LTE1N185	Plain weave 100% PA 6.6, TF coated	0.501
Neoprene I	Sedo Chemical Neoprene GmbH (Fürstenwalde/Spree, Germany)	N00S1	Neoprene laminated with jersey 100% Polyester	5.000
Neoprene II			Neoprene laminated with jersey 100% Polyester (face side) and 100% Nylon (reverse side)	3.095
Fake Leather I	-	-	Carded knit 100% Polyester, PU coated	0.831
Fake Leather II		-		0.923

The extracted values of ε_r and $\tan\delta$, reported on Table 4-3, were calculated following (4-1) and (4-2):

$$\varepsilon_r = \frac{\overline{\varepsilon_{rf1}} + \overline{\varepsilon_{rf2}}}{2} \quad (4-1)$$

$$\tan\delta = \frac{\overline{\tan\delta_{f1}} + \overline{\tan\delta_{f2}}}{2} \quad (4-2)$$

Where: $\overline{\varepsilon_{rf1}}$, $\overline{\varepsilon_{rf2}}$, $\overline{\tan\delta_{f1}}$ and $\overline{\tan\delta_{f2}}$ are the average values of ε_r and $\tan\delta$ extracted with the MUT positioned with the face-side (f_1) and the reverse-side (f_2) in contact with the resonator board, respectively.

Table 4-3 Average values obtained with the Resonator-Based Experimental Technique at 2.25 GHz, and their standard deviation (SD)

Sample	3D fabric I	3D fabric II	3D fabric III	3D fabric IV	3D fabric V	Cordura I	Cordura II	Neoprene I	Neoprene II	Fake Leather I	Fake Leather II
ε_r	1.10	1.10	1.12	1.13	1.11	1.58	1.56	1.37	1.30	1.45	1.43
SD	0.02	0.01	0.007	0.01	0.007	0.07	0.02	0.04	0.01	0.20	0.21
$\tan\delta$	0.005	0.006	0.017	0.018	0.004	0.008	0.008	0.001	0.001	0.017	0.012
SD	0.002	0.003	0.001	0.001	0.002	0.003	0.004	0.003	0.003	0.003	0.001

In resonator methods, such as the experimental technique presented here, the superficial roughness of the material may introduce some inaccuracies in the results due to the air gap between the sample and the resonator board. Figure 4-6 presents the extracted dielectric constants obtained by positioning the sample with each of the two faces contacting the board. We notice that the permittivity values vary according to the position of the sample on the patch. In particular, the largest variation is observed for the coated textiles. Even though the presence of this air gap can be accounted for during the characterization process, it is

important to analyse the superficial properties of the material in order to understand whether the results are correct and the material is compatible with this kind of characterization method.

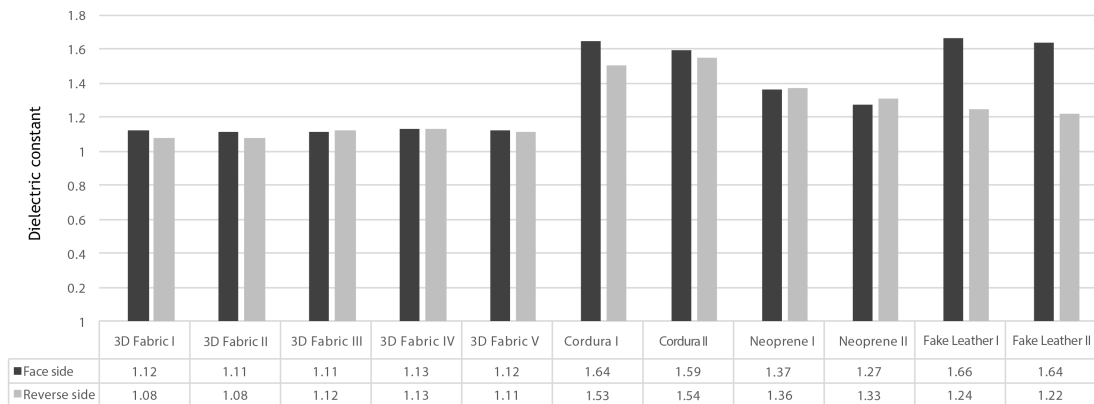


Figure 4-6 Results of the dielectric constant of textile materials when positioning face- and reverse-sides in contact with the resonator board

4.2 Surface Characterization Method

The influence of the surface parameters, such as superficial roughness and porosity, on the dielectric behaviour of the textiles have never been studied. Due to the results presented on Figure 4-6, detailed investigation of the influence of the surface parameters of the characterized textile was performed on this Subsection, in order to understand how these parameters can affect the performance of textile antennas.

4.2.1 Surface Roughness

The surfaces of the textile materials were characterized by measuring the superficial geometric roughness (SMD) with KES-F - 4 Surface Tester of Kawabata's Evaluation System for Fabrics, see Figure 4-7. The SMD is measured by pulling a U-shaped steel wire with 0.5 mm diameter through the fabric length under a normal force of 10 gf. In this way, a height profile of the fabric along its length is obtained. The standard mean deviation of this height profile is considered as surface roughness and is called geometric roughness [35]. This test was carried out in both the warp and the weft directions (5 measurements per each direction), for both face- and reverse-sides of the sample (20 measurements in total). The average value of these measurements is presented on Table 4-4. All measurements were performed under controlled environment conditions of 25°C and 65% of relative humidity, on DCTT at Universidade da Beira Interior.



Figure 4-7 KES-F - 4 Surface Tester of Kawabata's Evaluation System for Fabrics Laboratory of Physical Tests - DCTT, UBI)

4.2.2 Superficial Porosity

The superficial porosity (\emptyset_{sup}) was measured through image analysis using the DiameterJ tool [101], of the ImageJ software image analyser [102]. To obtain the superficial pores data, the first step was to take pictures of the textiles' surface, in a random area, with an optical microscope Nikon Eclipse LV100⁵. The images were taken using lenses of 5X magnitude for the 3D fabrics and 12X magnitude for the Neoprene, Cordura® and Fake Leather fabrics. The same amount of contrast and brightness was used in all pictures.

Using ImageJ software all images were converted to 8-bit greyscale level images. Then, the images were segmented in a binary image⁶ using algorithms and thresholding tools of DiameterJ. In this method, the fibre components were converted into white colour and the pores became black.

After the segmentation process, some white pixels could still remain in the pores areas. In this case, the morphological noise was removed using the binary commands - erode and dilate - of the ImageJ. The images were thus refined, eliminating the isolated pixel areas and highlighting the fibre edges.

Thereafter, the segmented image was analysed through the DiameterJ tool which gives the percentage of porosity as the ratio of the total number of black pixels to the total pixels in the image. The DiameterJ also gives the total number of pores found in the image. Figure 4-8 illustrates the image analysis process, and the obtained results are shown on Table 4-4.

⁵ Optical microscope images made at Printed Electronics Lab of EURECAT Technologic Centre (Mataró, Spain).

⁶ The segmentation process mean convert to binary formats with the pixel intensity values of 0 and 1, that is the image will only have black and white pixels, using the thresholding techniques.

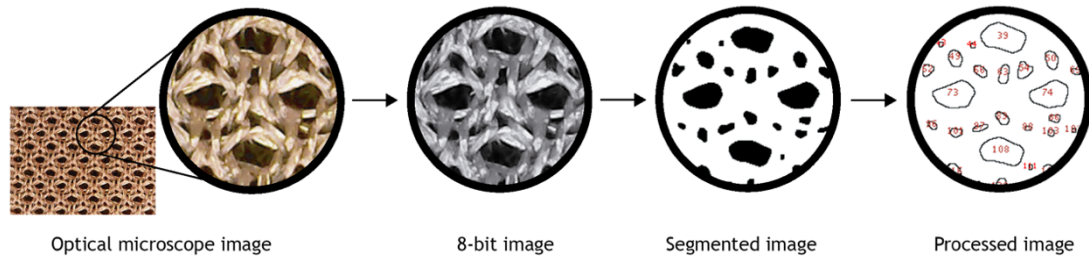
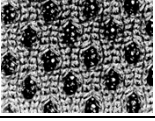
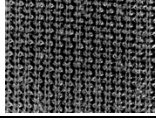
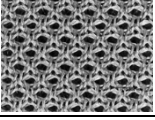
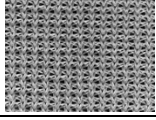
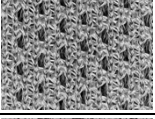
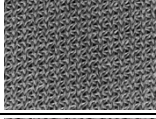
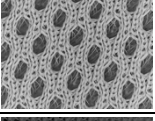
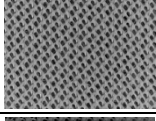
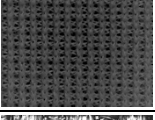
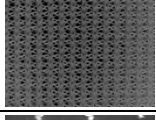
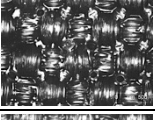
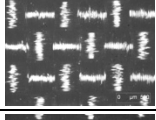
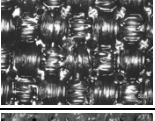
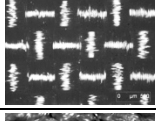
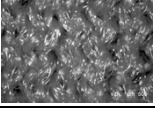
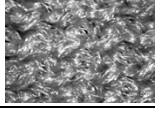


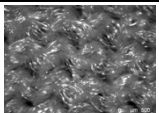
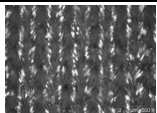
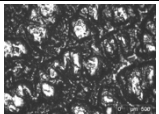
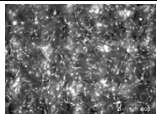
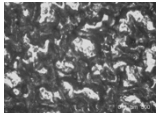
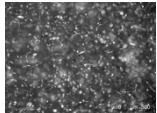
Figure 4-8 Process of the image analysis

4.2.3 Results

Table 4-4 presents the results obtained: the extracted dielectric constants, $\overline{\epsilon_{rf1}}$ and $\overline{\epsilon_{rf2}}$; the average of superficial roughness measurements, $\overline{SMD_{f1}}$ and $\overline{SMD_{f2}}$; the images used to extract the porosity and their respective results.

Table 4-4 Results of surface characterization

Sample	Face- side					Reverse- side				
	$\overline{\epsilon_{rf1}}$	Superficial porosity (% / cm ²)	Number of pores / cm ²	$\overline{SMD_{f1}}$ (μm)	Surface image	$\overline{\epsilon_{rf2}}$	Superficial porosity (% / cm ²)	Number of pores / cm ²	$\overline{SMD_{f2}}$ (μm)	Surface image
3D fabric I	1.12	35.43	89	5.320		1.08	17.96	244	9.130	
3D fabric II	1.11	23.45	126	4.988		1.08	21.07	269	10.700	
3D fabric III	1.11	18.90	219	5.743		1.12	22.71	165	2.578	
3D fabric IV	1.13	35.40	180	3.523		1.13	32.02	144	3.140	
3D fabric V	1.12	17.28	129	7.723		1.11	25.41	242	7.865	
Cordura I	1.64	0.5	<1	2.755		1.53	2	1	3.130	
Cordura II	1.59	0.7	<1	2.353		1.54	1.8	1	3.770	
Neoprene I	1.37	10.71	5	3.440		1.36	11.05	16	3.795	

Sample	Face- side					Reverse- side				
	$\overline{\epsilon_{rf1}}$	Superficial porosity (% / cm ²)	Number of pores / cm ²	$\overline{SMD_{f1}}$ (μm)	Surface image	$\overline{\epsilon_{rf2}}$	Superficial porosity (% / cm ²)	Number of pores / cm ²	$\overline{SMD_{f2}}$ (μm)	Surface image
Neoprene II	1.27	11.28	14	2.403		1.33	7.13	7	2.258	
Fake Leather I	1.66	1	<1	1.430		1.24	21.19	20	2.985	
Fake Leather II	1.64	1	<1	1.985		1.22	22.3	21	3.383	

As shown on Table 4-4, the surface features of the MUT may significantly influence the results obtained with the resonator-based experimental technique of dielectric characterization. Analysing the ϵ_r values on Table 4-4, one may verify that the dielectric constant extracted when placing the rougher face turning down contacting the resonator board presents a lower value. This is observed for all samples. Indeed, when positioning the rougher face in contact with the board more air is trapped on the interface between the MUT and the resonator board, lowering the measured value of ϵ_r .

Several structural parameters, such as stitch density and loop length, can influence the differences on the roughness of face and reverse sides of the textile materials. These features may be represented by the superficial roughness and porosity. Also, as one may observe on Table 4-4, the faces that have higher roughness \overline{SMD} also have the higher number of superficial pores per cm². This fact corroborates that, as expected, a higher number of superficial pores is related to a higher value of the surface roughness. Accordingly, positioning the faces with higher number of pores in contact with the board lowers the measured permittivity values. Considering all 176 ϵ_r measurements (8 measurements per probe, 2 probes per material and 11 materials) and plotting these data against the number of superficial pores per cm² of each face of the materials, an logarithmical regression is found, with $R^2 = 0.97574$, as shown on Figure 4-9.

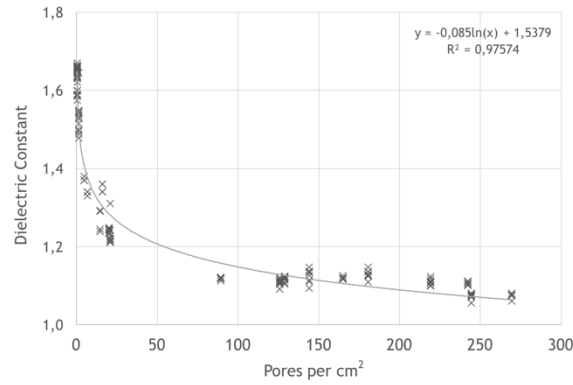


Figure 4-9 Relative dielectric constant vs Pores per cm² (logarithmical regression)

This means the dielectric constant value exponentially decreases with the increase of number of pores per cm², due to the presence of the air on the textile surface. Furthermore, the relative difference, Δ , of ϵ_r and \emptyset_{sup} among faces of the textile was calculated by (4-3), expressed in %:

$$\Delta = \frac{(\text{side 1} - \text{side 2})}{\text{side 2}} * 100 \quad (4-3)$$

where: *side 1* is the face with higher value and *side 2* is the face with lower value.

The results are plotted on Figure 4-10. A linear regression describes very well the relationship between the relative differences of ϵ_r and \emptyset_{sup} , with $R^2 = 0.99146$ as shown on Figure 4-10.

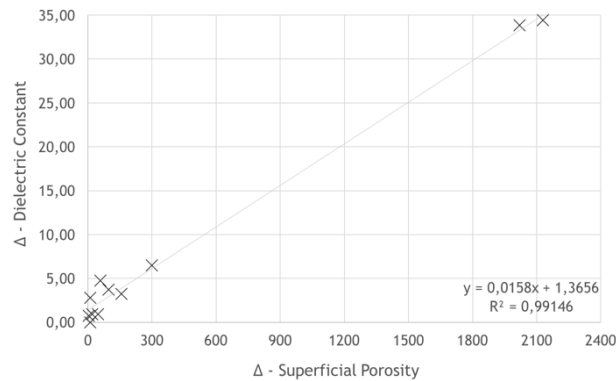


Figure 4-10 Relative difference of dielectric constant vs relative difference of superficial porosity (linear regression)

As presented on Figure 4-10, the largest relative difference between the ϵ_r of the face- and of the reverse-sides is observed for the coated textiles (Fake Leather I - 33.87 % and II - 34.42%). The 3D fabrics IV and II presented the lowest relative difference (0% and 2.78%, respectively). Coherently, these textiles also present the largest (Fake Leather I - 2019% and II - 2130%) and lowest (3D fabric IV - 10.56% and II - 11.30%) difference of superficial porosity among faces.

4.3 Structural Parameters Characterization

4.3.1 Bulk Porosity

The bulk porosity (\emptyset) of the textiles was calculated by (4-4).

$$\emptyset = 1 - \frac{\rho}{\rho_f} \quad (4-4)$$

Where: ρ (kg/m^3) is the density of the fabric, given by equation 4-5, and ρ_f is the nominal density of the polymeric components, described on Table 4-5.

$$\rho = \frac{m}{h} \quad (4-5)$$

Where: m is the mass per unit surface (g/m^2) and h is the thickness of the fabric (m). The results of the calculated bulk porosity of textiles are shown on Table 4-5.

Table 4-5 Results of bulk porosity

Sample	Density of polymeric components (kg/m^3)	Density (kg/m^3)	Porosity (%)
3D fabric I	PES = 1380	98.113	92.89
3D fabric II	PES = 1380	114.080	91.73
3D fabric III	PES = 1380	103.509	92.50
3D fabric IV	PES = 1380	136.514	90.11
3D fabric V	PES = 1380	87.198	93.68
Cordura I	PA 6.6 = 1120 PTFE = 2200	449.304	59.91
Cordura II	PA 6.6 = 1120 PU = 1150	469.061	58.91
Neoprene I	Neoprene = 1060 PES = 1380	224.80	79.98
Neoprene II	Neoprene = 1060 PES = 1380 PA = 1130	222.294	80.31
Fake Leather I	PES = 1380 PU = 1150	492.178	63.53
Fake Leather II	PES = 1380 PU = 1150	446.370	67.00

The results of bulk porosity also were analysed Plotting the 176 ε_r measurements against the bulk porosity results, a linear regression describes well the relationship between ε_r and \emptyset , with $R^2 = 0.97169$ as shown on Figure 4-11.

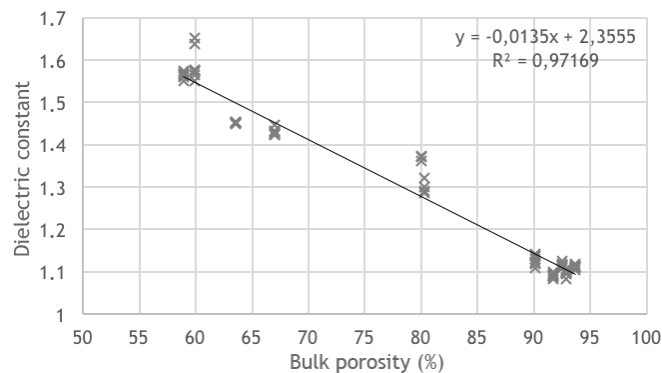


Figure 4-11 Relative dielectric constant vs bulk porosity (linear regression)

This is an expected result, as higher values of bulk porosity mean higher percentage of air into the fabric structure, lowering the dielectric constant of the fabric as air presents $\epsilon_r \approx 1$.

4.4 Significance of the Dielectric Results on the Design of Microstrip Patch Antennas

In order to analyse the impact of the differences of the ϵ_r values on the performance of textile antennas, six microstrip textile antennas were designed using the CST Microwave Studio 2016 full-wave simulator. All antennas were designed to resonate at 2.25 GHz, the same frequency used on the electromagnetic characterization procedure. Indeed, if the positioning of the MUT, placing the face or reverse-side in contact with the resonator board, leads to differences in the measured results of ϵ_r , it is important to verify the significance of these differences when manufacturing the microstrip antenna, when placing the patch in one or other face.

The antennas were manufactured using a commercial e-textile (Pure copper polyester taffeta fabric, Less EMF Inc., USA), with $R_s = 0.05 \Omega/\square$ and thickness equal to 0.080 mm, for the patch and the ground plane.

For the dielectric substrate, six diverse fabrics were considered, chosen among the previously characterized ones. The antennas were designed using the ϵ_r averaged value, shown on Table 4-3. For each substrate, two antennas were produced placing the patch on the face and on the reverse-side, respectively, as shown on Figure 4-12. The specification of these antennas is reported on Table 4-6.

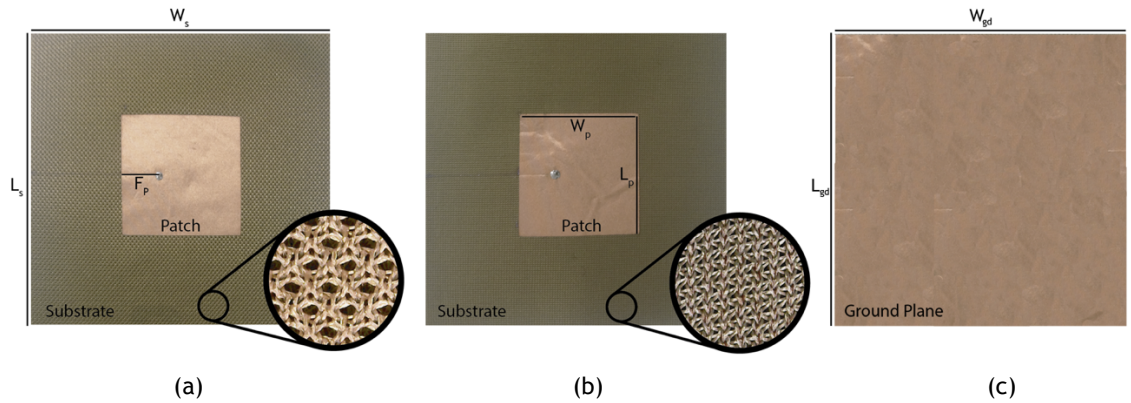


Figure 4-12 3D II textile antenna patch placed on (a) face side and (b) on reverse side of the fabric, and (c) rear of the antenna

Table 4-6 Dimensions of the textile antennas

Prototype	1	2	3	4	5	6
Sample	3D fabric I	3D fabric II	Neoprene I	Neoprene II	Fake Leather I	Fake Leather II
L_s - Substrate length (mm)	150	150	150	150	150	150
W_s - Substrate width (mm)	150	150	150	150	150	150
L_p - Patch length (mm)	57.8	57.5	51.0	53.4	53.3	53.0
W_p - Patch width (mm)	57.8	57.5	51.0	53.4	53.3	53.0
* F_p - Feed position (mm)	18.0	17.5	15.0	16.9	6.5	10.0

*Horizontal distance from the edge to the centre of the patch.

To ensure the geometric accuracy of the radiating element, a square patch was deliberately designed. All patches were cut with a laser cutting machine (LC6090C CCD, from Jinan G. Weike Science & Technology Co. Ltd., Jinan, China), on Department of Aerospace Science at Universidade da Beira Interior. The prototypes were produced by assembling the components with a thermal adhesive sheet I, and feed by SMA connector, with 50 Ω of impedance. After the construction, all prototypes were tested measuring the S_{11} , between 2 and 3 GHz, using a VNA, at Instituto de Telecomunicações - Aveiro. Figure 4-13 shows the comparison between the simulated and measured return loss.

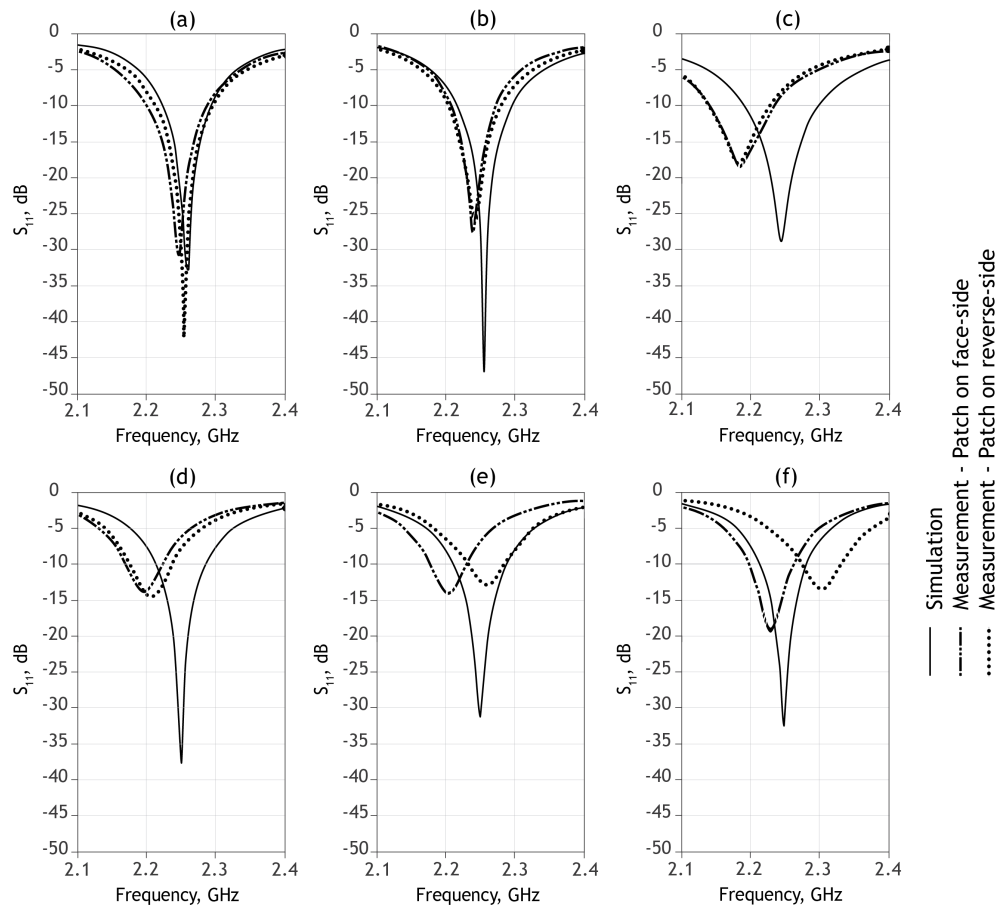


Figure 4-13 Simulated and measured S_{11} of textile antennas, (a) antenna 1 (b) antenna 2 (c) antenna 3 (d) antenna 4 (e) antenna 5 and (f) antenna 6

Table 4-7 Simulated and measured resonant frequencies

Prototype	Simulated resonant frequencies			Measured resonant frequencies					
				Patch on face-side			Patch on reverse-side		
	Initial frequency (GHz)	Central frequency (GHz)	Final frequency (GHz)	Initial frequency (GHz)	Central frequency (GHz)	Final frequency (GHz)	Initial frequency (GHz)	Central frequency (GHz)	Final frequency (GHz)
1	2.22	2.25	2.29	2.20	2.24	2.29	2.21	2.25	2.29
2	2.22	2.25	2.30	2.21	2.24	2.27	2.20	2.24	2.28
3	2.19	2.25	2.30	2.14	2.18	2.23	2.14	2.18	2.23
4	2.21	2.25	2.29	2.17	2.19	2.22	2.17	2.21	2.23
5	2.21	2.25	2.29	2.17	2.20	2.23	2.23	2.26	2.28
6	2.22	2.25	2.28	2.20	2.23	2.26	2.27	2.30	2.33

The prototype 1 has shown the best result resonating at the proposed frequency (2.25 GHz). Also, the measured bandwidth matches with the simulated (2.22 - 2.29 GHz) on both cases - when the patch is placed on the face (2.21 - 2.29 GHz) and on the reverse-side (2.20 - 2.29 GHz). Looking at the results of prototype 2, despite the small shift on the bandwidth, both measured antennas are resonating on 2.24 GHz, showing good agreement with the simulated values. It is important to notice that these small shifts may be caused by the manual manufacturing process.

Prototypes 3 and 4 have shown a larger shift on the resonant frequency. In fact, the neoprene is highly deformable and when heat was applied to assemble the conductive parts the neoprene has shrunk, reducing the thickness of both antennas in 1.5 mm. Despite this, the prototypes 3 and 4 still present an acceptable result, as one can see on Table 4-7, the resonate frequency still close to the simulated one.

The prototypes 5 and 6, whose dielectric substrates are fake leather fabrics, show the biggest difference of performances when positioning the patch in the face or reverse - side of the substrate. The resonant frequency of the prototypes whose patch was placed on the face-side, the less rough one, was shifted to a lower frequency (2.17 - 2.23 and 2.20 - 2.26 , respectively for antennas 5 and 6), proving that the substrate positioned this way presents a higher ϵ_r then the values considered on simulation, as expected. Similarly, in prototypes whose patch was placed in the reverse-side, the roughest one, the S_{11} was shifted to a higher frequency (2.23 - 2.28 and 2.27 - 2.33 GHz, respectively for antennas 5 and 6), that the substrate positioned this way has a lower ϵ_r than the value used on the simulation process. This is explained by the fact the bandwidth of the microstrip patch antenna is inversely proportional to the square root of the dielectric constant of the substrate [8], [32] .

In summary, prototypes 1, 2, 3 and 4, present a quite similar behaviour when placing the patch on the face or reverse- sides of the substrate. Indeed, as previously shown on Figure 4-6, the 3D and the neoprene fabrics used as substrate in these prototypes present low differences of the measured values of ϵ_r when placing the face or reverse-sides in contact to the resonator-board (less than 4.6%). On the contrary, prototypes 5 and 6 show different performance when placing the patch in one or other faces of the substrate as expected considering the higher

difference of values of ϵ_r (around 34%) measured placing the substrate in one and other positions, as previously presented on Figure 4-6. Despite these differences, prototypes 5 and 6 perform reasonably well, as the resonant frequency is close to the simulated one, as presented on Table 4-7.

Therefore, one may conclude that, despite the observed differences in results obtained for different positioning of the dielectric substrate, the average value of ϵ_r characterizes well the material and ensures a reliable performance of the textile antennas. Thus, the average value of ϵ_r measured by the resonator-based experimental technique is suitable to be considered for the design of microstrip patch antennas.

As one can see on Table 4-7, for all tested prototypes the measured resonance frequency was quite close to the simulated one. For samples presenting even larger structural differences between faces, the precision of the resonant frequency might be improved by adjusting the dielectric constant value by adding or subtracting the standard deviation value. Therefore, if the patch is placed over the roughest face, the ϵ_r is adjusted by subtracting the standard deviation to the measured averaged value of ϵ_r ; and the other way around.

4.5 Conclusions

The new Resonator-Based Experimental Technique was introduced to characterise several textile fabrics of interest. This method is based on the theory of resonance-perturbation, which consists in computing the electromagnetic parameters of the material under test, at a single frequency (2.25 GHz), by measuring the shift in the resonance frequency and in the value of the Q-factor of a microstrip patch antenna.

In general, the resonant methods yield higher accuracy than non-resonant ones and do not require complex sample preparation. Another advantage of the method is that it is only applied to the antenna substrate. Therefore, the procedure is not affected by arbitrary effects, such as, for example, the type of glue/adhesive sheet, the connector and the manufacturing technique of the probe, which can lead to the non-repeatability of the measurements and introduce variations in the final values.

The air-fibre mixture content on fabrics leads to a heterogeneous characterization process. In this work the studied materials showing higher bulk porosity also show lower dielectric constant values, which is due to the higher amount of air inside the fabric structure. The presented results corroborate that roughness correlates well with the number of pores on the surface: the textiles that present higher number of pores on the surface, also show higher \overline{SMD} values. Furthermore, when characterizing fabrics with the resonator-based experimental technique, placing the faces of higher \overline{SMD} in contact with the resonator board results in lower values of ϵ_r . Also, it is reported that the ϵ_r exponentially decreases with the superficial porosity increase.

Both of these facts occur because of the presence of the air on the surface, trapped in the superficial pores.

Besides the measured values of the dielectric constant differ when placing the face or reverse-sides in contact to the resonator board, and are thus influenced by the structure of the surface of the fabrics, this does not seem not be significant for the development of textile antennas. When designing microstrip patch antennas, the average of ϵ_r is well suited to ensure a reliable performance of the antenna.

5 Chapter

Textile Antenna for RF Energy Harvesting

The content of this chapter was partially published on IEEE International Symposium on Antennas and Propagation (2013), 24th IEEE Annual International Symposium on Personal, Indoor, and Mobile Radio Communications (2013), 7th International Symposium on Medical Information and Communication Technology (2014), 21th International Conference on Telecommunications (2104) and 5th STS Italia Conference A Matter of Design: Making Society through Science and Technology. The paper presented in this last conference was chosen as one of the ten best papers by young researchers and was awarded with a grant.

The Internet of Things (IoT) scenario is strongly related with the advance of the development of Wireless Body Sensor Network (WBSN) and Radio Frequency Identification (RFID) systems. Additionally, in the WBSN context, the integration of textile antennas for energy harvesting into smart clothing is a particularly interesting solution for a continuous wirelessly feed. Indeed, in the context of wearable devices the replacement of batteries is not easy to practice. This chapter describes the concept of the energy harvesting and presents a survey of textile antennas for RF energy harvesting. A dual-band printed monopole textile antenna for electromagnetic energy harvesting, operating at GSM 900 and DCS 1800 bands, is also proposed. The presented printed monopole antenna was developed in the framework of the PROENERGY PROJECT - Prototypes for Efficient Energy Self-Sustainable Wireless Sensor Networks, reference PTDC/EEA-TEL/122681/2010. The antenna aims to harvest energy to feed sensor nodes of a wearable health monitoring system. The gains of the antenna are around 1.8 dBi and 2.06 dBi allied with a radiation efficiency of 82% and 77.6% for the lowest and highest frequency bands, respectively.

5.1 Introduction

Nowadays, the socio-economic development and lifestyle trends indicate an increasing consumption of technological products and processes. The IoT scenario boosts the concept of wearable systems, as for instance health-monitoring systems ones [4], [103], [104]. The development of smart objects for IoT applications, include the capacity of identification of these objects in order to communicate and to interact with [4].

In this context, wearable technology has been addressed to make the person, mainly through his clothes, able to communicate with, and be part of, this technological network [105]. For instance, the wearable health-monitoring systems are not only endowed with sensing, processing, actuation and communication abilities, but also with energy harvesting and storage applications, emerging as a solution to the challenges of ubiquitous monitoring of people in several contexts.

The integration of WBSN on clothing puts the question about how to feed them. The batteries are an obvious choice, but they are bulky, require frequent replacement or recharging, and their short longevity is an ecological concern of current times. In this framework, the need for battery-free systems is increasing dramatically. Therefore, textile antennas for energy harvesting, emerge as a particularly interesting solution when the replacement of batteries is not easy to practice, such as in embedded systems.

Energy harvesting, or power scavenging, is the process of extracting energy from the surround environment and converting it into consumable electrical energy [106]. There are several sources of energy that can be harvested, such as acoustic, wind, solar, wave, mechanical and thermal.

Nowadays, RF energy is currently broadcasted from billions of radio transmitters and, thus, can be collected from the ambient environment or from dedicated sources [107]. Additionally, RF transmitters and receivers can be used when other potential intermittent energy scavenging sources (e.g., vibration and heat) are not available.

These radio waves present a widely available source of energy if effectively and efficiently harvested. Therefore, electromagnetic energy harvesting (EEH) holds a promising future for power supply of wearable low-power devices, offering a unique solution, enable for the implementation of a battery-free wireless sensing solution for 24 hours.

According to [108], there are two basic approaches, that will depend on the environmental condition, to harvest the electromagnetic energy:

1. Ambient source: in this approach, the harvester system uses the electromagnetic waves already present in the environment, such as solar [65], artificial light [109], or both [110], [111]. Also, can use the random RF sources, convenient from telecommunication systems, like Wi-Fi hotspots [112] and cell phone signals [113], [114], available specially in highly populated areas.
2. Dedicated source: in this approach, the harvester system is designed for a known RF source. This method can be more advantageous due to the previous knowledge about the RF source, that includes the frequency, directionality and polarization, as occur in the case of Wireless Power Transmission (WPT) [115].

This means, whereas in EEH the concept is harvesting the electromagnetic waves from the air, in WPT the electromagnetic beams are clearly directed in the direction of the device to power up, both of them working on far-field region [116].

Nevertheless, in the WPT context, there are other methods of transmitting energy wirelessly, working on near-field region, such as inductive coupling and magnetic resonance coupling [115], [117]. Also, it is possible to combine energy harvesting with wireless power transmission techniques, as presented in [108], [116]. This PhD Thesis will only focus on the electromagnetic energy harvesting, working on far-field region. The application, the range and field region from each wireless power transmission technique are described on Table 5-1.

Table 5-1 Wireless energy transfer techniques and applications

Wireless energy transfer technique	RF power transmission	Magnetic resonance coupling	Resonant inductive coupling
Range	Long - normally from several meters to kilometres (depend on the frequency and efficiency of the RF energy harvester)	Medium - from few centimetres to meters	Short - from few millimetres to centimetres
Field region	Far-field	Near-field	Near-field
Applications	Communication, sensor and powering - WSN and WBAN	Powering - cell phone charging, Plug-in Hybrid Electric Vehicle (PHEV) charging	Communication - Passive RFID tags, cell phone charging

Considering the recent advances in the wireless energy transfer technologies, not limited to the WSN and WBAN, in the near future, smart cities will be fully covered by small stations of dedicated sources, to wirelessly power wearable devices, such as augmented reality glasses and wellness devices [118].

5.2 Review of Textile Antennas for RF Energy Harvesting

The state-of-art of textile antennas for RF energy harvesting was based in search criteria that included 6 combinations of index terms, presented on Table 5-2, inquiring three main databases:

1. Scopus®: The largest interdisciplinary database across science, mathematics, technology, engineering, health and medicine, social science and humanities. The database includes 22.000+ peer-reviewed journals, 8 million conference papers, 28 million patents, summarising 67+ million scientific documents;
2. ISI - Web of Knowledge®: The oldest multidisciplinary scientific database, covering science, arts, humanities and 256+ disciplines. 160.000+ conference proceedings, 12.00+ journal, 50.00+ books, totalising 90+ million;
3. IEEE Xplore®: The Institute of Electrical and Electronics Engineers (IEEE) database, mainly covering materials from the IEEE and the Institution of Engineering Technology (IET), focus on computer science, electrical and electronics engineering fields. 195+ peer-reviewed journals, 1.000+ conference proceedings, 6.200+ technical standards and approximately 2.400 eBooks, providing more than 4 million scientific records.

The search was restricted to the combination of the index terms in the title, abstract and keywords, of the retrieved papers. Further, the search was limited to journal, conference and review papers, available until May of 2017. The search was generating 61, 43 and 71 results on Scopus®, ISI® and IEEE Xplore®, respectively. After excluding the papers that use rigid antennas or rigid materials, and eliminating the repeated works, a group of 20 papers remained. In this group, only papers using textile materials for both, conductive and dielectric parts and used for far-field RF energy harvesting were considered. In the following section, 12 works will be briefly described. The others 8 papers are related to the work developed in the framework of PROENERGY PROJECT - Prototypes for Efficient Energy Self-Sustainable Wireless Sensor Networks, reference PTDC/EEA-TEL/122681/2010. Therefore, will be partially described on the next Subsections and on Chapters 6 and 7. Table 5-2 presents the index terms used in the search and the final results for each database.

Table 5-2 Index terms and results of the search

	Database	Index terms					
		Textile antenna RF energy harvesting	Textile antenna electromagnetic energy harvesting	Textile antenna electromagnetic wireless power transmission	Textile antenna RF wireless power transmission	Wearable antenna electromagnetic energy harvesting	Wearable antenna RF energy harvesting
Results	Scopus®	[79], [100], [112], [113], [119]-[126]	[113], [114], [123], [125], [127], [128]	[123]	[123]	[113], [114], [123], [125], [127]-[130]	[79], [113], [120]-[126], [130], [131]
	ISI®	[79], [100], [112], [115], [119], [121]-[123], [126]	[114], [123], [127], [128]	[123]	[123]	[114], [123], [127], [128], [130]	[120]-[123], [126], [130], [131]
	IEEE Xplore®	[79], [100], [112], [113], [119]-[124], [126], [131]	[79], [100], [109], [113], [114], [122], [123], [132]	[79], [123]	[79], [123], [124], [131], [133]	[79], [109], [113], [114], [123], [130], [132]	[79], [112], [113], [119]-[124], [126], [130], [131]

Besides EEH and WPT, using rigid antennas, are nowadays hot research topics [106], [115], [117], [134], the development of textile antennas for wearable systems is a very new subject, that has emerged only in the past decade.

Some harvester systems that convert the received RF energy from ambient sources into DC power were called rectifying antennas, it is also known as rectennas. As explained in [135], the antenna performs the transduction of the RF energy into an electrical AC signal. A matching network is used to transfer a maximum AC power to the rectifier. Then, the rectifier converts the AC signal into a DC voltage, charging a load. In 2010, [130] Constanzo *et al.* presented the

first scheme of a triple-band ring textile rectenna for RF energy harvesting, operating at GSM 900, GSM 1800, and Wi-Fi frequencies.

This antenna was developed with a multilayer configuration and for its conductive parts the Global EMC shielding fabric with sheet resistance of $0.02 \Omega/\square$ was used. An unspecified fabric with $\epsilon_r = 1.23$ was used as a substrate support of the antenna. The Kapton® fabric with $\epsilon_r = 3.4$, $\tan\delta = 0.002$ and 1 mm of thickness, was used as the dielectric substrate. The predicted antenna efficiencies of this antenna are 61% at 900 MHz, 54% at 1.750 MHz, and 85% at 2.450 MHz. The integration of this triple-band ring textile rectenna, in a fully-autonomous RF energy harvesting, was further presented in [122], [124]. Later, the authors present the first scheme of a jacket, integrating this antenna into a harvester circuit [113], [125], [129].

In 2013, a circular patch slotted textile antenna was proposed for RF energy harvesting, operating at 2.45 GHz [100]. A denim fabric, with 1.6 mm of thickness, $\epsilon_r = 1.7$ and $\tan\delta = 0.085$, was used as dielectric substrate. This study investigated the performance of the antenna under bending conditions. The authors observed that when the antenna have small bending radius, major changes on the gain and radiation pattern of the antenna will occur. For example, in the normal state (no bending applied) the antenna shows a gain of 7.34 dBi, while under bending conditions ($R = 20\text{mm}$), the maximum gain obtained was 7.10 dBi.

Later, in 2014, Tallos *et al.* presented the draft of a coat with multiple body-worn embroidered textile antennas, to be integrated into a harvester system operating in the 2.45 GHz WLAN band [112]. This study has shown that body-worn textile antennas with rectifying circuits can supply enough power to feed low-power sensors.

In 2015, Adami *et al.* presented a textile patch antenna and a rectenna for 2.45 GHz RF power transfer and harvesting, to feed low-power sensors on clothing [79]. In both cases, a fabric composed of polyester and cotton (35% PES 65% CO) was used as dielectric substrate, having $\epsilon_r = 3.23$ and $\tan\delta = 0.06$. For the conductive parts, silver ink - Dupont 500 was applied, through the screen printing technique. Both, patch antenna and rectenna, were replicated using RF-4 as dielectric substrate, in order to compare the efficiency.

The textile patch antenna showed 11% of radiation efficiency against 30% efficiency of antenna made of RF-4. The authors indicate that the difference on the radiation efficiency is correlated to the dielectric losses of the substrates, as the fabric presents $\tan\delta = 0.06$ and RF-4 presents $\tan\delta = 0.0175$. Furthermore, the rectennas were tested varying the power source. For the highest power source used, the textile rectenna was capable to generate 100 μW . In comparison, the RF-4 rectenna generated 230 μW , being this difference coherent with the discrepancy in the radiation efficiency previously measured.

In 2016, a broadband spiral textile rectenna was presented and integrated on a RF energy harvesting system [119]. The designed system operates over a frequency range from 0.9 GHz to 4 GHz. In order to improve results, four different combinations of materials for the dielectric substrate and conductive parts, were proposed: (A) felt ($\epsilon_r = 1.14$ and $h = 5 \text{ mm}$) and Shieldit

Super® ($\sigma = 1.96 \times 10^5 \text{ S/m}$), (B) fleece ($\epsilon_r = 1.17$ and $h = 3 \text{ mm}$) and Shieldit Super® ($\sigma = 1.96 \times 10^5 \text{ S/m}$), (C) felt ($\epsilon_r = 1.14$ and $h = 5 \text{ mm}$) and stainless steel conductive yarns ($\sigma = 3.88 \times 10^4 \text{ S/m}$). Also, a rigid antenna (C) FR-4 ($\epsilon_r = 4.3$ and $h = 1.5 \text{ mm}$) and copper ($\sigma = 5.96 \times 10^7 \text{ S/m}$), was made in order to be the reference antenna to which compare the efficiency of the textile ones.

All antennas worked well, resonating at frequencies very close to the simulated ones. Moreover, antenna A shows the best result. Antenna B has a small shift in the resonance frequency due to the presence of air gaps between the fleece layer, while antenna C shows the higher shift because the improper attachment of the conductive yarns. Also, the measurements show that the spiral textile antenna A substrate had a higher fractional bandwidth in comparison with B. The harvester system was tested in two different indoor and outdoor scenarios, measuring 1.5 V and 0.5 V, respectively. The efficiency of the wearable system was around 30%.

Recently, in 2017, Ivši *et al.* have shown a spiral wideband textile antenna for RF energy harvesting, operating between 470 MHz up to 8 GHz, and a rectifier circuit to wirelessly feed on-body sensors [132]. To ensure the flexibility of the antenna, aiming the integration into cloth, the spiral antenna was embroidered with conductive yarns, using a denim fabric as dielectric substrate. This antenna was capable to cover all frequency ranges of interest - digital television, GSM and Wi-Fi. The measured gain was 1 dBi.

5.3 Spectrum Opportunities

The advance of technology stimulates the growing number of wireless transmitters, especially in highly populated urban areas, naturally increasing the power density of available RF in the environment. In order to identify the most promising frequencies for harvesting, measurements of the electromagnetic spectrum availability from 350 MHz to 3 GHz were performed, in the scope of the PROENERGY PROJECT - PTDC/EEA-TEL/122681/2010 and as reported in [121], [123].

The field trials were performed using the NARDA- SMR spectrum analyser with measuring antenna, and the Signal Hound spectrum analyser. By analysing the power density measurements in 40 different indoor/outdoor locations in Covilhã and Lisbon, was possible to identify the best opportunities that may be considered to conceive wideband or multiband antennas for electromagnetic energy harvesting. Figure 5-1 presents the locations of the measurements performed in Covilhã, and the average result of all measurements results is depicted on Figure 5-2.

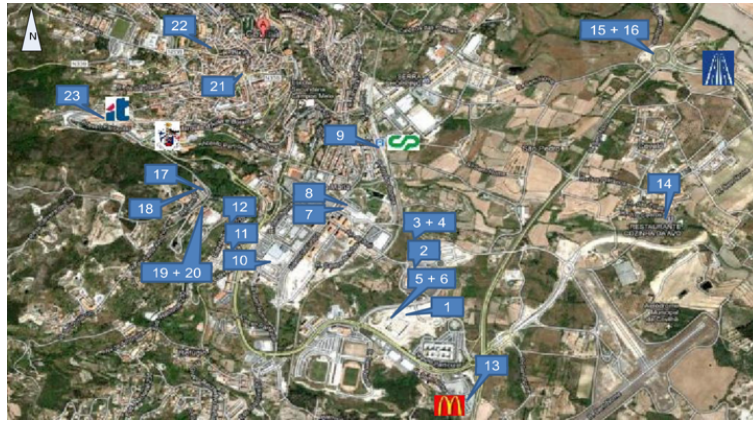


Figure 5-1 Measurements locations in Covilhã

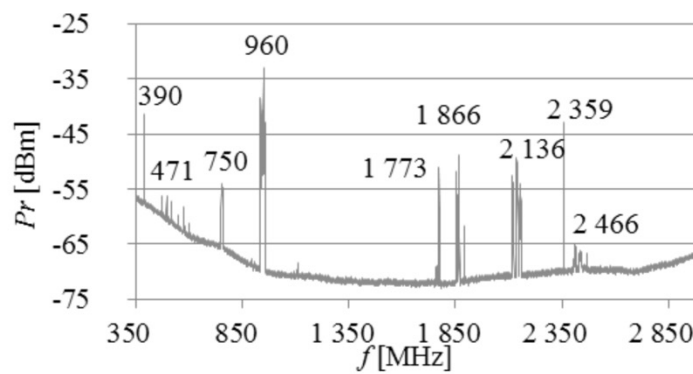


Figure 5-2 Average received power for all measurements

Observing the Figure 5-2, the sets of frequency bands with more available energy are:

- 390 to 392 MHz - Emergency broadcast stations;
- 750 to 759 MHz - Television broadcast stations;
- 934 to 960 MHz - GSM 900;
- 1.763 to 1.773 MHz - GSM 1800;
- 1.854 to 1.892 MHz - GSM 1800;
- 2.115 to 2.160 MHz - Universal Mobile Telecommunication System (UMTS);
- 2.359 MHz - Amateur, Services Ancillary to Broadcast / Services Ancillary to Programme (SAP/SAB) applications;
- 2.404 to 2.468 MHz - Wi-Fi.

5.4 Printed Monopole Textile Antenna

Based on the previous analysis, it is possible to conclude that the best set of frequency bands for energy harvesting is the mobile phone bands. Therefore, a dual-band printed monopole textile antenna to harvest in the GSM 900 and DCS 1800 bands was proposed.

The simulation of this antenna was made using CST Microwave Studio, using textile materials commercially available. For the dielectric substrate, a synthetic fabric (100% high tenacity PA 6.6), Cordura® (B. W. Wernerfelt Group, Søborg, Denmark), was chosen, as it is geometrically stable, presenting very low mechanical deformation. It also has low regain and minimizes the effect of the moisture absorption on lowering the resonance frequency of the antenna [128]. For the conductive parts, Zelt® (Less EMF Inc., Latham, USA) was considered. Table 5-3 describes the properties of the used textile materials.

Table 5-3 Textile materials used in the development of printed monopole

Dielectric Material						
Fabric	Mass per unit surface (g/m ²)	Composition	Finishing	Thickness (mm)	ϵ_r	$\tan\delta$
Cordura®	280	100% PA 6.6	Polyurethane coated	0.5	1.9	0.0098
Conductive Material						
Fabric	Mass per unit surface (g/m ²)	Composition	Finishing	Thickness (mm)	Conductivity (S/m)	
Zelt®	55.87	100% PA	Copper and tin plated	0.06	1.75105	

The proposed design of the antenna is presented on Figure 5-3 and its dimensions are given on Table 5-4. Also, Figure 5-3 shows the radiation pattern based on numerical simulations.

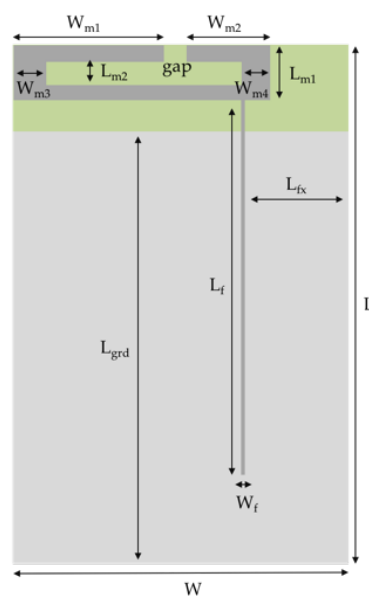


Figure 5-3 Design of dual-band printed monopole textile antenna

Table 5-4 Dimensions of the textile antenna

Parameter	Dimensions (mm)
$L, L_{\text{gnd}}, L_f, L_{fx}$	120, 100, 78, 30
$L_{m1}, L_{m2}, \text{gap}, W$	12, 5, 3.1, 80
$W_f, W_{m1}, W_{m2}, W_{m3}, W_{m4}$	1.5, 31, 21, 8, 4

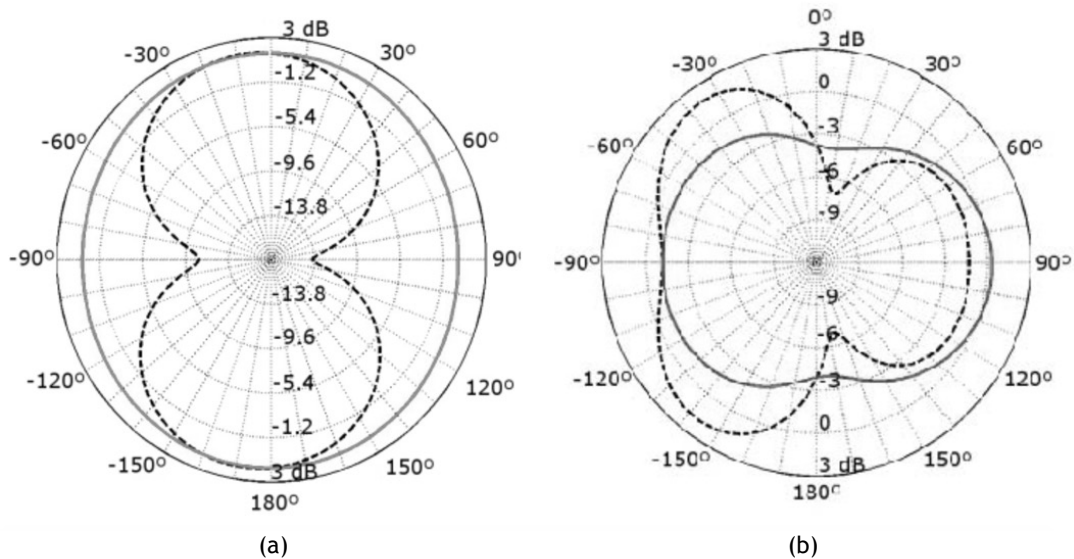


Figure 5-4 Simulated radiation pattern for the proposed printed monopole, YZ plane (dashed) and XZ plane (solid), for (a) 900 MHz and for (b) 1800 MHz

As one can see on Figure 5-4 radiation pattern of this antenna is clearly omnidirectional. An omnidirectional radiation, was chosen as the privileged direction of signal reception is unknown. The obtained gain, from numerical simulation, for the dual band antenna, is about 1.8 dBi and 2.06 dBi allied with 82% and 77.6% radiation efficiencies for the GSM 900 and DCS 1800 frequency bands, respectively.

Further, the printed monopole textile antenna was produced assembling the components with a thermal adhesive sheet (Fixorete Losango, JAU Têxteis, Serzedo, Portugal). Figure 5-3 shows the textile antenna after assemblage. The antenna is fed by a SMA connector, with 50 Ω of impedance. The return loss, presented in Figure 5-6, was measured using VNA at Instituto de Telecomunicações - Aveiro.

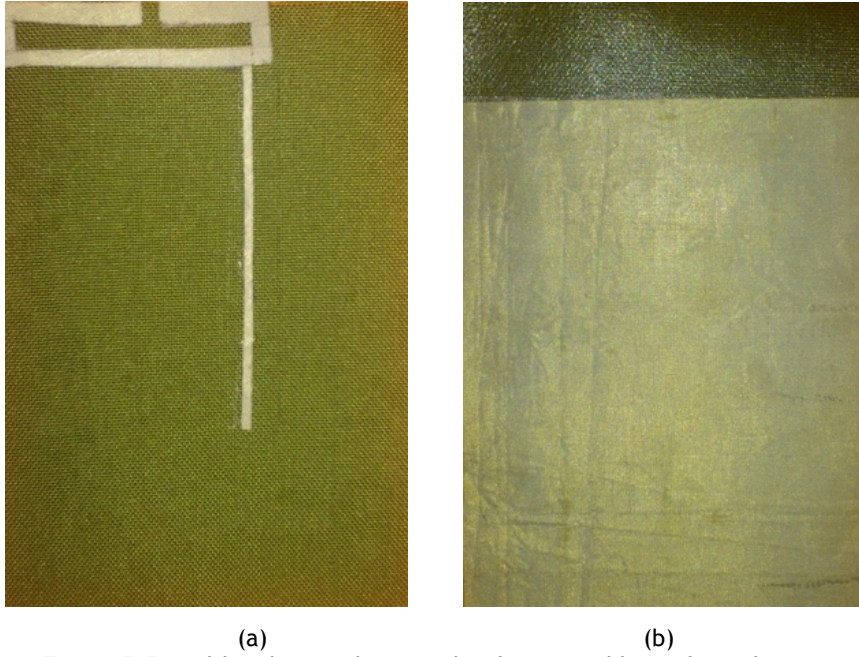


Figure 5-5 Dual-band printed monopole after assembly (a) front (b) rear

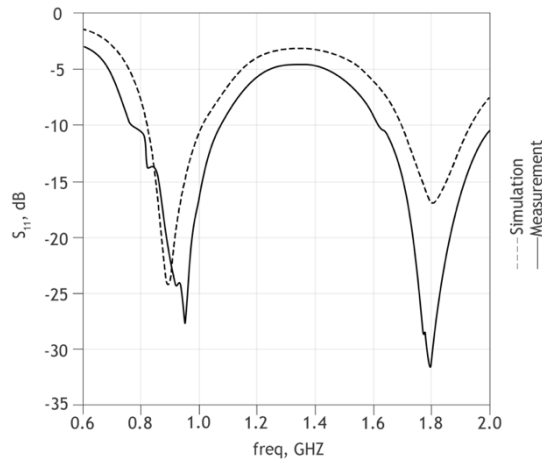


Figure 5-6 Simulated and measured S_{11} of the dual-band printed monopole

One may observe that this textile antenna presents an operating frequency range capable of completely covering the GSM 900 (880-960 MHz) and the DCS 1800 (1710-1880 MHz). Also, observing the S_{11} on Figure 5-6 some small differences between the simulated and the measured values are expected due to imprecisions related with the manual manufacturing process.

As presented on Subsection 5.1, it is possible to harvest RF electromagnetic energy from multiple sources. References [121], [126], [131] presents the fully integration of this printed monopole textile antenna in a harvester system. In summary, a five-stage Dickson voltage multiplier enables perpetual operation of an IRIS mote by a received RF power larger than 1 dBm. In addition, a TX91501 Powercast® RF transmitter was applied as dedicated source, providing a predictable and reliable RF energy power source to wirelessly charge battery-based

systems. With this system it was possible to charge sensor nodes up to 3 meters from the dedicated source. Figure 5-7 shows the printed monopole textile antenna connected to the 5-stage Dickson during the tests. This PhD Thesis is focussed on the development of textile antennas, but more information about the integration of this antenna on the harvester system and on power supply of sensors nodes for health monitoring can be found in references reporting complementary work made on the scope of PROENERGY PROJECT [121], [126], [131].

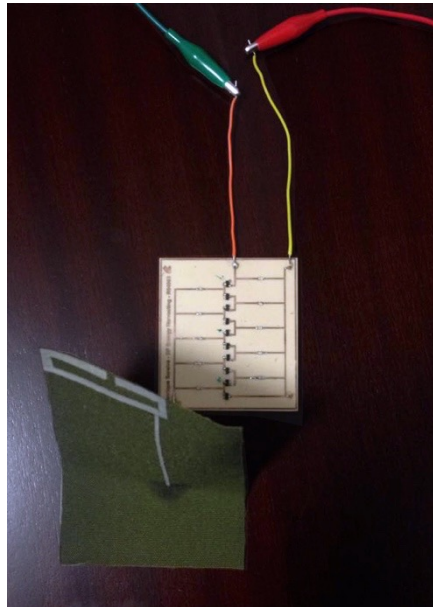


Figure 5-7 Printed monopole textile antenna connected to a 5-stage Dickson voltage multiplier

5.5 Conclusions

The advance of wearable technology and the miniaturization of the electronic devices are boosting the development of smart garments, for instance able to provide information about the state of user's health and environment.

Energy harvesting can be a solution for powering battery-free devices. This technology is considered essential for the industry in several areas of expertise, including medical, consumer electronics, fashion, automotive, and industrial control process. In the context of wearable systems, textile antennas are emerging as the solution for feeding low-power devices and/or Wireless Sensors Body Networks, where the change of batteries is not easy to perform.

Besides, the electromagnetic energy harvesting and the wireless power transmission are trendy research topics. A wearable systems using textile antennas is a very new subject, having emerged only in the past decade. For this reason, the state-of-the-art of textile antennas for RF energy harvesting is short. Also, the usage of electronic devices increases the availability of RF sources on the environment. Indeed, after field trials at Covilhã and Lisbon, two different cities in Portugal, the most available frequencies to harvest are from the emergency and television broadcasts, Amateur and GSM bands.

This Chapter has also presented a dual-band printed monopole textile antenna which was tested on the scope of the PROENERGY PROJECT - PTDC/EEA-TEL/122681/2010. It can be able to charge low-power devices, as well as extending the lifetime of tiny devices by using electromagnetic energy harvested at GSM 900 and DSC 1800. The printed monopole textile antenna was made using commercially available textiles. It has shown good behaviour on stand-alone measurements. The gains of the antenna are around 1.8 dBi and 2.06 dBi allied with a radiation efficiency of 82% and 77.6% for the lowest and highest frequency bands, respectively. After its integration on the harvester system, was possible to charge the nodes of WSN up to 3 meters from the dedicated source.

6 Chapter

Influence of the Manufacturing Techniques on the S_{11} Parameter of Printed Textile Antennas

The content of this Chapter was partially published on Sensors Journal (2016), 10th European Conference on Antennas and Propagation (2016), Electronic Conference on Sensors Applications (2016) and IEEE International Microwave Workshop Series on Advanced Materials and Process (2017). In this last conference, the paper was received an honourable mention in the student paper competition.

Beyond the selection of the textile materials to design an antenna, the process of manufacturing the antenna is also crucial, due to the very high deformability of the materials. In this Chapter, several techniques are tested through preliminary tests, to identify promising techniques and to discard inefficient ones, such as the gluing technique. Then, the influence of several parameters of the manufacturing techniques on the performance of the antenna are analysed, such as the use of steam during lamination, the type of adhesive sheet, the orientation of the conductive elements and others. Further, seven prototypes of the printed monopole textile antenna were manufactured by laminating and embroidering techniques. The measurement of sheet resistance has shown that the presence of the adhesive sheet used on the laminating process may reduce the conductivity of the conductive materials. Despite that, when measuring the return loss of printed monopole antennas produced by lamination, the results show the antennas have a good performance. The results also show that the orientation of the conductive fabric does not influence the performance of the antennas. However, when testing embroidered antennas, the results show that the direction and number of the stitches in the embroidery may influence the performance of the antenna.

6.1 Introduction

Beyond choosing the textile materials, the construction technique of the antenna is also crucial because the textile materials are highly deformable. The geometrical dimensions of the conductive patch and of the dielectric substrate should remain stable when connecting them, as the mechanical stabilization of both materials is essential to preserve the desired characteristics of the antenna. The geometrical precision of the conductive patch is also

critical, especially when the antenna has thin details, as the one proposed in 5.4.

As previously reviewed in Chapter 2, several techniques have been used to manufacture the textile antennas, using commercial available materials and low-cost procedures. The next Subsections describe and analyse several manufacturing techniques, aiming to improve the performance of the printed monopole textile antenna presented in previous Chapter 5.

6.2 Preliminary Results: Miscellaneous Techniques

In order to select the best procedures for manufacturing textile antennas, a textile antenna was designed to be reference and undergo preliminary tests. It is a microstrip patch antenna for 2.45 GHz, produced using the materials described on Table 5-3. It has a rectangular shape to guarantee the mechanical stability during the tests. The antenna was designed to be fed by a microstrip line, using a SMA connector, with $50\ \Omega$ of impedance. The design and dimensions of the microstrip patch antenna are described in Figure 6-1 and Table 6-1, respectively.

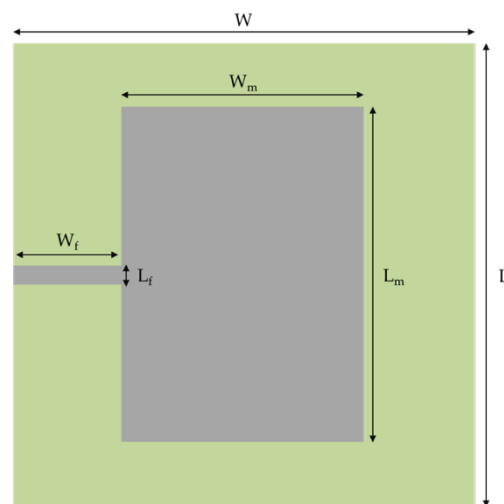


Figure 6-1 Design of the microstrip patch antenna used to test several manufacturing techniques

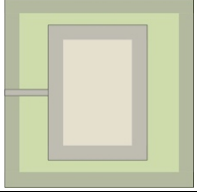
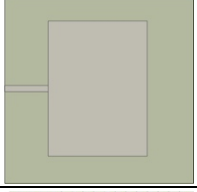
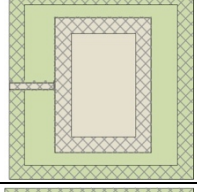
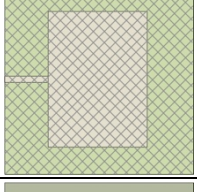
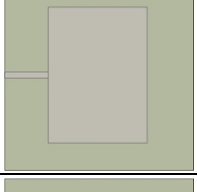
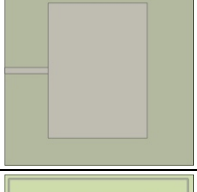
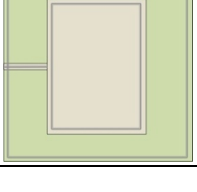
Table 6-1 Dimensions of the microstrip patch antenna

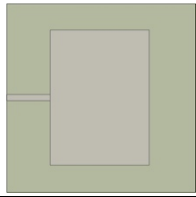
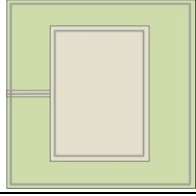
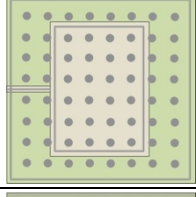
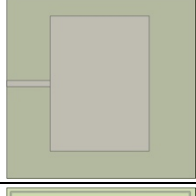
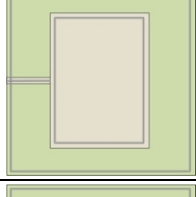
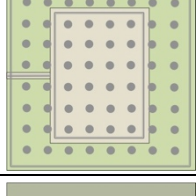
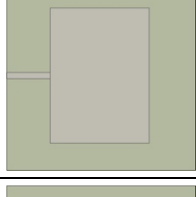
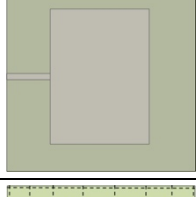
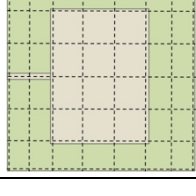
Parameter	Dimensions (mm)
W, L	80, 80
W_m, L_m	41.5, 58
W_f, L_f	19.25, 2.3

Sixteen prototypes of the microstrip patch antenna were produced, as described in Table 6-2, using four manufacturing techniques: laminating, sewing, gluing and coating. Through the laminating technique, three adhesive sheets were tested, varying in terms of porosity, thickness and composition. Images of two of these thermal adhesive sheets are shown below in

Table 6.4. The glued antennas were produced using three different glues available on the market, being one specific for textiles. Considering the high risk of short cuts between the patch and the ground plane, as reported on 2.2, one sewed antenna was made, sewing with non-conductive thread. Also, two antennas were fabricated through the coating process. In one of them, the prototype 14, the assembly is completely wrapped by the coat eliminating the material interface between the substrate and the conductive parts. Table 6-2 describes the prototypes and the materials used on the assembly process.

Table 6-2 Description of the manufacturing techniques used to produce the microstrip patch antennas

Manufacturing technique	Prototype	Description of assembly process	Material	Schema
Laminating technique	1	Adhesive sheet only on the edges of the conductive parts, applied by the ironing operation.	Fixorete Contínuo (JAU Têxteis, Portugal), $h = 0.01$ mm, 100% PA	
	2	Adhesive sheet covering all surface of the conductive parts, applied by the ironing operation.	Fixorete Contínuo (JAU Têxteis, Portugal), $h = 0.01$ mm, 100% PA	
	3	Adhesive sheet only on the edges of the conductive parts, applied by the ironing operation.	Fixorete Losango (JAU Têxteis, Portugal), $h = 0.01$ mm, 100% PA	
	4	Adhesive sheet covering all surface of the conductive parts, applied by the ironing operation.	Fixorete Losango (JAU Têxteis, Portugal), $h = 0.01$ mm, 100% PA	
	5	Adhesive sheet covering all surface of the conductive parts, applied by the ironing operation.	Fast2Fuse (C&T Publishing, USA), $h = 0.1$ mm, 100% PES	
Gluing technique	6	Textile glue applied covering all surface of the conductive parts.	Super Cola Pano (Acrilex, Brazil)	
	7	Textile glue - Super Cola Pano (Acrilex, Brazil) applied only on the edges of the conductive parts.	Super Cola Pano (Acrilex, Brazil)	

Manufacturing technique	Prototype	Description of assembly process	Material	Schema
	8	Super Glue applied covering all surface of the conductive parts.	Super Glue 3 Loctite (Henkel AG & Co., Germany)	
	9	Super Glue applied only on the edges of the conductive parts.	Super Glue 3 Loctite (Henkel AG & Co., Germany)	
	10	Super Glue drops applied on every 1 cm, covering all surface area of the conductive parts. To ensure the stability of the antenna, the glue was also continuously applied on the edges of the conductive parts.	Super Glue 3 Loctite (Henkel AG & Co., Germany)	
	11	Permanent glue applied covering all surface of the conductive parts.	UHU Permanent Adhesive (UHU GmbH & Co., Germany)	
	12	Permanent glue applied only on the edges of the conductive parts.	UHU Permanent Adhesive (UHU GmbH & Co., Germany)	
	13	Permanent glue drops applied on every 1 cm, covering all surface area of the conductive parts. To ensure the stability of the antenna, the glue was also continuously applied on the edges of the conductive parts.	UHU Permanent Adhesive (UHU GmbH & Co., Germany)	
Coating technique	14	PU coat applied completely covering both sides of the antenna. Any glue or adhesive was applied between the conductive and dielectric layers.	PU coating prepared at Dyeing Laboratory of Universidade da Beira Interior	
	15	PU coat applied only between the conductive and dielectric layers.	PU coating prepared at Dyeing Laboratory of Universidade da Beira Interior	
Sewing technique	16	Grid pattern sewed on Juki DU-1181N industrial sewing machine, with non-conductive thread using straight stitch (5 stitches per cm).	Coat Astra thread (Coat Industrial, Scotland), 100% PES	

The S_{11} of all prototypes was measured with a VNA at Instituto de Telecomunicações - Aveiro and the results are shown on Figure 6-2. The coating process has severely affected the electrical properties of the conductive fabric, decreasing its conductivity. For this reason, the antennas produced with this technique did not result in viable antennas and the results of prototypes 14 and 15 were eliminated, not being presented on Figure 6-2.

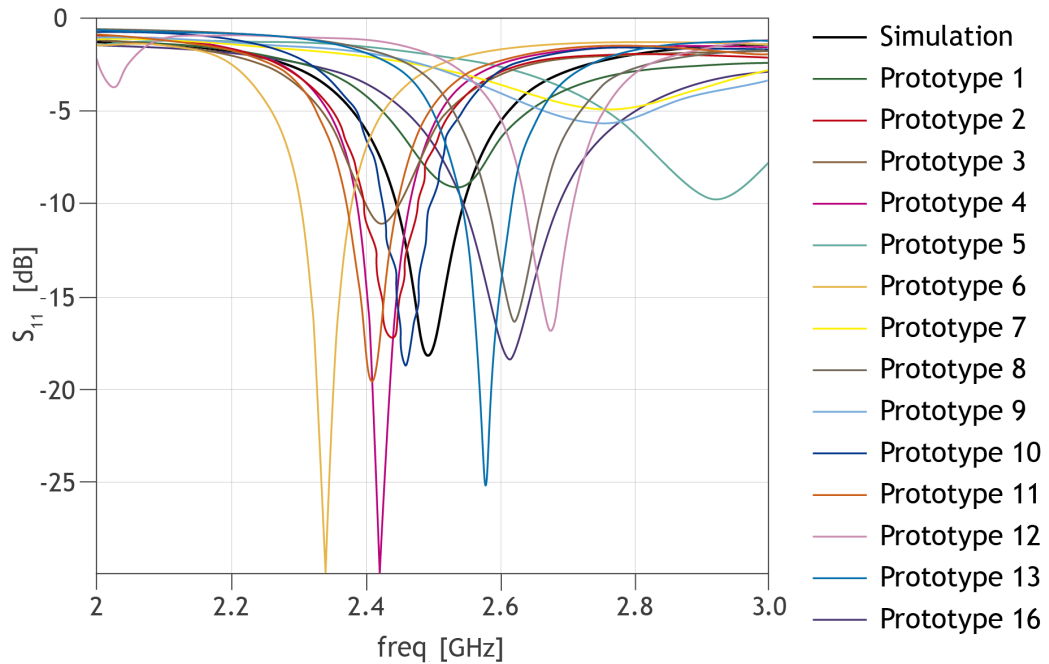


Figure 6-2 S_{11} of the microstrip patch antennas

Taking in account the inaccuracies due to the manual process, which cause small shifts on the resonance frequency, the prototypes 2, 4, 8, 10, 11, 13 and 16 show good results as one can see on Figure 6-2. The prototype 10 presents the best result, nearly matching the simulated S_{11} .

Focussing on the laminating technique, it is important to report that the prototypes 1, 2, 3 and 4 were assembly ironing during 12 seconds (6 seconds for each conductive layer). However, due the higher thickness of the Fast2Fuse adhesive sheet, the prototype 5 was maintained under heating press for 20 seconds. This has caused a shrinkage of the dielectric substrate, resulting in less five millimetres on L dimension and less two millimetres on W dimension. Also, such thick interlining predictably changes the permittivity value of the substrate as add an interlayer between it and the conductive layer. The association of these both phenomena contributes to the mismatch of prototype 5, whose resonance frequency is significantly different from the simulated one.

The sewed antenna, prototype 16, has presented a satisfactory result. Also, the grid pattern of seams contributes to create air gaps between the substrate and conductive parts, decreasing the permittivity value of the Cordura® as more air is trapped approaching thus the permittivity

to 1. This way, the resonance frequency of the prototype 16 was shifted to a higher frequency, as one can observe in Figure 6-2. Air gaps between substrate and conductive layers are also clearly and visually observed on prototypes 1, 3, 9 and 12. As consequence the resonance frequency of these antennas are also shifted to higher values than the simulated one, as shown in Figure 6-2.

Unexpectedly, the glued prototypes show the worse results. Moreover, the process to apply a thin and smooth layer of glue is difficult to practice in draws of fine details as the one of the printed monopole textile antenna, proposed in 5.4. Likewise, despite the satisfactory results of the sewed antennas, it is not possible to use the sewing technique to reproduce the printed monopole textile antenna, due to its fine details. For these reasons, in the next Subsection, among the techniques preliminarily considered, only the laminating manufacturing technique will be deeper analysed.

6.3 Laminating Manufacturing Technique

As briefly surveyed on Chapter 2, the laminating process is the most common manufacturing technique used to assembly printed textile antennas. It consists in assembling the components with the thermal adhesive sheet, through the ironing operation. The geometrical dimensions of the components should remain stable to preserve the desired characteristics of the antenna.

Moreover, despite the adhesive remains at the interface of the material, in [29] authors affirm the adhesive layer introduces extra losses in the substrate and the conductivity may thus decrease after the laminating process, lowering the efficiency of the textile antenna. Moreover, the usage of thermal adhesive layers may also influence the conductivity properties of the conductive textile elements of the antenna, which is then important to analyse.

6.3.1 Influence of using Thermal Adhesive Sheet on the Sheet Resistance of Conductive Fabrics

In order to verify the influence of the adhesive sheet used in the laminating process on the conductivity of the materials and thus on the performance of the textile antennas, measurements of sheet resistance were performed, following the ASTM standard F 1896 - Test Method for Determine the Electrical Resistivity of a Printed Conductive Material [47].

In this standard process, the resistance is measured with an ohmmeter, i.e. a resistance measuring electronic device. In this case, a sourcemeter Keithley 2602A was used. To calculate the sheet resistance, the measured value of resistance is divided by the number of squares contained in the probe, given by the length divided by the width of the probe. The sheet resistance is thus given in Ω/\square . Figure 6-3 illustrates the set-up of the resistance measurement tests. The laminated probes were prepared using a Press MTA2012 FESPA, model SWH-2. The

conductive materials under test (MUT) and the dimensions of the testing probes are described in Table 6-3. Table 6-4 presents the characteristics of the adhesive sheets used in lamination.

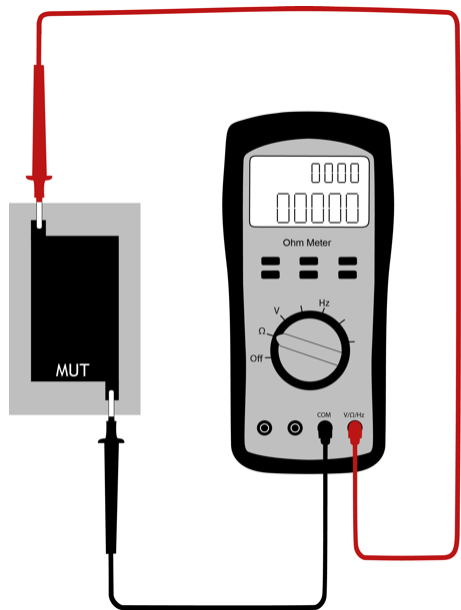
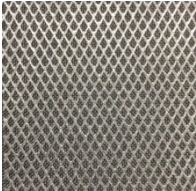
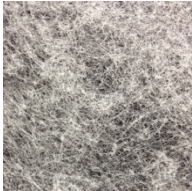


Figure 6-3 Set-up of resistance measurement test

Table 6-3 Conductive materials under test

Conductive material	Composition	Thickness (mm)	Sheet resistance given by the manufacturer (Ω/\square)	Dimensions of the probe (mm)	
				Length (L)	Width (W)
Zelt [®]	100% PA - Copper and tin plated	0.06	<0.09	60	30
Pure copper polyester taffeta fabric (similar to Electron [®])	100% PES - Copper plated	0.08	<0.05		

Table 6-4 Characteristics of the thermal adhesive sheets used on the lamination process

Adhesive sheet	I	II
Type	Fixorete Losango <i>Grid network</i>	Fixorete Contínuo <i>Continuous web</i>
Image		
Composition	100% PA	
Thickness (mm)	0.01	
Mass per unit surface (g/m ²)	280	210

The resistance measurements were performed under controlled environmental conditions, 24°C and 35% relative humidity, at the Printed Electronics Lab of EURECAT Technologic Centre, in Mataró, Spain. The planning of experiments consisted in testing two conductive materials, Zelt® and Pure copper taffeta fabric, and analyse the influence of three main variables of the lamination process that are: usage of steam, type of adhesive layer and superficial features of the laminated substrate. Therefore, the conductive textile materials were tested in the following conditions:

- A. stand-alone;
- B. stand-alone after wet heat treatment, of 12 seconds on 200°C with steam;
- C. with adhesive sheet type I (grid network) and II (continuous web), after applying the adhesive sheets at 200°C, under 10 bar, during 6 seconds, without steam;
- D. laminated to three different textile substrates, the 3D spacer fabric I and II, and Cordura II, described on previous Table 4-3. For each conductive material, six laminated probes were prepared, placing the conductive MUT in each of the two surfaces, face and reverse side, of all three substrates, and laminating at 200°C, under 10 bar, for 12 sec., without steam. The following Figure 6-4 schematises the laminated probes prepared per substrate, placing the MUT over the two faces, the rougher and smother ones.

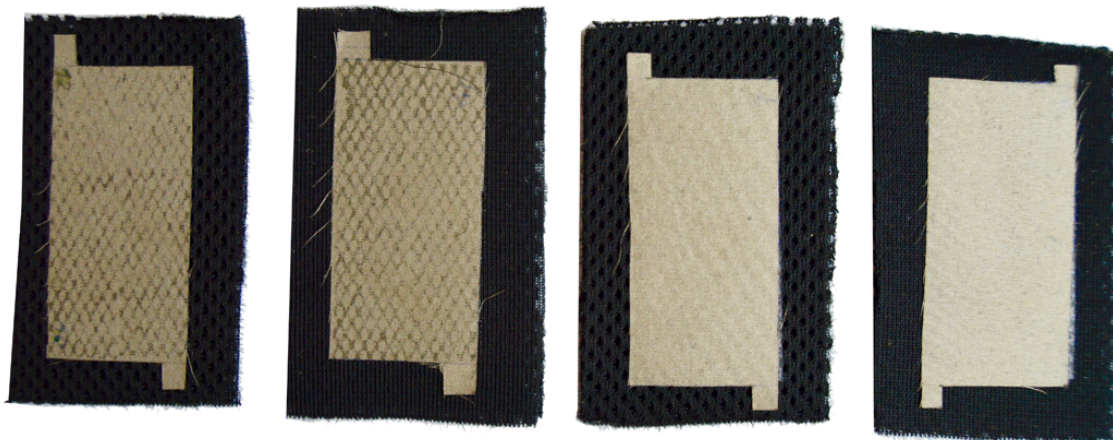


Figure 6-4 Example of the group D of probes, for 3D I substrate.

For all MUT of groups A, B and C, three probes were prepared and tested three times. Figure 6-5 and Table 6-5 present the averaged values of these 9 measurements and their standard deviation.

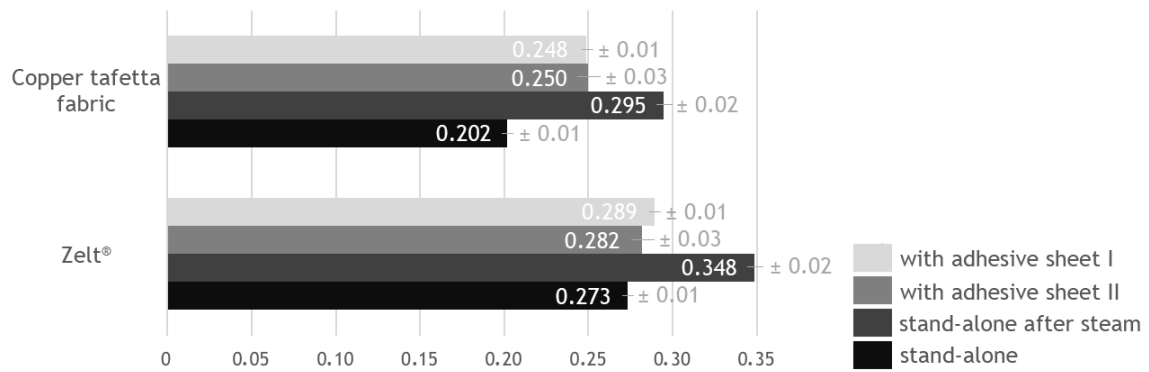


Figure 6-5 Results of sheet resistance measurements ($[\Omega/\square]$, $n = 9$)

As one can see in Figure 6-5, for both conductive MUT the lowest value of sheet resistance is obtained when testing the material stand-alone. As expected, the measured value is higher than the one given by the producer, but closest to the value reported in [68]. As expected, the Pure copper polyester taffeta fabric presents a lower sheet resistance than Zelt®. As one may observe, major changes occur when steam is applied on the conductive fabrics, the sheet resistance increasing 27.5% and 46.2% after applying steam, for Zelt® and Pure copper polyester taffeta fabric, respectively. This can be explained by the fact copper is more susceptible to the oxidation caused by the steam than the copper and thin alloy is, as reported in [76]. When no steam is applied, and adhesive sheet is placed on one surface of the conductive materials, pressing at 200°C, under 10 bar for 6 seconds, a small increase on sheet resistance is observed. In the case of Pure copper polyester taffeta fabric, when laminating the adhesive sheet I and II on the conductive material, the R_s increases 23.28% and 24%, respectively. In the case of Zelt®, the increase of R_s is much lower, being 5.88% and 3.26% when applying the adhesive sheets I and II, respectively.

Table 6-5 Results of sheet resistance measurements of laminated probes $[\Omega/\square]$

		Dielectric Substrate					
Conductive Material	Adhesive Sheet	3D Fabric I		3D Fabric II		Cordura II	
		Face-side ($n = 9$)	Reverse-side ($n = 9$)	Face-side ($n = 9$)	Reverse-side ($n = 9$)	Face-side ($n = 9$)	Reverse-side ($n = 9$)
Pure copper polyester taffeta fabric	I	0.259 ± 0.01	0.231 ± 0.02	0.251 ± 0.02	0.240 ± 0.02	0.214 ± 0.00	0.233 ± 0.00
	II	0.261 ± 0.01	0.247 ± 0.02	0.259 ± 0.01	0.227 ± 0.01	0.222 ± 0.01	0.230 ± 0.01
Zelt®	I	0.303 ± 0.02	0.275 ± 0.01	0.327 ± 0.02	0.306 ± 0.01	0.308 ± 0.00	0.323 ± 0.00
	II	0.337 ± 0.02	0.307 ± 0.02	0.304 ± 0.02	0.285 ± 0.01	0.294 ± 0.00	0.311 ± 0.01

Observing the results of the laminated 3D fabrics in Table 6-5, it is possible to note that, independently of the type of adhesive sheet, the lowest R_s is obtained when the conductive MUT is laminated on the reverse-side of the 3D substrates, which is the face presenting the highest superficial roughness value, as previously characterised (see Table 4-4). Laminating onto a rougher face corresponds to lowering the number of contact points. This way, less glue

of the adhesive sheet penetrates deeply on the structure of the conductive fabric, preserving so the continuity of the electric flow through the conductive fabric.

In turn, when the MUT is laminated onto the face-side of the substrate, which is the smoother surface, this creates a higher number of contact points, contributing for a deeper penetration of the adhesive into the MUT. In this case, the presence of the adhesive will create barriers that cause discontinuity in the electrical current flow. As result, R_s increases.

In the case of the substrate Cordura II, despite the reverse-side is rougher than the face-side (Table 4-4), the MUT laminated on its reverse-side shows the highest R_s . Indeed, as the face-side is coated, the glue of the adhesive sheet is easily absorbed by the coating, thus remaining as an interface material, improving continuity for the current flow in this face and as result the R_s decreases.

Also, for both conductive MUT, independently of the substrate, the lowest R_s was generally obtained when using the adhesive sheet I. Figure 6-6, shows the Scanning Electron Microscope (SEM) images of the face where the adhesive was not applied. As one can see in the SEM images, even in this face there is the presence of adhesive. In (a) is possible to observe that, due to the shape of the adhesive sheet I (grid network), the glue covers a limited zone of pores, that is highlighted by the red arrows. Therefore, some area remains without adhesive and thus not interfering with the current flow. While in (b) the adhesive sheet II (continuous web) covers all pores of the surface, thus making more difficult for the electric current flow going through and thus the R_s increases.

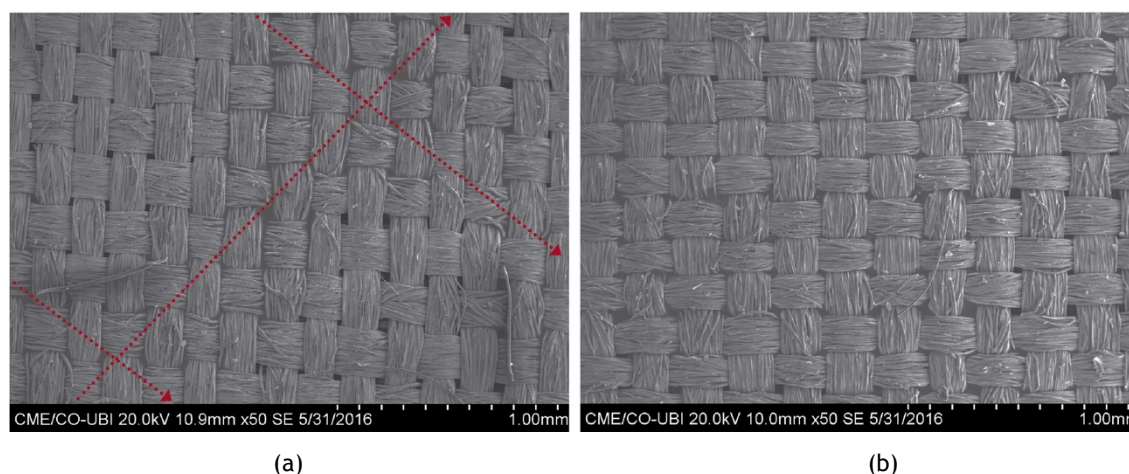


Figure 6-6 SEM image of the surface of Zelt® after applying in the other face, in (a) the adhesive sheet I and in (b) the adhesive sheet II

6.3.2 Laminated Printed Monopole Antenna

In order to confirm the results obtained on previous section, two printed monopole antennas were assembly by the laminating technique and their performance was analysed. These textile printed monopole antennas were the same one presented in Section 5.4, made using Zelt® for

the conductive part and the Cordura[®] fabric as dielectric substrate. To insure the geometrical accuracy, all patches were cut by a laser cutting machine (Jinan G. Weike Science & Technology Co. Ltd., Jinan, China), on the Department of Aerospace Science at Universidade da Beira Interior.

To investigate the consequence of using steam on the laminating process, and its influence on the return loss of the printed monopole antenna, prototype A was assembled applying steam during the ironing process, while in prototype B steam were not used. Both prototypes, A- with and B- without steam, were assembled using the thin thermal adhesive sheet I, following the ironing conditions presented on Table 6-6.

Table 6-6 Ironing conditions

Temperature (°C)	Pressure (bar)	Time (s)	Vacuum table
200	10	12 (6 for patch + 6 for ground plane)	Yes

To feed the antenna a SMA connector, with 50 Ω of impedance, was used. Considering the experience obtained during the manufacturing process of the printed monopole reported on Section 5.4, and the experimental knowledge of how difficult it is welding on Zelt[®], the SMA connector was glued using the conductive glue Elecolit[®], with 70% of silver (Panacol - Elosol GmbH, Taunus, Germany). After, an extra layer of an elastic and conductive glue, the Wire Glue[™] Advanced Microcarbon Technology (Andres Products, Andover, USA), was applied to protect the previous silver layer and reinforce the connection between the SMA connector and the Zelt[®]. The S_{11} of prototypes A and B were measured with a VNA at Instituto de Telecomunicações - Aveiro, and the obtained results are shown on Figure 6-7.

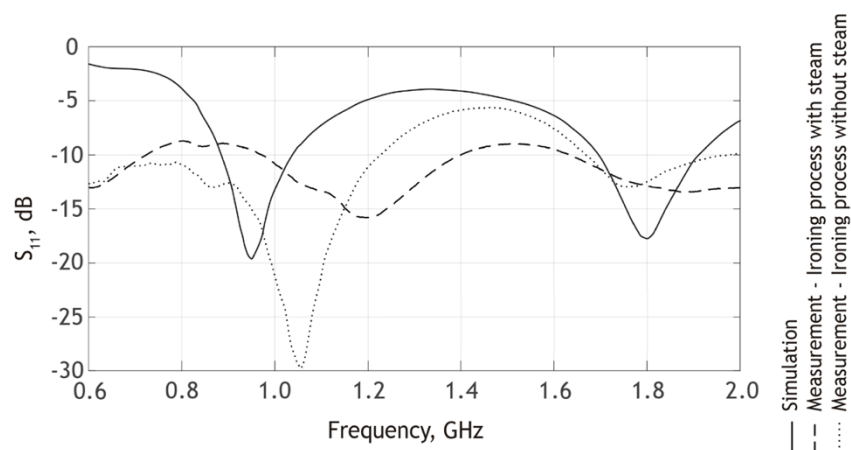


Figure 6-7 Comparison between ironing processes with and without steam

According to the measured results presented on Figure 6-7, one can see a higher mismatch on the frequency of the antenna made using steam during the ironing process. In order to investigate the cause of this mismatch, the thickness of the antenna was measured, using KES-

F-3 Compressional Tester of Kawabata's Evaluation System for fabrics. The thickness of the antenna made without steam is 0.62 mm, and the thickness of the antenna made with steam is 0.60 mm. This difference can be due to the higher compaction of the materials when steam is applied. As one can see in the SEM images of cross section of the antenna shown on Figure 6-8, in the antenna without steam the adhesive sheet (highlighted by yellow arrows in image (a)) remains at the interface between the conductive and dielectric layers. However, when steam is applied, the adhesive sheet merges with the textile structure (highlighted by green arrows in image (b)).

Based on the results and analysis presented on Subsection 6.3.1, this effect is responsible for a decrease in the conductivity due to the presence of the glue among the conductive yarns. Moreover, the presence of the adhesive sheet into the Cordura® fabric will presumably change, even if slightly, its permittivity. Nevertheless, it is worth noting that it is important to further study and quantify the effect of steam in the performance of the antenna, in order to consider it in the design of the antenna improving this way the modelling and simulation of its performance.

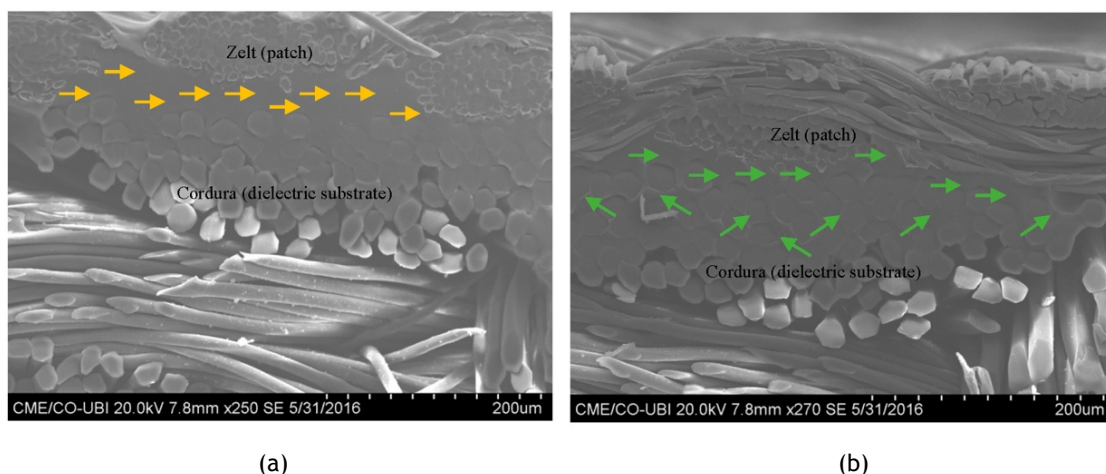


Figure 6-8 SEM images: cross-section of the antenna assembled (a) without steam and (b) with steam

6.3.3 Influence of the Cutting Direction of the Conductive Fabrics

The cutting process of the conductive material is critical, mainly when the antenna has very thin lines as for instance the W_f dimension of the printed monopole (see 5.4). Beyond the cutting precision, the alignment of the fabric with the cutting direction may also influence the performance of the antenna. Therefore, in order to analyse the influence of the orientation of the conductive woven (Zelt®) in the S_{11} parameter, an extra prototype of printed monopole was fabricated:

- Prototype C: patch of antenna was cut on bias of the fabric (45°).

This prototype was tested and its results were compared to the ones of prototype B, whose patch was cut parallel to the warp of the fabric. One should note that Zelt® is a plain weave

woven with the same amount of yarns per cm^2 (45 yarns) in the warp and in the weft, and for this reason only the warp direction was considered. Both prototypes were assembled using the thermal adhesive sheet I, without steam, following the ironing conditions presented on Table 6-6. Figure 6-9 presents the simulated and measured values of S_{11} parameter of both antennas.

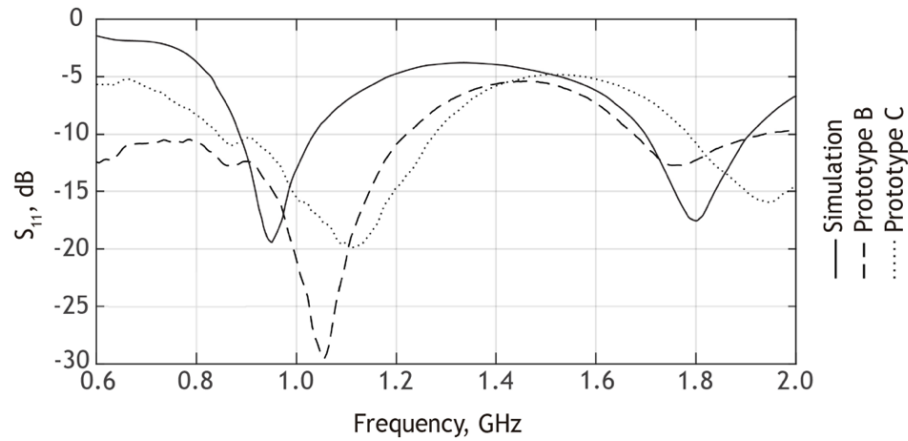


Figure 6-9 Simulated and measured return loss of laminated antennas

Both antennas, produced by the lamination technique, have shown good results, as the S_{11} parameter shows. The orientation of the conductive patch does not seem to influence the performance of these antennas. As one can see on Figure 6-9, the measurements match the simulation fairly well, although there is a small shift of the frequency. This shift of frequency might be due to the narrow manufacturing tolerances that exist even when cutting the fabric by laser. Still, the reflection coefficient is low at the operating frequencies, meaning that the antenna presents a good impedance match in both GSM and DCS bands.

6.4 Embroidery Manufacturing Technique

Embroidering is a promising method in terms of repeatability and mass-manufacturing as the embroidered antennas do not need a cutting neither lamination process, thus reducing the production costs. For this reason, several embroidered antennas have been proposed, for instance spiral antennas [25-26], RFID tags [27-28], and antennas without a ground plane [29-31]. This Section explores the embroidering technique to produce antennas that can be easily applied in clothing as an emblem. This way the embroidering technique might enlarge the dissemination of the textile antennas into clothing.

The experimental study on embroidering is based on the same printed monopole antenna, previously presented at Section 5.4. As this antenna requires a ground plane, the embroidering manufacturing process has to be adapted in order to eliminate the short cuts between the patch and the ground plane. Therefore, the construction technique of these embroidered antennas was: firstly, embroidering the patch in a thin textile; secondly, cut the embroidery; and, finally, attach the embroidery to the dielectric substrate using the thermal adhesive sheet. This process

is the same one used to produce the traditional emblems for cloth customization. Further, the SMA connector was glued using conductive glues, as described in previous Subsection 6.3.2.

Five antennas were developed with this technique, using an automatic embroidering machine (SWF MA-6, SWF Central, Creve Coeur, USA), on the Department of Textile Science and Technology at Universidade da Beira Interior, see Figure 6-10. The patches were embroidered in the Atlantic fabric (B. W. Wernerfelt Group, Søborg, Danmark) using Silverpam yarn (Tibtech Innovations, Roncq, France). Table 6-7 describes the characteristics of these materials used on the embroidering process of the printed monopole textile antennas.

Table 6-7 Characteristics of the materials used to develop embroidered printed monopoles

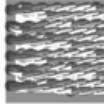
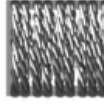
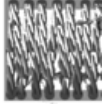
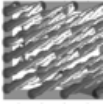
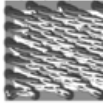
Conductive material	Yarn	Linear mass (dtex)	Composition	Finish	Conductivity (mS/m)
	Silverpam	250	100% PA	Silver plated	0.005
Embroidery base	Fabric	Mass per unit surface (g/m ²)	Composition	Finish	Thickness (mm)
	Atlantic	120	100% PES	Oil + water repellent	0.3



Figure 6-10 SWF MA-6 automatic embroidering machine

The orientation of the stitch was considered by performing stitches along four different directions for antennas 1, 3, 4, and 5. The number of stitches was considered by varying the float of the stitch for antennas 2 and 3. To avoid differences in the fringe effect on the feed line ($W_f \times L_f$) due the different directions of the stitches, all antennas have feed lines embroidered with a horizontal step stitch. The parameters of the embroidery are described in Table 6-8, and Figure 6-11 shows the embroidered patches.

Table 6-8 Parameters of the embroidered antennas

Antenna prototype	1	2	3	4	5
Description of stitch	Horizontal step stitch	Satin with vertical step	Vertical step stitch, with horizontal step	Diagonal step stitch (direction: 152° / quadrant 2), with horizontal step	Diagonal step stitch (direction: 30° / quadrant 1), with horizontal step
Draft of stitch					
Number of stitches	1255	2084	1378	1360	1361
Yarn consumption (g)	0.27	0.39	0.22	0.23	0.27
Yarn consumption per embroidered area (g/m ²)	489	706	398	416	489

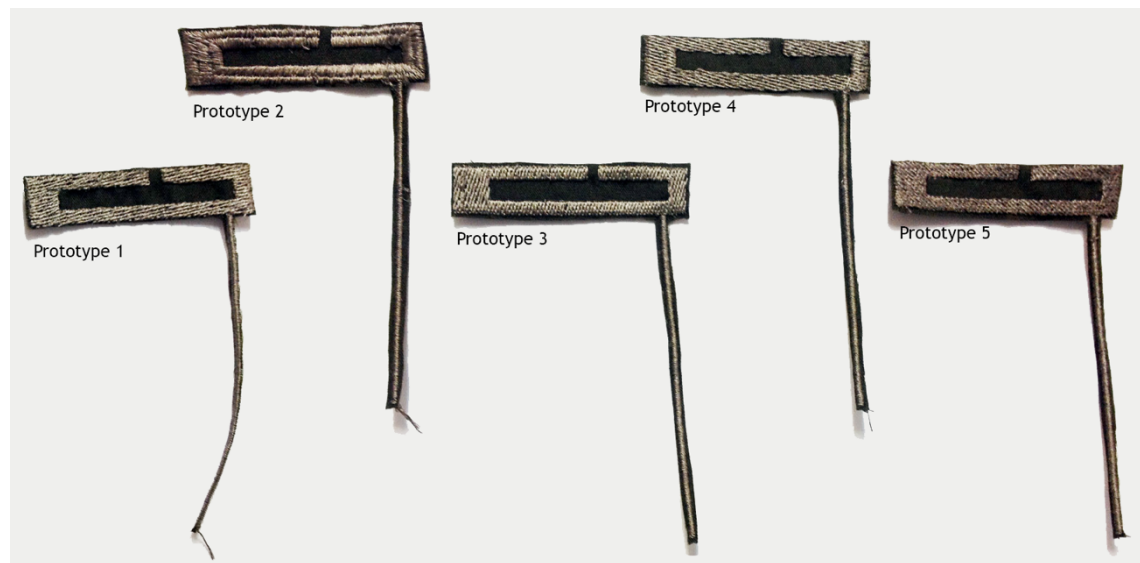


Figure 6-11 Embroidered patches of printed monopole textile antenna

Figure 6-12 shows the simulated and measured values of the S_{11} parameter of these antennas, measured with a VNA, at Instituto de Telecomunicações - Aveiro. It is clear that the measurements match closely to the simulations. A prototype 3 is the one with the best match of the return loss.

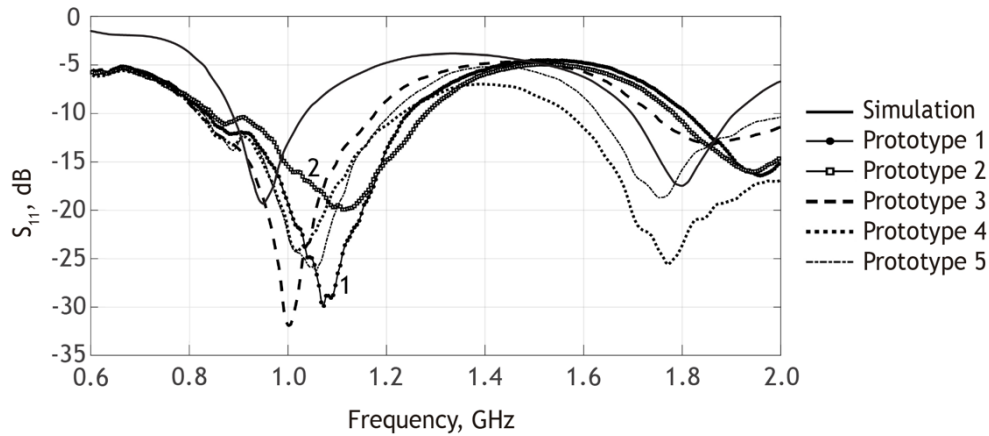


Figure 6-12 Simulated and measured return loss of embroidered antennas

The prototype 3 presents the closest result to the simulation line. This can be due to the fact the embroidery stitch direction is parallel of the feed line, homogenizing the current flow [75]. Prototypes 4 and 5 present very similar behaviours that might indicate the angle of the diagonal direction is not influencing it. Coherently, prototype 1 shows the higher shift of the frequency that can be due to the fact the direction of the embroidery stitch is perpendicular to the feed line. Additionally, prototype 2 was made using a vertical stitch, as well as prototype 3, having however, a higher number of stitches. This may make the current flow less continuous, due the constant breaks and higher number of air gaps in the embroidery as already reported by other authors [36]. This probably reduces the conductivity of the patch, which explain the difference between the magnitudes of the return loss of prototypes 3 and 2.

6.5 Conclusions

Considering the manufacturing techniques, seams can be considered since non-conductive threads are used to avoid short cuts between the patch and the ground plane. Textile glue is not enough to completely assembly the conductive fabrics. Although gluing with permanent glue and super glue works well, gluing is a problematic technique as it is difficult to apply a smooth and continuous portion of glue.

In the laminating technique, a thin adhesive sheet must be used to minimise its interference on the permittivity of the dielectric material. Also, the presence of the glue of the adhesive sheet affects the sheet resistance of the conductive fabric. The choice of a patterned adhesive sheet, such as sheet I, whose pattern is a grid network, can reduce the discontinuity of the current flow. On the laminating process, when the conductive material is assembled to a smooth face of the substrate, its sheet resistance will increase due to the high number of contact points which cause discontinuities on the electric current flow. Therefore, when producing antennas using substrates with different faces, as for instance the 3D spacer fabrics, to preserve the conductivity of the material of the patch, it should preferably be assembled to the rougher face of the substrate.

When laminating, the ironing process without steam seems to be preferable as it better preserves the electromagnetic performance of the materials. Additionally, this work also shows that the orientation of the conductive fabric used for the patch, plain weave woven, is not influencing the performance of the laminated antenna.

When embroidering antennas, it is preferable to use stitches that are parallel to the feed line, to ensure a continuous current flow. In addition, this work shows that the number of stitches in the embroidery may contribute to increase the conductivity of some elements, thus improving the performance of the antenna. Therefore, it is a parameter that should be considered when manufacturing embroidered antennas.

Finally, embroidering is a promising technique to customize the application of antennas on clothing and fashion, as embroidered antennas may be addressed as emblems are.

7 Chapter

Smart Coat with a Fully Embedded Antenna for RF Energy Harvesting

The content of this Chapter was partially published on Sensors Journal (2016), Smart Fabric and Wearable Technologies Conference (2015), 10th European Conference on Antennas and Propagation (2016) and Electronic Conference on Sensors Applications (2016). This Chapter presents the E-Caption: Smart and Sustainable Coat. It has an embedded dual-band printed monopole textile antenna for RF energy harvesting, operating at GSM 900 and DCS 1800 bands. This printed antenna is fully integrated, as its dielectric is the textile material composing the coat itself. The E-Caption illustrates the innovative concept of textile antennas that can be manipulated as simple emblems. The comparison of results obtained, before and after the integration of the antenna into cloth, shows that the integration and the presence of the human body does not affect the behaviour of the antenna.

7.1 Introduction

The recent technological developments made electronic devices become imperative and indispensable, being present in our daily routines, all over the world. The development of smart and wearable textile products requires bringing technologies to the consumer in an acceptable and desirable format.

In the framework of textile antennas for RF energy harvesting, as reviewed on 5.2, different designs have been proposed in the past decade. Nevertheless, only two works [112], [113], known to the author, have outlined the integration of these antennas in smart clothing. This leads to conclude that, despite the advance on the manufacturing techniques of the textile antennas, their integration into clothing is still a difficult task.

Until now, the printed textile antennas have been produced separately and are then posteriorly integrated in the lining of the garment, into pockets or simply glued to the cloth. Only on the RFID context textile antennas have been integrated in products in a pleasing way, for instance for commercial advertisement proposes, where antennas are dissimulated in brand names and

logotypes [73], [141]. Nevertheless, none author has analysed the influence of its integration on clothing on its performance.

7.2 Integration into Clothing

This Chapter proposes an innovative solution that presents the first printed monopole textile antenna (presented on 5.4) manufactured directly in the clothing as it is made with the same textile materials composing the cloth. This innovative solution to integrate antennas into cloths is illustrated on Figure 7-1. The antenna is integrated into the clothing by manipulating it as a simple emblem. In the future, the antennas can be incorporated into patterns and drawings, mixing conductive and non-conductive embroideries, creating fashionable emblems that function as antennas. These “emblem” antennas may be accessible to the end user for customization of smart cloth, for several applications.

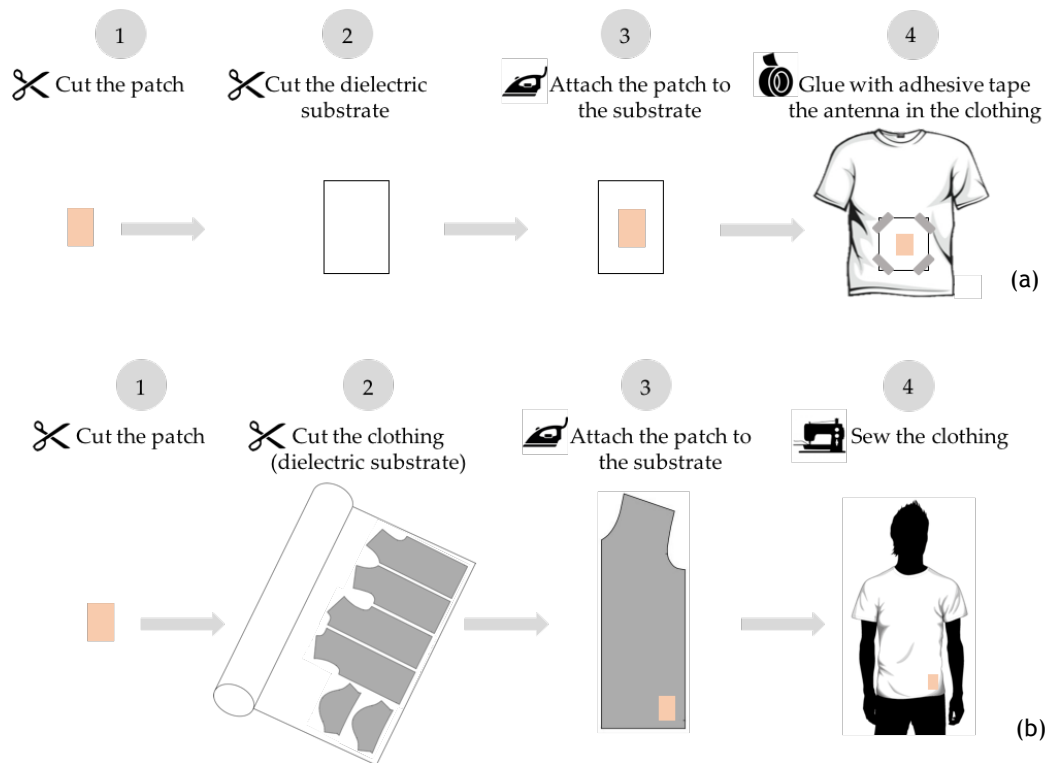


Figure 7-1 Comparison of techniques of integration of antennas into cloth (a) typical integration and (b) “emblem” approach

The curvature of the human body consists of a superposition of bends in arbitrary directions. This hinders the integration of the conventional and rigid antennas into clothing. Due the flexibility and drapability of fabrics, textile antennas have been used for on-body applications.

However, when the textile fabric adapts to the surface topology it bends and deforms, causing changes to its electromagnetic properties and thus influencing the antenna performance [28], [29], [36]. Indeed, the bending and the elongation of the dielectric fabric influences its

permittivity and its thickness, which affects the resonance frequency of the antenna and especially the bandwidth, as explained in [28], [36].

The relationship between the performance of ex-situ textile antennas and the curvature of the human body have been studied in the last decades. To simulate the curvature of arms and legs, the authors have used PVC pipes to bend the antenna in different radius of curvature, along the width and length dimensions [36], [58], [142]. The measurements in the bended antennas, have shown a detuning of resonance frequency, independently of the direction of bending and of the radii of the pipes, in comparison to the resonance frequency of antennas on flat state [36], [58], [142]. Also, under bend conditions, as smaller bend the radius the is, as lower the resonance frequency becomes [36], [142].

The place to integrate the printed monopole antenna on the coat, has to be a place with large curvature radius, in order to minimize the influence of bending on the performance of the antenna. In this framework, considering the unobtrusive areas to integrate wearable devices identified in [143], the chosen area to place the antenna was “waist and hips”, as it is also an area easily accessible as one can see on Figure 7-2.

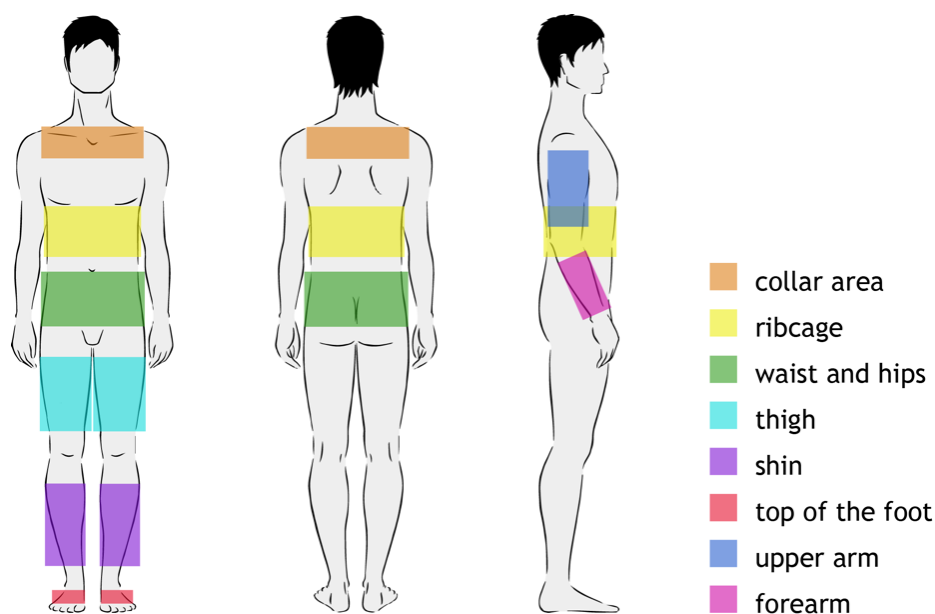


Figure 7-2 Unobtrusive areas to integrate wearable devices, according to [143]

7.3 E-Caption: Smart and Sustainable Coat

The integration of textile antennas for energy harvesting into smart clothing emerges as a particularly interesting solution when the replacement of batteries is not easy to practice, such as in wearable devices. A fully-embedded antenna in clothing contributes for the integration of electronic devices in less obtrusive ways, improving the good aesthetic and the technical design, making the garment more comfortable and desirable to the final consumer. This might

enhance niche markets where form and function work together in order to create new attractive textile products that can assist the user in many aspects of their daily routine.

The E-Caption: Smart and Sustainable Coat was developed combining these concepts. It is a smart coat for electromagnetic harvesting, named E-Caption: Smart and Sustainable Coat, in which the antenna has a substrate that is continuous and was cut according to the pattern-making of the coat, thus being part of it [127]. The integrated printed monopole textile antenna was manufactured based in the results presented on Chapter 6. That means, the patch was cut parallel to the warp, using laser cutting machine, and was produced by laminating manufacturing technique, without steam on the process. Also, the SMA connector was glued using conductive glues. The coat is made of Cordura® and of a 3D fabric (Reference 3003, LMA—Leandro Manuel Araújo, Ltda., Matosinhos, Portugal). Figure 7-3 shows the E-Caption coat with the integrated printed monopole textile antenna for RF energy harvesting. Also, Figure 7-4 presents the logotype of E-Caption created for marketing proposes, such as when the E-Caption was presented on a television show (see Appendix E). Figure 7-5 shows the integrated 5-stage Dickson multiplier voltage, and illustrate the system operation.



Figure 7-3 E-Caption: Smart and Sustainable Coat (Credits: Sophia Cueto Photography and Make Up Artist, Model: Benilde Reis)



Figure 7-4 Logotype of E-Caption: Smart and Sustainable Coat

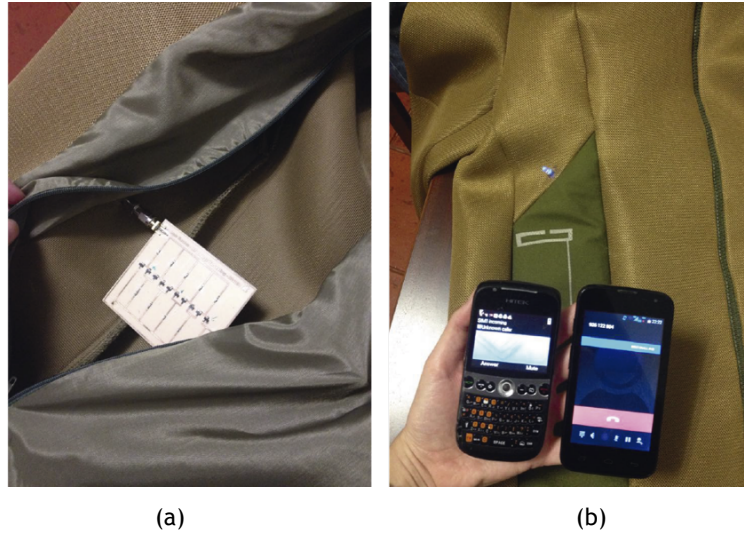


Figure 7-5 Textile printed monopole antenna integrated on clothing. (a) 5-stage Dickson voltage multiplier integrated on lining of E-Caption to harvest the RF energy and (b) the in-situ antenna harvesting the RF energy from the cell phones and turning on the LED

7.4 Influence of the Human Body on the Performance of E-Caption

Despite the concern about the influence of the human body on the performance of antennas, detuning the resonance frequency and changing the radiation patterning [68], [144]-[147], none results about the influence of the body on the performance of textile antennas already integrated into clothing were presented in the literature up to now. Thus, this Subsection will describe the performance of the antenna belonging to the E-Caption: Smart and Sustainable Coat. The coat was tested in the anechoic chamber, at Instituto de Telecomunicações - Aveiro, as shown on Figure 7-6.



Figure 7-6 Performance of the antenna in the anechoic chamber (a) in free space and (b,c) on-body measurements

Figure 7-7 presents the variation in the S_{11} parameter obtained through numerical simulation and measured in free space, before and after the integration into the smart coat. It is possible to see the agreement between the simulated and measured values even in the on-body measurements. In both situations, the textile antenna presents an operating frequency range capable of completely covering the GSM 900 (880-960 MHz) and the DCS 1800 (1710-1880 MHz).

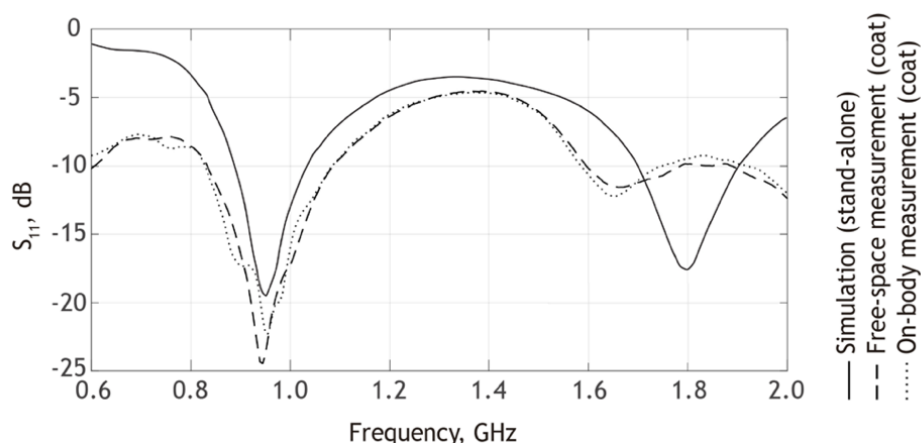


Figure 7-7 Simulated and measured return loss, before/after dressing the coat

The Figure 7-8 shows the radiation pattern of the antenna fully integrated into the smart coat structure, the free-space and on-body measurements. Even after integrated into clothing, the radiation pattern of the antenna is clearly omnidirectional. The results depicted on Figure 7-8 corresponds to the XZ plane. This is the only possible and measurable plane, as can be seen in previous Figure 7-6, due to the configuration and placement of the antenna on the coat. Nevertheless, it is the most relevant plane in order to evaluate the omnidirectional characteristic of the antenna. Moreover, given the position of the antenna on the coat, it is clear that the direction at which the antenna will present less influence from the coat or from the person occurs at nearly 30° in the broadside direction. This is confirmed by the results depicted on Figure 7-8.

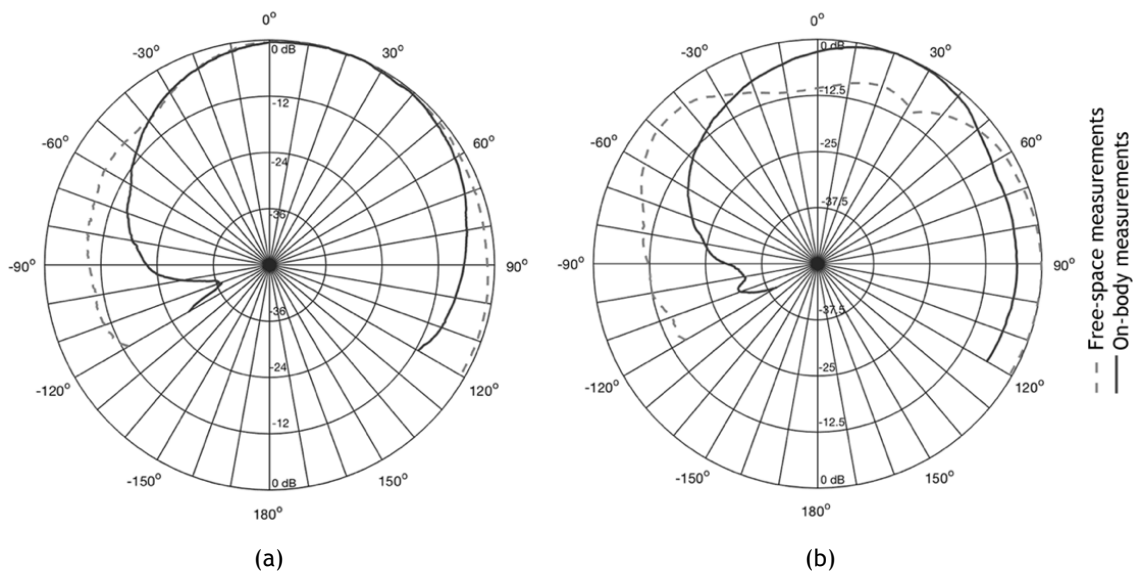


Figure 7-8 Measured radiation pattern of the textile antenna into the coat, free-space and on-body measurements at (a) 900 MHz and (b) 1800 MHz

According to the results presented in Figure 7-8, one may conclude that, as expected, the mass of the coat and mainly of the person influence the radiation characteristic of the antenna. In the measurement of the empty jacket, when the coat places between the probe antenna and the test antenna, around 160° , there is a reduction in the gain of the antenna, which is due to the presence of a large dielectric body, that is, the coat. Nevertheless, the antenna shows a nearly omnidirectional pattern.

The on-body antenna performs differently. Since the human body is conductive, it absorbs and reflects radiofrequency waves. The results on Figure 7-8 show that when the body is behind the test antenna, at 30° broadside, a slight increase in gain is measured. However, when the body is between the probe and the test antenna, at 160° , it will absorb a high amount of radiation and will reflect the rest in the opposite direction, shielding the test antenna and, thus, create a null of radiation at this point. This happens for both frequencies, being clearer at 1800 MHz.

7.5 Conclusions

In the future, garments will not only communicate social conditions or protect the human body against the extremes of nature, but will also provide information and communication tools. Clothes are becoming able to communicate wirelessly without the need of large and expensive equipment. This is possible because textile technologies can produce new types of sensors and antennas that are so small, flexible, and inexpensive that they can be applied in different types of clothing, shoes, and accessories.

The effective integration of wearable systems contributes to the advance of the IoT. Based on the wearability guidelines, the innovative concept of producing textile antennas to integrate into clothing by simply manipulating it as an “emblem” has emerged, may improve the usage of the wearable technologies. In the future, the wearable antennas can be incorporated into

textile patterns and drawings, creating fashionable antennas. These “emblem” antennas may be easily acceded by the end user, for customization of smart cloth for several applications.

The E-Caption: Smart and Sustainable Coat is the first prototype of this concept, integrating an “emblem” antenna capable of completely covering GSM900 (880-960 MHz) and the DCS1800 (1710-1880 MHz) bands, for IoT applications. In this context, the integration of textile antennas for energy harvesting into smart clothing can be a solution for recharging wearable devices, such as low-power electronics and WBSN.

Embedding antennas in clothing contributes for the advance of the integration of electronic devices in less obtrusive way, making the smart clothes more comfortable. In the E-caption, the antenna is manufactured directly on the clothing, having a continuous dielectric substrate made with the textile materials composing the coat. Therefore, a continuous substrate of the antenna does not influence its performance. Moreover, the presented results show that, despite the masses of the coat and of the body influence the radiation characteristic of the integrated antenna, the antenna still shows a nearly omnidirectional radiation pattern.

8 Chapter

Development of a Continuous Substrate Integrating the Ground Plane

The exponential growth in the wearable market is boosting the industrialization process of manufacturing textile antennas. The patch of planar antennas can be easily cut, embroidered or screen printed by machines. The conception of an optimal industrial substrate that meets all the mechanical and electromagnetic requirements is still a challenge. Following the continuous substrate concept presented in previous Chapter 7, this Chapter presents a continuous Substrate Integrating the Ground Plane (SIGP). The SIGP is a novel textile material, which is a double fabric that integrates the dielectric substrate and the conductive ground plane in a single textile, eliminating thus one laminating step in the manufacturing process of microstrip patch antennas. Three SIGP materials, that are weft knitted spacer fabrics, were developed in partnership with the company Borgstena Textile Portugal Lda, creating synergy between academy and industry. The tests of the performance of SIGP show that the integration of the ground plane into the substrate changes the dielectric constant of the material. Despite this, after the accurate dielectric and electrical characterization, the SIGP I has shown a good performance as dielectric substrate of microstrip patch antenna for energy harvesting.

8.1 Introduction

According to the Wearable Technology 2017-2027: Markets, Players and Forecasts report by IDTechEx [148], the market for wearable devices will reach over \$150 billions per year until 2027. Technical textiles will follow the same path as well [9]. For this reason, the industrialization of the manufacturing processes, aiming the mass production of textile antennas, emerge with great relevance.

Although the patch of microstrip antennas may have fine details, they can be easily cut or embroidered by industrial machines, as previously discussed on Chapter 6. Therefore, the focus of this Chapter will be on the industrial production of a dielectric substrate together with the ground plane. Based on previous results reported in Chapter 7, which have proven that a continuous substrate does not influence the performance of the textile antenna, this chapter

presents a new continuous substrate which, in plus, integrates the ground plane. This new material is from now designated SIGP - Substrate Integrating the Ground Plane.

The SIGP is thus a novel textile material that integrates the dielectric substrate and the conductive ground plane in a single sheet, as one can see on Figure 8-1. This way, the manufacturing process of the textile microstrip patch antennas may become easier and faster. The integration of the ground plane into the substrate can contribute to decrease the losses and mismatches caused by the incurrences due to the hand-made manufacturing process. Also, the continuous ground plane, shields the antenna radiation, ensuring that the human body is exposed only to a very small fraction of the radiation.



Figure 8-1 Continuous Substrate Integrating the Ground Plane - 3D Weft knitted spacer fabric (white) with an integrated conductive layer (gold)

The concept of integrating the antenna in a multiple fabric, was already presented in [80], [149], [150]. In these works, the authors present a 3D Integrated Microstrip Antenna, which is woven into a 3D orthogonal fabric. This microstrip antenna, for aerospace application, was developed to work as radar L-band (1.5 GHz). It was made using copper yarns in the conductive parts and aramid (Kevlar 129) yarns in the dielectric layer. Despite the measured resonance frequency is 1.8 GHz, higher than the planned one, this antenna shows a great result as proves that the antenna can be integrated in a unique material, composed of multiple layers.

8.2 Method and Materials

The SIGP is a weft knitted spacer fabric, produced in a double circular machine, the V-LEC6BS Knitting Machine (Monarch Knitting Machinery Ltd., Leicester, England). Figure 8-2 presents this machine, which has a routable needle cylinder and needle dial, being capable to produce a 3D weft knit with differentiated conductive and dielectric faces. The SIGP was developed and manufactured at Borgstena Textile Portugal Lda, following the manufacturing process of the Patent US 6779369 B2 [151]. Figure 8-3 presents the scheme of the needles and yarns on the knitting machine.

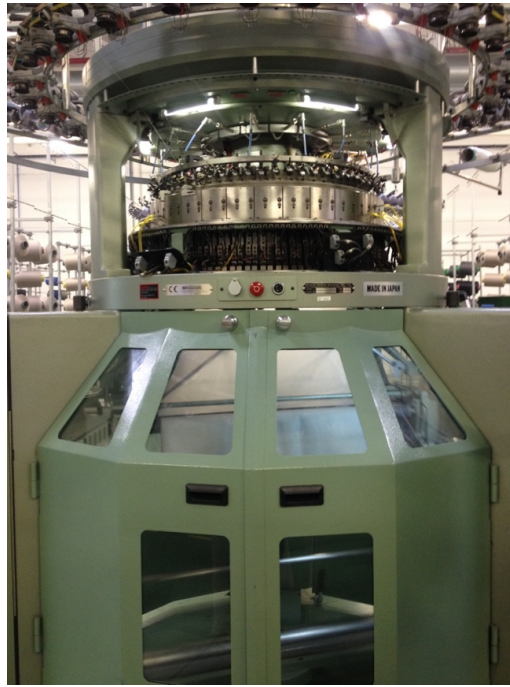


Figure 8-2 V-LEC6BS Knitting Machine by Monarch Knitting Machinery Ltd. (Courtesy Borgstena Textile Portugal)

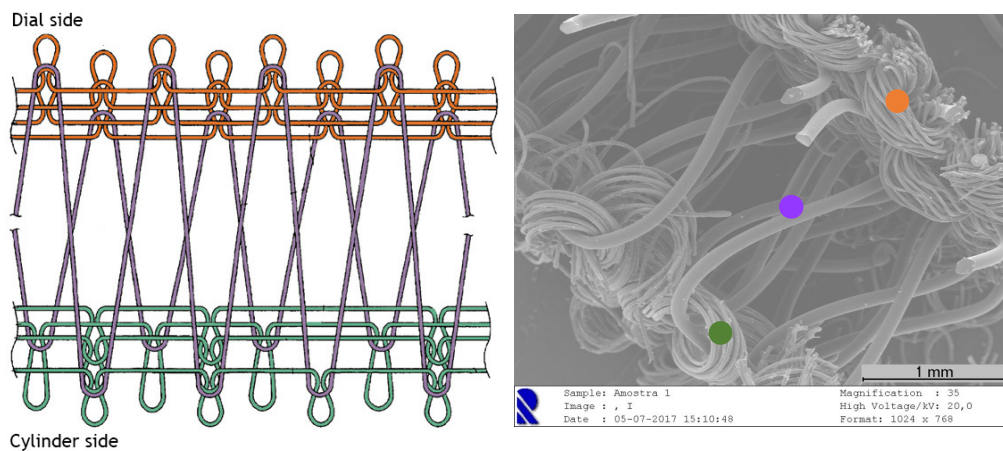


Figure 8-3 Scheme of the Substrate Integrating the Ground Plane. (a) knitting structure diagram, being the green, orange and purple yarns correspondent to the conductive, dielectric and spacer yarns, respectively, based on [151]; (b) SEM image of the SIGP I, with 35X amplification

Based on the knitting structure presented in Figure 8-3, three different SIGP were developed, using the following yarns:

- for the dielectric substrate a 100% PES yarn.
- for the spacer yarn, a Monofilament FH yarn, 100% PET, 225 dtex, produced by Monosuisse AG (Emmenbrücke, Switzerland).
- for the conductive layer two different yarns, “Shieldex® 117/17 dtex Z-turns HC+B” and “Shieldex® 22/1 dtex + 113/32 dtex PES”, produced by Shieldex Trading (Palmyra, USA).

The Shieldex® 117/17 yarn (Shieldex® 117/17 dtex Z-turns HC+B) is a high tenacity PA 6.6 filament yarn, composed by 17 twisted filaments coated with 99% pure silver. The linear mass of this yarn is 141 dtex and it presents a resistivity $<500 \Omega/\text{m}$ (values given by the manufacturer). The Shieldex® 22/1 yarn (Shieldex® 22/1 dtex + 113/32 dtex PES) is a twisted yarn composed by two different materials: a PA 6 monofilament plated with 99% pure silver twisted with 32 PES filaments. The linear mass of this yarn is 145 dtex and it presents a resistivity $<30.000 \Omega/\text{m}$ (values given by the manufacturer).

The choice of these two materials is founded on the linear mass (dtex) of the yarns that must be suitable for work with the V-LEC6BS knitting machine and of course on their electrical conductivity. The price of the yarns was considered as well. Thus, the Shieldex® 117/17 yarn was selected because of its highly conductivity, suitable for producing antennas. The Shieldex® 22/1 yarn was selected because of its price (82€/Kg, in October 2016), being four times less expensive than the other one (307€/Kg, in October 2016). These yarns were worked separately and also mixed, looking for a good compromise between conductivity and price.

The three developed SIGP are listed below:

- SIGP I - Ground plane made using the Shieldex® 117/17 yarn;
- SIGP II - Ground plane made using the Shieldex® 22/1 yarn;
- SIGP III - Ground plane made mixing both conductive yarns, alternating yarns every two courses.

Previous Figure 8-1 presents an image of the SIGP I material, which is composed of one conductive face made of Shieldex® 117/17 yarn, and one dielectric face made of 100% PES yarn.

Also, a control and reference material was produced using the 100% PES yarn on both sides of the spacer knit. This control material aims to serve as reference to compare with and to analyse the influence of the integration of the ground plane in the properties of the dielectric substrate. The structural parameters and the electromagnetic properties of these spacer knits will be described in the next Subsections.

8.3 Structural Parameters

The thickness and the surface roughness of the samples were measured using the KES-F - 3 Compressional Tester of Kawabata's Evaluation System for Fabrics. The tests were performed at the Textile Department of UBI, under controlled environmental conditions, 25°C and 65% RH, testing 5 probes of each SIGP, for determining the total thickness. The thickness of the conductive layer was measured through SEM image analysis, at the Laboratory of Electron Microscopy of UBI. The superficial porosity was calculated through the image analyser method previously presented on Chapter 4, using SEM images with 35X amplification. Table 8-1 summarises the structural parameters of the SIGP. Table 8-2 shows the structural parameters of the reference spacer knit.

Table 8-1 Summary of structural parameters of the produced SIGP

SIGP	Thickness (mm)	Thickness of conductive layer (mm)	Density (number of loops/cm)				Superficial Porosity (%)	
			Dielectric face		Conductive face		Conductive face	Dielectric face
			wales	courses	wales	courses		
I	2 ± 0.01	0.043	18	13	18	13	45.71	45.04
II							43.90	
III							44.50	

Table 8-2 Structural parameters of the reference spacer knit

	Thickness (mm)	Density (number of loops/cm)				Superficial Porosity (%)	
		Face side		Reverse side		Face side	Reverse side
		wales	courses	wales	courses		
Reference spacer knit	2 ± 0.01	18	13	18	13	45.02	45.01

As one can see on Table 8-1, despite the same number of loops in both dielectric and conductive faces, the superficial porosity is slightly different. As previously explained in Chapter 4, the superficial porosity depends on the structure of the knit as well as on the properties of the yarns. In these materials, the knit structure is unique and for this reason, the small variations in the superficial porosity of the conductive face are due to the differences of the diameter and title of the conductive yarns. Indeed, the SIGP I, which is made of Shieldex® 117/17 yarn, the thinnest conductive yarn (141 dtex), presents the highest superficial porosity. Accordingly, the SIGP II that was made of Shieldex® 22/1 yarn, the thickest one (145 dtex), presents the lowest superficial porosity. While the SIGP III shows an intermediate superficial porosity value, as expected as it is made of a mixture of both conductive yarns.

8.4 Characterization of the Electromagnetic Properties

8.4.1 Dielectric Constant

As the SIGP has a conductive layer, the Resonator-Based Experimental Technique previously presented in Chapter 4 cannot be used to characterize the dielectric properties. For this reason, the dielectric constant was measured through the Microstrip Resonator Patch Method [20]. As presented in 3.3.4, this method consists in designing a microstrip patch antenna using an estimated ε_r value, and calculating the real ε_r based on the shift of the measured resonant frequency of the tested antenna.

Thus, one microstrip patch antenna was designed to resonate at 2.45 GHz and to be manufactured using the three SIGP materials. The antenna was simulated in the CST Microwave Studio 2017 full-wave simulator, using estimated values of $\varepsilon_r = 1.10$ and $\tan\delta = 0.006$. These estimated values were based on the obtained results for the 3D fabrics, during the dielectric

characterization in Chapter 4. For manufacturing the radiant element, i.e. the conductive patch, the Pure copper polyester taffeta fabric (previous Table 6-3) was used and assembled by laminating technique. As the conductivity of the ground plane is unknown, the antenna was simulated considering the conductivity value of the Pure copper polyester taffeta fabric. Figure 8-4 presents the design and the dimensions (mm) of this microstrip patch antenna.

As control, a prototype using the reference spacer knit was also manufactured, using the Pure copper polyester taffeta fabric for both patch and ground plane.

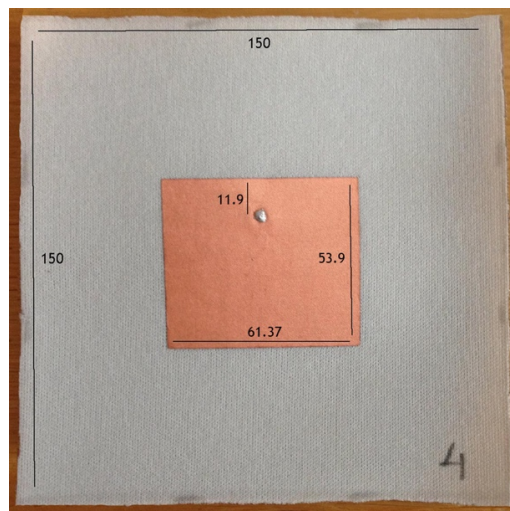


Figure 8-4 Microstrip patch antenna designed for the dielectric characterization, dimensions in mm

All patches were cut on laser cutting (Jinan G. Weiike Science & Technology Co. Ltd., Jinan, China), on Department of Aerospace Science at Universidade da Beira Interior; and the antennas were assembled by the laminating process, using the Adhesive Sheet II (previous Table 6-4). Due to the knitted structure, it was impossible welding the SMA connector in the ground plane as usually performed in some previous antennas. For this reason, the SMA connector was glued to the ground plane using a conductive glue Elecolit® and to ensure the mechanical stability an extra coating of Slow-Cure™ Epoxy (Bob Smith Industries Inc., Atascadero, USA) was applied. In the patch side, the SMA connector was welded on the conductive fabric, as usual. The antennas were tested using a VNA, at Instituto de Telecomunicações - Aveiro and Figure 8-5 presents the obtained results.

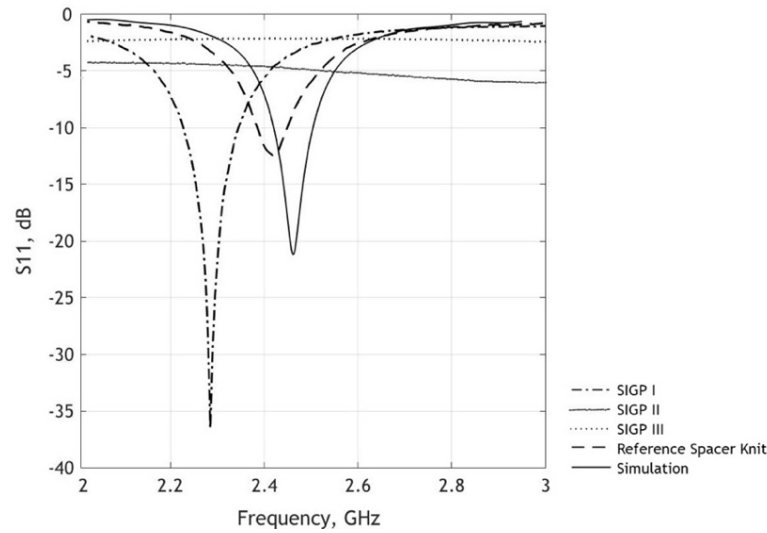


Figure 8-5 Measured S_{11} of the microstrip patch antenna designed for the dielectric characterization

As one can see on Figure 8-5, the prototype 4, that is the control antenna which was made with the reference spacer knit and the conductive fabric (Pure copper polyester taffeta), presents the best agreement with the simulated S_{11} . This was expected, as the simulation was made using the conductivity value of the Pure copper polyester taffeta fabric. This result shows that the estimated values of $\epsilon_r = 1.10$ and $\tan\delta = 0.006$ characterize well the dielectric behaviour of the reference spacer knit.

Prototypes 2 and 3 do not work, due to the low conductivity of the ground plane. These results are thus discarded. Prototype 1 presents an acceptable performance. Comparing the return loss of prototypes 1 and 4, it is possible to see that the integration of the ground plane on the substrate increases the dielectric constant value, as the resonant frequency of prototype 1 shifted for a lower frequency. This can be explained by the fact the integration of the ground plane reduces the thickness of the substrate, thus changing the Q-factor of the antenna as described in 2.2.1.1. Indeed, the total thickness value is 2 mm for all knit spacer fabrics herein considered. However, the SIGP fabrics already include the ground plane, whose thickness is 0,043 mm (Table 8-1), and thus its dielectric substrate is thinner than 2 mm. While the control antenna has a substrate 2 mm thick overlapped by the conductive fabric whose thickness is equal 0,08 mm (Table 6-3).

Based on these results, a new simulation of the prototype 1 was made, changing the ϵ_r value until the new simulated return loss be in agreement with the already measured return loss, to then extract the real ϵ_r value. Figure 8-6 plots the result of the S_{11} obtained in the new simulation and the previously result obtained testing the prototype 1.

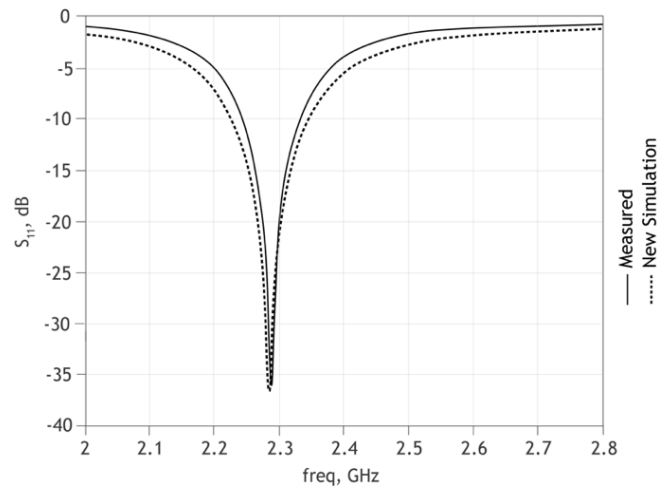


Figure 8-6 Plot of the previously measured S_{11} and of the new simulation of the prototype 1

Through comparing these two return losses, the new value $\epsilon_r = 1.28$ is extracted, according to the method presented at 3.3.4. Assuming this ϵ_r as the real value of the substrate, one may estimate the conductivity of the ground plane of SIGP I as $\sigma = 50$ kS/m. The validation of these results is further presented in Section 8.5.

8.4.2 Surface Resistance

To characterize the conductivity of the ground plane, the sheet resistance was measured following the ASTM Standard F 1896 - Test Method for Determine the Electrical Resistivity of a Printed Conductive Material [47], already presented in 6.3.1. The tests were performed at the Department of Aerospace Science of UBI, under the environmental conditions of 25°C and 50% RH. Four probes of each SIGP were measured with an Agilent HP 34401A Multimeter. Also, the conductivity was calculated by the Equation 2-5. Table 8-3 reports the measured results.

Table 8-3 Electrical properties of the SIGP

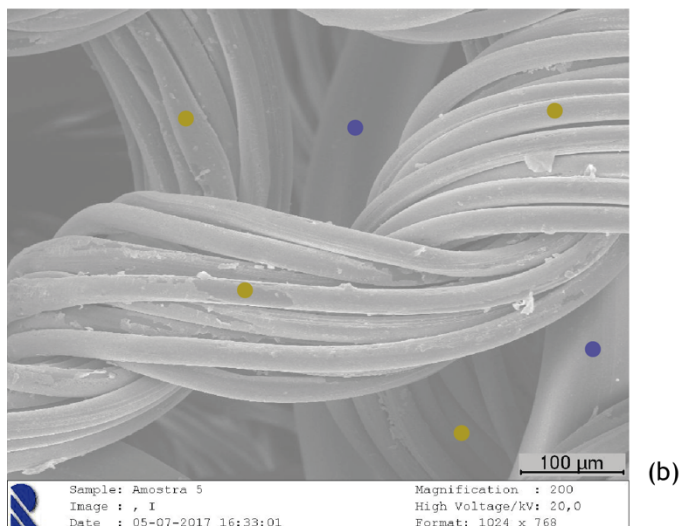
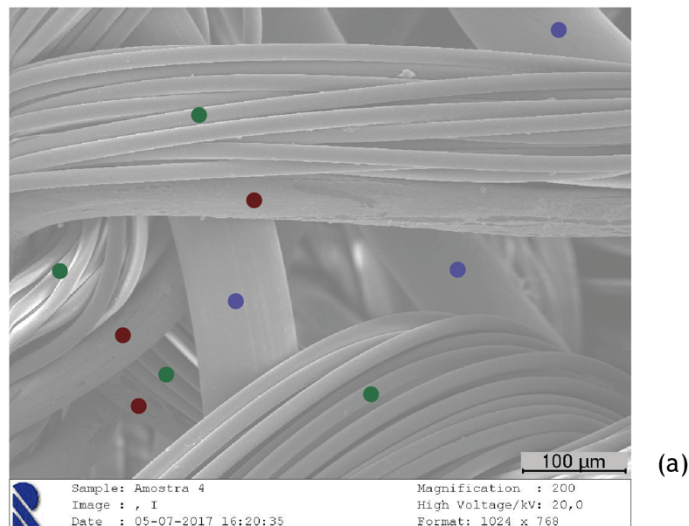
SIGP	Dimensions of the probe (mm)		Sheet resistance (Ω/\square)	Conductivity (kS/m)
	Length (L)	Width (W)		
I	30	60	0.428 ± 0.03	54
II			22.332 ± 1.99	1
III			2.224 ± 0.31	10

As expected, the ground plane of SIGP I material, made of the most conductive yarn (Shieldex[®] 117/17), has shown the best result, presenting the lowest R_s value. Accordingly, the ground plane of SIGP II material, made of the less conductive yarn (Shieldex[®] 22/1), presents the highest R_s value. While the ground plane of the SIGP III material presents an intermediate R_s value. The conductivity of the knitted fabric depends on the properties of the conductive yarns composing it. Observing the SEM images, with 200X of amplification, presented in Figure 8-7,

it is possible to see in (a) that all filaments of the Shieldex® 117/17 yarn are coated with silver. While in (b) one can observe that in the Shieldex® 22/1 yarn there exists only one conductive plated monofilament that is twisted with non-conductive filaments. This observation corroborates the results obtained for the sheet resistance of the ground plane. Also, in (c) it is possible to observe loops establishing some but few contacts between the Shieldex® 22/1 and Shieldex® 117/17 yarns. The SIGP III material, compared to the SIGP II one, presents a better performance, but its sheet resistance is still too high due to the few contacts between both conductive yarns.

Finally, the measured conductivity of the ground plane of SIGP I, which is 54 kS/m, agrees very well with the result estimated through the measurement on the microstrip patch antenna, which is 50 kS/m, as reported in previous section.

- Plated filament of the Shieldex® 22/1
- PES filaments of the Shieldex® 22/1
- Coated filaments of the Shieldex® 117/17
- Spacer yarn - 100% PES



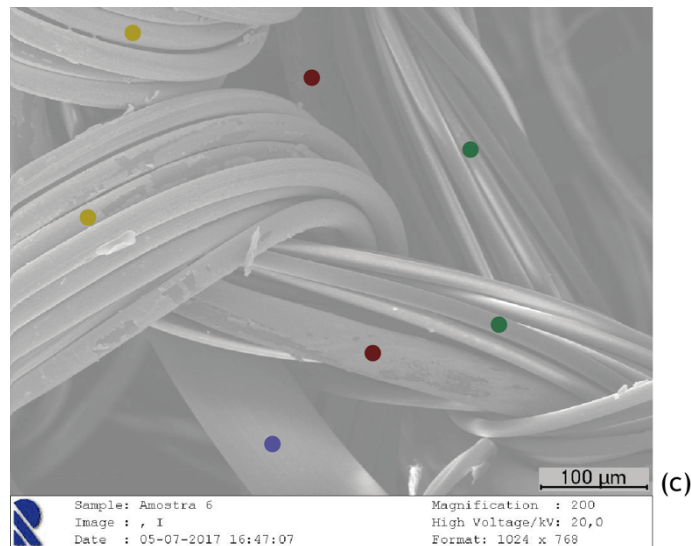


Figure 8-7 SEM images of the conductive side of the Substrate Integrating the Ground Plane (a) SIGP I, (b) SIGP II and (c) SIGP III

8.5 Validation of the Performance of SIGP

To validate the results obtained in previous section 8.4, a new microstrip patch antenna for energy harvesting at ISM band (Industrial, Scientific and Medical), between 2.4 and 2.5 GHz, was designed using the SIGP I as substrate and ground plane and the Pure copper polyester taffeta fabric as patch. This bandwidth also serves to support to the services of WLAN, Bluetooth, and among others. Figure 8-8 presents the design and the dimensions (mm) of this microstrip patch antenna.

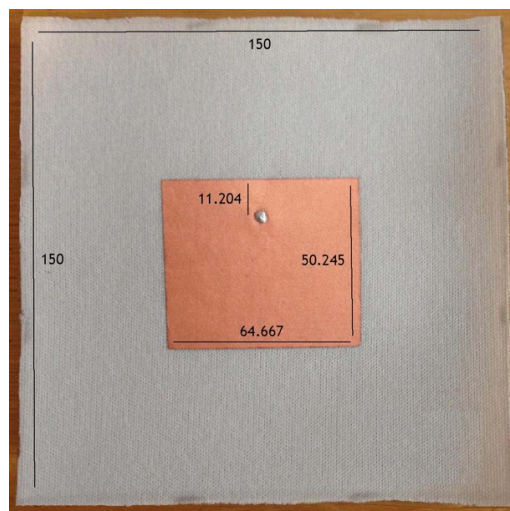


Figure 8-8 Microstrip patch antenna for energy harvesting at ISM band, dimensions in mm

This antenna was produced using the same manufacturing conditions as the antennas presented in previous 8.4.1. The microstrip patch antenna was tested using a VNA, at Instituto de Telecomunicações - Aveiro and Figure 8-9 presents the results.

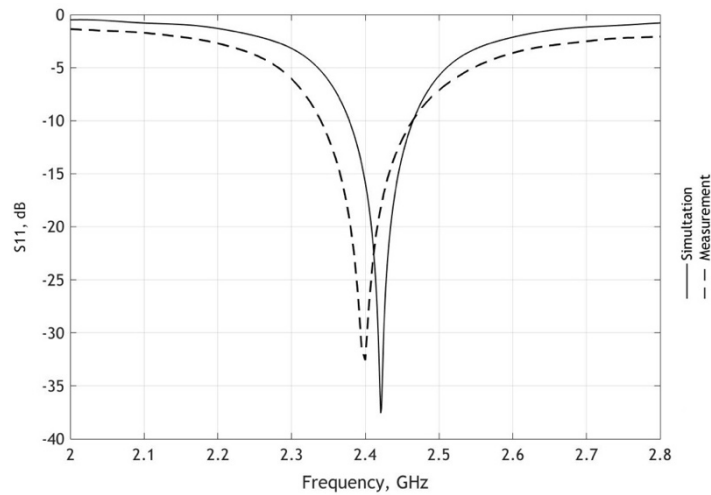


Figure 8-9 S_{11} of the microstrip patch antenna for energy harvesting at ISM band

As one can see on Figure 8-9, the antenna shows a good impedance, validating so the results of the electromagnetic characterisation presented in previous Subsections. The small shift presented on S_{11} , as the simulated frequency is 2.42 GHz and the measured frequency is 2.40 GHz, is not significant and can be explained due to the inaccuracies on the manufacturing process, such as the gluing of the SMA connector.

8.6 Conclusions

This chapter presents the development and validation of a continuous Substrate Integrating the Ground Plane (SIGP). The integration of the textile ground plane into the surface of the textile substrate, all in one fabric that has multiple layers, is the first step to the industrialization of the textile microstrip patch antennas. The knitting spacer technologies, warp and weft technologies, are particularly suited for this propose as allow the production of thick fabrics with different surfaces. The weft knitted spacer fabrics with an integrated conductive layer, herein developed and presented, have shown how promising is this approach. The SIGP I presented good dielectric and electrical properties, being thus suitable to be used for industrial fabrication and mass production of textile microstrip patch antennas and further smart clothing and wearables.

In this Chapter the electrical properties of the spacer knitted fabrics were characterized using the ASTM Standard F 1896. Also, the dielectric constant was characterized through the microstrip patch radiator method.

Three SIGP materials, which are weft knitted spacer fabrics, were developed using two types of conductive yarns. The SIGP I, made using a highly conductive yarn in which all filaments are coated, shows the best conductivity result and best performance when tested on antenna. The SIGP II, made using a less conductive yarn in which only one plated monofilament is conductive, and the SIGP III, made with a mix of both yarns, are not conducting enough to be applied on antennas as the S_{11} results show. Despite the conductivity is too low for the requirement of

antennas, these weft knitted spacer fabrics are interesting materials as complement for other applications, such as electromagnetic shielding, textile switches and other interactive textiles. Being cheaper materials, these SIGP II and III fabrics may complement other more expensive ones and contribute thus to develop affordable smart clothing and wearables.

The integration of the ground plane on the surface of the substrate changes the dielectric properties of the substrate material, increasing its dielectric constant value. This is mainly due to the decrease of the thickness of the substrate. Further, a microstrip patch antenna for energy harvesting at ISM band was designed and manufactured using the novel knit material SIGP I. This antenna presented a great impedance adaptation, proving that the Substrate Integrating the Ground Plane is suitable for the development of textile antennas. This result is very promising for boosting the industrial fabrication of microstrip patch textile antennas and their mass production and dissemination into the IoT network, guiding future developments of smart clothing and wearables.

9 Chapter

Final Remarks

9.1 General Conclusions

In the near future, the IoT developments will boost the use of garments which will not only communicate social conditions or protect the human body against the extremes of nature, but will also provide information and communication tools, will also harvest energy to feed wearable systems. Clothes are becoming able to communicate wirelessly without the need of large and expensive equipment, neither the need of replacing batteries. This is possible because textile technologies can produce new types of flexible devices, such as antennas that are small, flexible and inexpensive and can thus be applied in different types of clothing, as well as shoes and accessories. Textile antennas have thus been emerged to extend the interaction ability of clothing, giving rise to the development of smart cloth. Furthermore, planar antennas of the type microstrip patch are antennas secure to use in the vicinity of the body as radiate perpendicularly to a ground plane, which shields the antenna radiation, ensuring that the human body is exposed only to a very small fraction of the radiation.

This PhD Thesis focuses on the wearable textile antennas, giving an overview about the influence of the textile materials on the performance of textile microstrip patch antennas. Such antennas are usually formed by assembling conductive (patch and ground plane) and dielectric (substrate) layers. For this reason, the knowledge about the electromagnetic properties of textiles and about the assembly manufacturing techniques is crucial. Specific electrical highly conductive textiles are available on the market and have been successfully used. Ordinary textile fabrics have been used as substrates and it is thus important to study and characterize their electromagnetic properties. Woven, knits and nonwovens are inhomogeneous, highly porous, compressible and easily influenced by the environmental hygrometric conditions, making their electromagnetic characterization difficult. Despite there are no standard methods, several authors have been adapting techniques for the dielectric characterization of textiles. Thus, this PhD thesis reviews the resonant and non-resonant techniques that have been used to characterize the dielectric properties of textiles. Despite the resonant techniques only characterize the material in a single frequency, for low-loss materials the resonant methods generally provide higher accuracy and sensibility than non-resonant ones. Some methods require a complex sample preparation, such as the methods of transmission lines. Thus, the results obtained through this method can be influenced by the

conditions of some variables, as for example, the type of e-textile or conductive metal that is used, the used glue/adhesive sheet, the connector and the manufacturing technique to make the probe. To alleviate the problems and complexity of the sample preparation and the influence of the conductive material on the dielectric characterization process, a new Resonator-Based Experimental Technique was presented and performed.

This method is based on the theory of resonance-perturbation, which consists in computing the electromagnetic parameters of the material under test, at a single frequency (2.25 GHz), by measuring the shift in the resonance frequency and in the value of the Q-factor of a microstrip patch antenna. Eleven textile materials were characterized and the results show differences in the ϵ_r values, when placing the face or reverse-side of textiles in contact with the resonator board. These differences are due to the air gap between the surface of the material and the board. Based on this observation, superficial properties of the textile materials were investigated. The results highlight that, as expected, the faces with higher surface roughness also present the higher number of pores on the surface. This way, when characterizing textile fabrics with the resonator-based experimental technique, placing the faces of higher surface roughness in contact with the resonator board results in lower values of ϵ_r . Also, the ϵ_r exponentially decreases with the superficial porosity increase. Both of these observed facts occur because of the presence of the air on the surface, trapped in the superficial pores. Despite the measured value of the dielectric constant ϵ_r differs when placing the face or reverse-sides in contact to the resonator board, and is thus influenced by the structure of the surface of the MUT, the average value of ϵ_r represents well the bulk material and may be considered when designing antennas. The observed superficial differences of the substrate do not seem significant for the development of textile antennas, even when using substrates with clearly different faces.

Energy harvesting can be a solution for powering battery-free devices, contributing to the growth of wireless wearable devices. In this context, the textile antennas are emerging as the solution for feeding low-power devices and/or Wireless Sensors Body Networks, where the change of batteries is not easy to perform. This PhD Thesis also presents a dual-band printed monopole textile antenna which was developed on the scope of the PROENERGY PROJECT - PTDC/EEA-TEL/122681/2010. It can be able to charge low-power devices, as well as extending the lifetime of tiny devices by using electromagnetic energy harvested at GSM 900 and DSC 1800. The printed monopole textile antenna was made using commercially available textiles, Zelt® for the conductive parts and Cordura® as dielectric substrate. To improve the performance of this antenna, several manufacturing techniques were preliminary tested to identify promising techniques and to discard inefficient ones. The results of these tests allow to conclude that:

- **Coating technique:** applying PU coating on Zelt® reduces significantly the conductivity of the conductor Zelt® material and the antenna does not work;

- **Seam technique:** can be considered since non-conductive threads are used to avoid short cuts between the patch and the ground plane and the conductive elements are hold and remain in the conductive fabric;
- **Gluing technique:** textile glue is not strong enough to completely assembly the conductive fabrics;
despite permanent glue and super glue work well, gluing is a problematic technique as it is difficult to apply a controlled smooth and continuous coat of glue;
- **Laminating technique:** in the laminating technique, a thin adhesive sheet must be used to minimise its interference on the permittivity of the dielectric material;
the presence of the glue of the adhesive sheet affects the sheet resistance of the conductive fabric and may decrease it;
the choice of a patterned adhesive sheet can minimize the discontinuity of the current flow and so preserve the conductivity;
when the conductive material is assembled to the smoother face of the substrate, its sheet resistance increases due to the high number of contact points which cause discontinuities on the electric current flow;
the ironing process without steam seems to be preferable as it better preserves the electromagnetic performance of the materials;
additionally, a plain weave woven, such as Zelt[®], shows that the orientation of the conductive fabric used for the patch does not influence the performance of the laminated antenna.
- **Embroidery technique:** is preferable to use stitches that are parallel to the feed line, to ensure a continuous current flow;
the number of stitches in the embroidery may contribute to increase the conductivity of some elements, thus improving the performance of the antenna.

The effective integration of wearable systems contributes to the advance of the IoT. Based on the wearability guidelines, the innovative concept of producing textile antennas to integrate into clothing by simply manipulating it as an “emblem” has emerged. This concept may improve the usage of the wearable technologies. In the future, the wearable antennas might be incorporated into textile patterns and drawings, creating fashionable antennas. These “emblem” antennas may be easily acceded by the end user, for customization of smart cloth for several applications.

The E-Caption: Smart and Sustainable Coat is the first prototype demonstrating this concept. It integrates an “emblem” version of the presented printed monopole textile antenna for energy harvesting. In the E-caption, the antenna is manufactured directly on the clothing, having a continuous dielectric substrate made with the textile materials composing the coat. Therefore, it is shown that a continuous substrate of the antenna does not influence its performance. Moreover, the results show that, despite the masses of the coat and of the body influence the radiation characteristic of the integrated antenna, the antenna still shows a nearly omnidirectional radiation pattern.

In order to contribute to the industrialization of textile antennas, based on the results obtained, a new continuous Substrate Integrating the Ground Plane was developed (SIGP). It is a novel textile material, which is a double fabric that integrates the dielectric substrate and the conductive ground plane in a single textile, eliminating thus one laminating step in the manufacturing process of microstrip patch antennas. In this thesis, three SIGP were produced using two types of conductive yarns, being one a highly conductive yarn well suitable for the design of antennas:

- **SIGP I** - made using a highly conductive yarn in which all filaments are coated, shows as expected the best conductivity result and best performance when tested on antenna;
- **SIGP II** - made using a less conductive yarn in which only one plated monofilament is conductive;
- **SIGP III** - made with a mix of both yarns, it is not conducting enough to be applied on antennas as the S_{11} results show.

Despite SIGP II and III present too low conductivity for the requirement of antennas, these weft knitted spacer fabrics are interesting materials as complement for other functionalities, such as electromagnetic shielding, textile switches and other interactive textiles. Being cheaper materials, these SIGP II and III fabrics may complement other more expensive ones and contribute thus to develop affordable smart clothing and wearables.

To characterize the dielectric properties of SIGP I, the microstrip resonator patch technique was used. The results show that the integration of the ground plane on the surface of the substrate changes the dielectric properties of the substrate material, increasing its dielectric constant value, ϵ_r . This is mainly due to the decrease of the thickness of the substrate.

Further, a microstrip patch antenna for energy harvesting at 2.45 GHz was designed and manufactured using the SIGP I. This antenna presents a great impedance adaptation, proving that the substrate integrating the ground plane (SIGP) is suitable on the development of textile antennas. Finally, the integration of the ground plane in the substrate, fabricated through an industrial process, may boost the industrial fabrication of microstrip patch textile antennas and their mass production. The SIGP associated with the “emblem” antenna concept are important contributions giving novel guidelines for the advance of the integration of electronic devices in less obtrusive ways.

9.2 Future Works

This PhD thesis has established guidelines to integrate antennas into clothing that rise new approaches for developing smart clothing. It would be interesting to continue the work of this PhD Thesis, merging fashion design to textile engineering in order to create functional and fashionable smart clothing which includes antennas. Having these double formations, this is an ongoing research for me and the opportunity to undertake business actions.

Thus, a new version of E-Caption coat is already under development, as one can see in Appendix E. The E-Caption 2.0 - Smart and Safety Coat, is a Personal Protective Equipment (PPE) developed to warning the tower climbers to the radiation level exposure. As the first version of E-Caption, this coat will be a proof-of-concept of the textile antennas used for energy harvesting.

Until now, the tower climbers carry a portable radiation monitor for exposure to RF and non-ionizing radiation, that has a LED display, alarm and vibration notifications. Despite the great performance of this equipment, it is typically heavy, big (about 200 mm x 150 mm) and expensive (between \$599.00 and \$2.500).

The E-Caption 2.0 is made using the continuous SIGP III in order to protect the tower climbers by shielding the RF radiation. Also, the left front side will be made using the SIGP I, integrating a textile RF harvest system manufactured directly on the SIGP. This development is based on the System-on-Substrate (SoS) concept [152], [153], where every part of the system is placed on the same substrate. Furthermore, several LED's will be placed in this front of the coat to warning the user for the radiation levels.

The analysis and study of this prototype may go deeper in diverse scientific subjects. After finishing the manufacturing process of E-Caption 2.0, measurements of S_{11} and radiation pattern of the textile antenna, on free space and on-body, should be performed. Also, the efficiency and wearability of the system may be tested. It would be interesting to analyse the washing conditions in order to test the stability of the antenna, and establish the wear and maintenance conditions of the SIGP and the assemblies performed. Further, tests of Specific Absorption Rate (SAR) may be performed to measure if and how much energy the body absorb from the harvest system and to characterise the shielding efficiency of SIGP II.

This new coat is expected to contribute for the advance of Personal Protective Equipment (PPE) for tower climbers. The E-Caption 2.0 will be able to disseminate the applicability of textile antennas for energy harvesting into clothing, also contributing to the development of wearable wireless devices and smart clothing aiming to reach the specific market of PPE ⁷.

⁷ Appendix F.

References

- [1] H. Kopetz, "Internet of Things," in *Real-Time Systems: Design Principles for Distributed Embedded Applications*, New York: Springer, 2011, pp. 307-323.
- [2] Lopes Research LLC, "An Introduction to the Internet of Things," *CISCO*, 2013.
- [3] Commission of the European Communities "Internet of Things – An action plan for Europe", Brussels, 2009, pp. 1-12.
- [4] D. Miorandi, S. Sicari, F. De Pellegrini, and I. Chlamtac, "Ad Hoc Networks Internet of things : Vision , applications and research challenges," *Ad Hoc Networks*, vol. 10, no. 7, pp. 1497-1516, 2012.
- [5] L. Columbus, "Roundup Of Internet of Things Forecasts And Market Estimates, 2015," *Forbes Magazine*, 2015.
- [6] H. Khaleel, Ed., *Innovation in Wearable and Flexible Antennas*. Southampton, UK: WIT Press, 2015.
- [7] P. Salonen, M. Keskilammi, J. Rantanen, and L. Sydanheimo, "A Novel Bluetooth Antenna on Flexible Substrate for Smart Clothing," *IEEE Int. Conf. Syst. Man, Cybern.*, vol. 2, pp. 789-794, 2001.
- [8] C. A. Balanis, *Antenna Theory Analysis and Design*, Third. New Jersey: Wiley Interscience, 2005.
- [9] D. Agis, D. Bessa, J. Gouveia, and P. Vaz, "Tecnologia: A Tecnologia Ultrapassa a Humanidade," in *Vestindo o Futuro: Microtendências para as Indústrias Têxtil, Vestuário e Moda até 2020*, Porto: ATP - Associação Têxtil e Vestuário Portugal, 2010, pp. 226-276.
- [10] A. Bonfiglio and D. E. De Rossi, *Wearable Monitoring Systems*. New York: Springer, 2010.
- [11] T. Kirstein, D. Cottet, J. Grzyb, and G. Troster, "Wearable Computing Systems: Electronic Textiles," in *Wearable Electronics and Photonics*, New York: Springer, 2005, pp. 177-196.
- [12] R. Gonçalves, R. Magueta, P. Pinho, and N. B. Carvalho, "Dissipation Factor and Permittivity Estimation of Dielectric Substrates Using a Single Microstrip Line Measurement," *Appl. Comput. Electromagn. Soc. J.*, vol. 31, no. 2, pp. 118-125, 2016.
- [13] L. F. Chen, C. K. Ong, C. P. Neo, V. V. Varadan, and V. K. Varadan, *Microwave Electronics: Measurement and Materials Characterization*. Chichester: John Wiley & Sons, Ltd, 2004.

- [14] J. Baker-Jarvis, R. Geyer, J. Grosvenor, M. D. Janezic, C. A. Jones, B. Riddle, C. M. Weil, and J. Krupka, "Dielectric Characterization of Low-loss Materials: A Comparison of Techniques," *IEEE Trans. Dielectr. Electr. Insul.*, vol. 5, no. 4, pp. 571-577, 1998.
- [15] J. Baker-Jarvis, M. D. Janezic, and D. C. DeGroot, "High-Frequency Dielectric Measurements," *IEEE Instrumentation & Measurement Magazine*, pp. 24-31, 2010.
- [16] W. E. Morton and W. S. Hearle, *Physical Properties of Textile Fibres*, Fourth Edi. Cambridge: Woodhead Publishing in Textiles, 2008.
- [17] M. Pourova, R. Zajicek, L. Oppl, and J. Vrba, "Measurement of Dielectric Properties of Moisture Textile," in *14th Conference on Microwave Techniques*, 2008, pp. 1-4.
- [18] C. Hertleer, A. V. Laere, H. Rogier, and L. Van Langenhove, "Influence of Relative Humidity on Textile Antenna Performance," *Text. Res. J.*, vol. 80, no. 2, pp. 177-183, 2009.
- [19] J. Lilja, P. Salonen, T. Kaija, and P. De Maagt, "Design and Manufacturing of Robust Textile Antennas for Harsh Environments," vol. 60, no. 9, pp. 4130-4140, 2012.
- [20] S. Sankaralingam and G. Bhaskar, "Determination of Dielectric Constant of Fabric Materials and Their Use as Substrates for Design and Development of Antennas for Wearable Applications," *IEEE Trans. Instrum. Meas.*, vol. 59, no. 12, pp. 3122-3130, 2010.
- [21] K. Bal and V. K. Kothari, "Permittivity of Woven Fabrics : A Comparison of Dielectric Formulas for Air-Fiber Mixture," *EEE Trans. Dielectr. Electr. Insul.*, vol. 17, no. 3, pp. 881-889, 2010.
- [22] K. Bal and V. K. Kothari, "Measurement of Dielectric Properties of Textile Materials and Their Applications," *Indian J. Fibre Text. Res.*, vol. 34, pp. 191-199, 2009.
- [23] J. S. Thorp, M. Akhtaruzzaman, and D. Evans, "The Dielectric Properties of Alumina Substrate for Microelectronic Packaging," *J. Mater. Sci.*, vol. 25, no. 9, pp. 4143-4149, 1990.
- [24] J. Coonrod, "Understanding When to use FR-4 or High Frequency Laminates," *Onboard Technology Magazine*, pp. 26-30, 2011.
- [25] M. N. O. Sadiku, "Elements of Electromagnetics", 4th ed., New Delhi: Oxford University Press, 2007.
- [26] R. Shawl, B. Longj, D. Werner, and A. Gavrin, "The Characterization of Conductive Textile Materials Intended for Radio Frequency Applications," *IEEE Antennas Propag. Mag.*, vol. 49, no. 3, pp. 28-40, 2007.
- [27] B. Gupta, S. Sankaralingam, and S. Dhar, "Development of Wearable and Implantable Antennas in the Last Decade: A Review," in *10th Mediterranean Microwave Symposium*, 2010, pp. 251-267.

- [28] P. Salonen, Y. Rahmat-samii, M. Schafhth, and M. Kivikoski, "Effect of Textile Materials on Wearable Antenna Performance: A Case Study of GPS Antenna," in *IEEE Antennas and Propagation Society Symposium (APS)*, 2004, vol. 1, pp. 459-462.
- [29] A. Tronquo, H. Rogier, C. Hertleer, and L. Van Langenhove, "Applying Textile Materials for the Design of Antennas for Wireless Body Area Networks," in *1st European Conference on Antennas and Propagation (EuCAP)*, 2006, pp. 1-5.
- [30] C. Hertleer, A. Tronquo, H. Rogier, and L. Van Langenhove, "The Use of Textile Materials to Design Wearable Microstrip Patch Antennas," *Text. Res. J.*, vol. 78, no. 8, pp. 651-658, Aug. 2008.
- [31] S. Brebels, J. Ryckaert, C. Boris, S. Donnay, W. De Raedt, E. Beyne, and R. P. Mertens, "SOP Integration and Codesign of Antennas," *IEEE Trans. Adv. Packag.*, vol. 27, no. 2, pp. 341-351, 2004.
- [32] J. Vandensande, H. Pues, and A. Van de Cappelle, "Calculation of the Bandwidth of Microstrip Resonator Antennas," in *9th European Microwave Conference*, 1979, no. 2, pp. 116-119.
- [33] C. Hertleer, H. Rogier, L. Vallozzi, and L. Van Langenhove, "A Textile Antenna for Off-Body Communication Integrated Into Protective Clothing for Firefighters," *IEEE Trans. Antennas Propag.*, vol. 57, no. 4, pp. 919-925, 2009.
- [34] International Organization for Standarization, "ISO 5084:1996 Determination of thickness of textiles and textile products," 1996.
- [35] S. Kawabata, "Measurement of the Mechanical Properties of Fabrics," in *The Standarization and Analysys of Hand Evaluation*, Second Edi., Osaka: The Textile Machinery Society of Japan, 1980, pp. 28-57.
- [36] I. Locher, M. Klemm, T. Kirstein, and G. Tröster, "Design and Characterization of Purely Textile Patch Antennas," *EEE Trans. Adv. Packag.*, vol. 29, no. 4, pp. 777-788, 2006.
- [37] T. Kaija, J. Lilja, and P. Salonen, "Exposing Textile Antennas for Harsh Environment," in *The Military Communications Conference*, 2010, pp. 737-742.
- [38] X. Wang, W. Xu, and L. Wenbin, "Study on the Electrical Resistance of Textiles Under Wet Conditions," *Text. Res. J.*, vol. 79, pp. 753-760, 2009.
- [39] R. R. Bonaldi, E. Siores, and T. Shah, "Electromagnetic shielding characterization of several conductive fabrics for medical applications," *J. Fiber Bioeng. Informatics*, vol. 2, no. 4, pp. 245-253, 2010.
- [40] S. Brzeziński, T. Rybicki, I. Karbownik, G. Malinowska, E. Rybicki, L. Szugajew, M. Lao, and K. Sledzińska, "Textile materials for electromagnetic field shielding made with the use of nano- and micro-technology," *Cent. Eur. J. Phys.*, vol. 10, no. 5, pp. 1190-1196, 2012.

- [41] S. Brzeziński, T. Rybicki, I. Karbownik, G. Malinowska, E. Rybicki, L. Szugajew, M. Lao, and S. K., "Textile Multi-layer Systems for Protection against Electromagnetic Radiation," *Fibers Text. Estearn Eur.*, vol. 17, no. 2, pp. 66-71, 2009.
- [42] S. Gimpel, U. Mohring, H. Muller, A. Neudeck, and W. Scheibner, "Textile-Based Electronic Substrate Technology," *J. Ind. Text.*, vol. 33, no. 3, pp. 179-189, 2004.
- [43] V. Kaushik, J. Lee, J. Hong, S. Lee, S. Lee, J. Seo, C. Mahata, and T. Lee, "Textile-Based Electronic Components for Energy Applications: Principles, Problems, and Perspective," *Nanomaterials*, vol. 5, no. 3, pp. 1493-1531, 2015.
- [44] W. Zeng, L. Shu, Q. Li, S. Chen, F. Wang, and X. M. Tao, "Fiber-Based Wearable Electronics: A Review of Materials, Fabrication, Devices, and Applications," *Adv. Mater.*, vol. 26, pp. 5310-5336, 2014.
- [45] W. A. Maryniak, T. Uehara, and M. A. Noras, "Surface Resistivity and Surface Resistance Measurements - Using a Concentric Ring Probe Technique," *Trek Appl. Note*, vol. 1005, pp. 1-4, 2003.
- [46] American Society for Testing and Materials, "ASTM Standards D 257-99.," in *Standard test methods for D-C resistance or conductance of insulating materials*, 1999.
- [47] American Society for Testing and Materials, "Test Method for Determining the Electrical Resistivity of a Printed Conductive Material," F 1896, 2004.
- [48] American Association of Textile Chemists and Colorists, "AATCC Test Method 76-2011," in *Electrical Surface Resistivity of Fabrics*, 2011, pp. 1-3.
- [49] International Organization for Standardization, "ISO 10965:2011," in *Textile floor coverings - Determination of electrical resistance*, 2011, pp. 1-5.
- [50] International Organization for Standardization, "ISO 21178:2013," in *Light conveyor belts - Determination of electrical resistances*, 2013, pp. 1-20.
- [51] Y. Ouyang and W. J. Chappell, "High Frequency Properties of Electro-Textiles for Wearable Antenna Applications," *IEEE Trans. Antennas Propag.*, vol. 56, no. 2, pp. 381-389, 2008.
- [52] D. Cottet, J. Gryzb, T. Kirstein, and G. Troster, "Electrical characterization of textile transmission lines," *IEEE Trans. Adv. Packag.*, vol. 26, no. 2, pp. 182-190, 2003.
- [53] J. Lilja, P. Salonen, P. De Maagt, and N. K. Zell, "Characterization of Conductive Textile Materials for SoftWearAntenna Characterization of conductive textiles," in *IEEE Antennas and Propagation Society (APS)*, 2009, pp. 1-4.
- [54] P. Salonen, Y. Rahmat-samii, H. Hurme, and M. Kivikoski, "Effect of Conductive Material on Wearable Antenna Performance : A Case Study of WLAN Antennas," in *IEEE Antennas and Propagation Society Symposium (APS)*, 2004, pp. 455-458.

- [55] J. Lilja and P. Salonen, "Textile material characterization for softwear antennas," in *Antennas and Propagation Society International Symposium (APSURSI)*, 2009, pp. 1-7.
- [56] L. Vallozzi, F. Boeykens, and H. Rogier, "Cylindrically-bent rectangular patch antennas : novel modeling techniques for resonance frequency variation and uncertainty," in *9th European Conference on Antennas and Propagation (EuCAP)*, 2015, pp. 1-5.
- [57] P. Salonen and Y. Rahimat-Samii, "Textile Antennas : Effects of Antenna Bending on Input Matching and Impedance Bandwidth," in *IEEE Aerospace and Electronic Systems Magazine*, 2007, no. 3, pp. 10-14.
- [58] N. Amaro, C. Mendes, and P. Pinho, "Bending Effects on a Textile Microstrip Antenna," in *Antennas and Propagation Society International Symposium (APS-URSI)*, 2011, pp. 282-285.
- [59] S. Dey, N. Saha, and A. Alomainy, "Design and Performance Analysis of Narrow Band Textile Antenna for Three Different Substrate Permittivity Materials and Bending Consequence," in *Loughborough Antennas and Propagation Conference(LAPC)*, 2011, pp. 1-5.
- [60] P. Salonen and H. Hurme, "A Novel Fabric WLAN Antenna for Wearable applications," *IEEE Antennas Propag. Soc. Symp.*, vol. 2, pp. 100-103, 2003.
- [61] C. Hertleer, H. Rogier, L. Vallozzi, and F. Declercq, "A textile antennas based on high-performance fabrics," in *2nd European Conference on Antennas and Propagation*, 2007, pp. 1-5.
- [62] S. Zhu and R. Langley, "Dual-Band Wearable Antennas Over EBG Substrate," *Electron. Lett.*, vol. 43, no. 3, 2007.
- [63] L. Vallozzi, V. P. Torre, C. Hertleer, H. Rogier, M. Moeneclaey, and J. Verhaevert, "Wireless communications for firefighters using dual-polarized textile antennas integrated in their garment," *IEEE Trans. Antennas Propag.*, vol. 58, pp. 1357-1368, 2010.
- [64] A. Dierck, F. Declercq, and H. Rogier, "Review of active textile antenna co-design and optimization strategies," in *IEEE International Conference on RFID-Technologies and applications*, 2011, pp. 194-201.
- [65] F. Declercq, A. Georgiadis, and H. Rogier, "Wearable aperture-coupled shorted solar patch antenna for remote tracking and monitoring applications," in *5th European Conference on Antennas and Propagation*, 2011, pp. 2992-2996.
- [66] S. Zhu and R. Langley, "Dual-band wearable textile antennas over EGB substrate," *IEEE Trans. Antennas Propag.*, vol. 57, pp. 926-935, 2009.
- [67] S. Agneessens, S. Member, S. Lemey, T. Vervust, and H. Rogier, "Wearable, Small, and Robust: the Circular Quarter-Mode Textile Antenna," *IEEE Antennas Propag. Lett.*, vol. 1225, pp. 1536-1225, 2015.

- [68] S. Agneessens and H. Rogier, "Compact Half Diamond Dual-Band Textile HMSIW On-Body Antenna," *IEEE Antennas Propag. Mag.*, vol. 62, no. 5, pp. 2374-2381, 2014.
- [69] M. Bozzi, A. Georgiadis, and K. Wu, "Review of substrate-integrated waveguide circuits and antennas," *ET Microwaves, Antennas Propag.*, vol. 5, no. 8, p. 909, 211AD.
- [70] O. Caytan, S. Lemey, S. Agneessens, D. Vande Ginste, P. Demeester, C. Loss, R. Salvado, and H. Rogier, "Half-Mode Substrate-Integrated-Waveguide Cavity-Backed Slot Antenna on Cork Substrate," *IEEE Antennas Propag. Lett.*, vol. 15, pp. 162-165, 2015.
- [71] S. Lemey, O. Caytan, D. Vande Ginste, P. Demeester, and H. Rogier, "SIW Cavity-backed Slot (Multi-) Antenna Systems for the Next Generation IoT Applications," in *Wireless Sensors and Sensors Networks (WISNet), 2016 IEEE Topical Conference on*, 2016, pp. 75-77.
- [72] K. Elmahgoub, T. Elsherbeni, F. Yang, A. Z. Elsherbeni, L. Sydänheimo, and L. Ukkonen, "Logo-antenna based RFID tags for advertising application," *Appl. Comput. Electromagn. Soc. J.*, vol. 25, no. 3, pp. 174-181, 2010.
- [73] J. Tak, S. Member, J. Choi, and S. Member, "An All-textile Louis Vuitton Logo Antenna," *IEEE Antennas Propag. Lett.*, vol. 1225, pp. 3-6, 2015.
- [74] M. L. Scarpello, I. Kazani, C. Hertleer, H. Rogier, and D. Vande Ginste, "Stability and efficiency of screen-printed wearable and washable antennas," *IEEE Antennas Wirel. Propag. Lett.*, vol. 11, pp. 838-841, 2012.
- [75] A. Tsolis, W. G. Whittow, A. A. Alexandridis, and J. C. Vardaxoglou Yiannis, "Embroidery and Related Manufacturing Techniques for Wearable Antennas: Challenges and Opportunities," *Electronics*, no. 3, pp. 314-338, 2014.
- [76] F. Declercq, H. Rogier, and C. Hertleer, "Permittivity and Loss Tangent Characterization for Garment Antennas Based on a New Matirx-Pencil Two-Line Method," *IEEE Trans. Antennas Propag.*, vol. 56, no. 8, pp. 2548-2554, 2008.
- [77] Y. Ouyang, E. Karayianni, and W. J. Chappell, "Effect of Fabric Patterns on Electrotexile Patch Antennas," in *IEEE Antennas and Propagation Society International Symposium*, 2005, no. 1, pp. 246-249.
- [78] J. C. G. Matthews and G. Pettitt, "Development of Flexible, Wearable Antennas," *IEEE Antennas Propag. Soc. Symp.*, pp. 273-277, 2009.
- [79] S. Adami, D. Zhu, Y. Li, E. Mellios, B. H. Stark, and S. Beeby, "A 2.45 GHz Rectenna on Screen-Printed on Polycotton for On-Body RF Power Transfer and Harvesting," in *IEEE Wireless Power Transfer Conference*, 2015, pp. 1-4.
- [80] L. Yao and Y. Qiu, "Design and Fabrication of Microstrip Antennas Integrated in Three Dimensional Orthogonal Woven Composites," *Compos. Sci. Technol.*, vol. 69, no. 7-8, pp. 1004-1008, 2009.

- [81] W. L. Balls, "Dielectric Properties of Raw Cotton," *Nature*, vol. 158, pp. 9-11, 1946.
- [82] U. C. Hasar, "A New Microwave Method for Electrical Characterization of Low-Loss Materials," *IEEE Microw. Wirel. Components Lett.*, vol. 19, no. 12, pp. 801-803, Dec. 2009.
- [83] A. Moretti, G. N. Malheiros-silveira, E. Hugo, and M. S. Gonçalves, "Characterization and Validation of a Textile Substrate for RF Applications," in *Microwave & Optoelectronics Conference (IMOC), 2011 SBMO/IEEE MTT-S International*, 2011, pp. 546-550.
- [84] M. Mantash, A. C. Tarot, S. Collardey, and K. Mahdjoubi, "Investigation of Flexible Textile Antenna and AMC Reflectors," *Int. J. Antennas Propag.*, pp. 1-10, 2012.
- [85] M. Klemm and G. Troster, "Textile UWB Antennas for Wireless Body Area Networks," *IEEE Antennas Propag.*, vol. 54, no. 11, pp. 3192-3197, 2006.
- [86] A. S. A. Bakar, M. I. Misnon, D. K. Ghodgaonkar, N. Khadri, J. H. Salleh, W. Y. W. Ahmad, M. D. M. Ramli, Y. M. Taib, and Z. Salleh, "Comparison of Electrical Physical and Mechanical Properties of Textile Composites Using Microwave Nondestructive Evaluation," in *RF and Microwave Conference*, 2014, pp. 164-168.
- [87] E. Hakansson, A. Amiet, A. Kaynak, H. Eva, A. Amiet, and A. Kaynak, "Dielectric characterization of conducting textiles using free space transmission measurements: Accuracy and methods for improvement," *Synth. Met.*, vol. 157, pp. 1054-1063, 2007.
- [88] B. Kapilevich, B. Litvak, M. Anisimov, D. Hardon, and Y. Pinhasi, "Complex Permittivity Measurements of Textiles and Leather in a Free Space: An Angular-Invariant Approach," *Int. J. Microw. Sci. Technol.*, pp. 1-7, 2012.
- [89] J. Lesnikowski, "Dielectric permittivity measurement methods of textile substrate of textile transmission lines," *Electr. Rev.*, vol. 88, no. 3, pp. 148-151, 2012.
- [90] J. Lilja, P. Salonen, P. D. Maagt, and N. K. Zell, "Characterization of Conductive Textile Materials for Softwear Antenna," in *Antennas and Propagation Society International Symposium (APSURSI) 2009*, 2009, pp. 1-5.
- [91] O. Himdi and M. Lafond, "Printed Millimeter Antennas - Multilayer Technologies," in *Advanced Millimeter-Wave Technologies: Antennas, Packaging and Circuits*, D. Lui, U. Pfeiffer, J. Gryzb, and B. Gaucher, Eds. Chichester: Wiley Interscience, 2009.
- [92] D. Gershon, J. P. Calame, Y. Carmel, T. M. A. Jr, D. Gershon, J. P. Calame, Y. Carmel, and T. M. Antonsen, "Adjustable resonant cavity for measuring the complex permittivity of dielectric materials Adjustable resonant cavity for measuring the complex permittivity of dielectric materials," vol. 3207, no. 2000, pp. 12-15, 2007.
- [93] U. Faz, U. Siart, T. F. Eibert, S. Member, and T. Hermann, "Electric Field Homogeneity Optimization by Dielectric Inserts for Improved Material Sensing in a Cavity Resonator,"

vol. 64, no. 8, pp. 2239-2246, 2015.

- [94] A. Kumar and D. G. Smith, "Microwave Properties of Yarns and Textiles Using a Resonant Microwave Cavity," *IEEE Trans. Instrum. Meas.*, vol. 26, no. 2, pp. 95-98, 1977.
- [95] B. Roy and S. K. Choudhury, "Characterization of Textile Substrate to Design a Textile Antenna," in *Microwave and Photonics (ICMAP), 2013 International Conference on*, 2013, pp. 1-5.
- [96] I. J. Bahl and S. S. Stuchly, "Analysis of a Microstrip Covered with a Lossy Dielectric," *IEEE Trans. Microw. Theory Tech.*, vol. 28, no. 2, pp. 104-109, 1980.
- [97] M. Bogosanovich, "Microstrip Patch Sensor for Measurement of the Permittivity of Homogeneous Dielectric Materials," *IEEE Trans. Instrum. Meas.*, vol. 49, no. 5, pp. 1144-1148, 2000.
- [98] S. Hausman, Ł. Januszkiewicz, M. Michalak, T. Kacprzak, and I. Krucińska, "High Frequency Dielectric Permittivity of Nonwovens," *Fibers Text. Estearn Eur.*, vol. 14, no. 5, pp. 60-63, 2006.
- [99] A. Technologies, "Measuring Dielectric Properties Using Agilent's Materials Measurement Solutions." USA, pp. 1-4, 2014.
- [100] M. F. Ismail, M. K. A. Rahim, M. R. Hamid, and H. A. Majid, "Circularly Polarized Textile Antenna with Bending Analysis," in *IEEE International RF and Microwave Conference (RFM)*, 2013, pp. 460-462.
- [101] N. A. Hotaling, K. Bharti, H. Kriel, and C. G. J. Simon, "DiameterJ: A validated open source nanofiber diameter measurement tool," *Biomaterials*, vol. 61, pp. 327-338, 2015.
- [102] A. C. Schineider, W. S. Rasband, and K. W. Eliceiri, "NIH Image to ImageJ: 25 years of image analysis," *Nat. Methods*, vol. 9, pp. 671-675, 2012.
- [103] S. Warren and B. Natarajan, "Wireless Communication Technologies for Wearable Systems," in *Wearable Monitoring Systems*, New York: Springer, 2011, pp. 51-80.
- [104] A. Pantelopoulos and N. G. Bourbakis, "A Survey on Wearable Sensor-Based Systems for Health Monitoring and Prognosis," *IEEE Trans. Syst. mam Cybern. - Part C Appl. Rev.*, vol. 40, no. 1, pp. 1-12, 2010.
- [105] M. Stoppa and A. Chiolerio, "Wearable Electronics and Smart Textiles: A Critical Review," *Sensors*, vol. 14, no. 7, pp. 1957-11992, 2014.
- [106] S. Chalasani and J. M. Conrad, "A Survey of Energy Harvesting Sources for Embedded Systems," in *IEEE SoutheastCon*, 2008, pp. 442-447.
- [107] H. Jabbar, Y. S. Song, and T. T. Jeong, "RF energy harvesting system and circuits for charging of mobile devices," *IEEE Trans. Consum. Electron.*, pp. 247-253, 2010.

- [108] A. Constanzo, M. Dionigi, D. Masotti, M. Mongiardo, G. Monti, L. Tarricone, and R. Sorrentino, "Electromagnetic Energy Harvesting and Wireless Power Transmission: A Unified Approach," *Proc. IEEE*, vol. 102, no. 1692-1711, 2014.
- [109] S. Lemey, S. Agneessens, P. Van Torre, K. Baes, H. Rogier, and J. Vanfleteren, "Autonomous Wearable RFID-Based Sensing Platform for the Internet-of-Things," in *Applied Computational Electromagnetics Society Symposium*, 2017, pp. 1-2.
- [110] S. Lemey, S. Agneessens, and H. Rogier, "Textile SIW Antennas as Hybrid Energy Harvesting and Power Management Platforms," in *European Microwave Conference (EuMC)*, 2015, pp. 20-23.
- [111] S. Lemey and H. Rogier, "Substrate integrated waveguide textile antennas as energy harvesting platforms," in *International Workshop on Antenna Technology (iWAT)*, 2015, pp. 23-26.
- [112] R. K. Tallos, Z. Wang, and J. L. Volakis, "Wi-Fi Energy Harvesting System Using Body-worn Antennas," in *Antennas and Propagation Society*, 2014, pp. 1405-1406.
- [113] D. Masotti, A. Costanzo, and S. Adami, "Design and Realization of a Wearable Multi-Frequency RF Energy Harvesting System," in *5th European Conference on Antennas and Propagation*, 2011, pp. 517-520.
- [114] R. Gonçalves, N. Carvalho, P. Pinho, C. Loss, and R. Salvado, "Textile antenna for electromagnetic energy harvesting for GSM900 and DCS1800 bands," in *Antennas and Propagation Society International Symposium (APSURSI) 2013*, 2013, pp. 1206-1207.
- [115] N. B. Carvalho, G. Apostolos, A. Constanzo, H. Rogier, A. Collado, J. A. García, S. Lucyszyn, P. Mezzanotte, J. Kracek, D. Masotti, A. J. S. Boaventura, M. N. R. Lavin, M. Pinuela, D. C. Yates, P. D. Mitcheson, M. Mazanek, and V. Pankrac, "Wireless Power Transmission : R & D Activities Within Europe," *IEEE Trans. Microw. Theory Tech.*, vol. 62, no. 4, pp. 1031-1045, 2014.
- [116] D. Belo, A. Georgiadis, and N. B. Carvalho, "Increasing Wireless Powered Systems Efficiency by Combining WPT and Electromagnetic Energy Harvesting," in *IEEE Wireless Power Transfer Conference*, 2016, pp. 2-4.
- [117] X. Lu, P. Wang, D. Niyato, D. I. Kin, and Z. Han, "Wireless Networks with RF Energy Harvesting: A Contemporary Survey," *IEEE Commun. Surv. Tutorials*, vol. 17, no. 2, pp. 757-789, 2015.
- [118] O. Galinina, H. Tabassum, K. Mikhaylov, S. Andreev, E. Hossain, and Y. Koucheryavy, "On Feasibility of 5G-Grade Dedicated RF Charging Technology for Wireless-Powered Wearables," pp. 1-9, 2015.
- [119] R. M. El Khosht, M. A. Feshawmy, M. A. El Shorbagy, M. N. Farag, A. E. El Said, H. F. Hammad, and A. T. Abdel-Hamid, "A Foldable Textile-Based Broadband Archimedean

- Spiral Rectenna for RF Energy Harvesting,” in *16th Mediterranean Microwave Symposium (MMS)*, 2016, pp. 1-4.
- [120] C. Loss, R. Gonçalves, C. Lopes, R. Salvado, and P. Pinho, “Textile Antenna for RF Energy Harvesting Fully Embedded in Clothing,” in *10th European Conference on Antennas and Propagation (EuCAP)*, 2016.
 - [121] N. Barroca, H. Saraiva, P. T. Gouveia, J. Tavares, L. Borges, F. Velez, C. Loss, R. Salvado, P. Pinho, R. Gonçalves, N. Carvalho, R. Chavéz-Santiago, and I. Balasingham, “Antennas and Circuits for Ambient RF Energy Harvesting in Wireless Body Area Networks,” in *Proceedings of the Annual International Symposium on Personal, Indoor and Mobile Radio Communications*, 2013, pp. 527-532.
 - [122] M. Dini, M. Filippi, A. Costanzo, A. Romani, M. Tartagni, M. Del Prete, and D. Masotti, “A Fully-Autonomous Integrated RF Energy Harvesting System for Wearable Applications,” in *European Microwave Conference (EuMC)*, 2013, pp. 987-990.
 - [123] J. Tavares, N. Barroca, H. Saraiva, L. Borges, F. Velez, C. Loss, R. Salvado, P. Pinho, R. Gonçalves, and N. Carvalho, “Spectrum Opportunities for Electromagnetic Energy Harvesting from 350 MHz to 3 GHz,” in *7th International Symposium on Medical Information in Communication Technology*, 2013, pp. 126-130.
 - [124] A. Constanzo, D. Masotti, and M. Del Prete, “Wireless power supplying flexible and wearable systems,” in *European Conference on Antennas and Propagation (EuCAP)*, 2013, pp. 2843-2846.
 - [125] D. Masotti and A. Constanzo, “Design of Wearable Rectennas Harvesting from Multi-Tone Ambient RF sources,” in *Proceedings of the 4th International Symposium on Applied Sciences in Biomedical and Communication Technologies*, 2011, pp. 1-5.
 - [126] H. M. Saraiva, L. M. Borges, N. Barroca, J. Tavares, P. T. Gouveia, F. Velez, C. Loss, R. Salvado, P. Pinho, R. Gonçalves, R. Chavéz-Santiago, and I. Balasingham, “Experimental Characterization of Wearable Antennas and Circuits for RF Energy Harvesting in WBANs,” in *IEEE Vehicular Technology Conference*, 2014, pp. 1-5.
 - [127] C. Loss, R. Gonçalves, C. Lopes, P. Pinho, and R. Salvado, “Smart Coat with a Fully-Embedded Textile Antenna for IoT Applications,” *Sensors*, vol. 16, no. 6. 2016.
 - [128] R. Salvado, C. Loss, R. Gonçalves, and P. Pinho, “Textile Materials for the Design of Wearable Antennas : A Survey,” *Sensors*, vol. 12, pp. 15841-15857, 2012.
 - [129] A. Constanzo, D. Masotti, and M. Aldrigo, “Compact, Wearable Antennas for Battery-Less Systems Exploiting Fabrics and Magneto-Dielectric Materials,” *Electronics*, vol. 3, no. 3, pp. 474-490, 2014.
 - [130] A. Costanzo, F. Donzelli, D. Masotti, and V. Rizzoli, “Rigorous Design of RF Multi-Resonator Power Harvester,” in *4th European Conference on Antennas and Propagation*

(EuCAP), 2010, pp. 1-4.

- [131] L. M. Borges, N. Barroca, H. M. Saraiva, J. Tavares, P. T. Gouveia, F. Velez, C. Loss, R. Salvado, P. Pinho, R. Gonçalves, R. Chavéz-Santiago, and I. Balasingham, "Design and Evaluation of Multi-Band RF Energy Harvesting Circuits and Antennas for WSNs," in *21 st International Conference on Telecommunications*, 2014, pp. 308-31.
- [132] B. Ivši, M. Babi, A. Galoi, and D. Bonefa, "Feasibility of Electromagnetic Energy Harvesting Using Wearable Textile Antennas," pp. 485-488, 2017.
- [133] J. O. Ha, S. H. Jung, M. C. Park, K. H. Lee, and Y. S. Eo, "A Fully Integrated 3 - 5 GHz UWB RF Transceiver for WBAN Applications," in *EEE International Microwave Workshop Series on RF and Wireless Technologies for Biomedical and Healthcare Applications (MTT-S)*, 2013, pp. 1-3.
- [134] S. Lemey, H. Rogier, F. Declercq, B. S. Lemey, S. M. leee, and F. Declercq, "Textile Antennas as Hybrid Energy-Harvesting Platforms," *Proc. IEE*, vol. 102, no. 11, pp. 1833-1857, 2014.
- [135] V. Kuhn, F. Seguin, C. Lahuec, and C. Person, "Matching Network Improvement for RF Energy Harvesters in Body Sensor Area Network Context," in *European Microwave Conference (EuMC)*, 2015, pp. 1-10.
- [136] S. Zhang, D. Speight, A. Paraskevopoulos, D. Fonseca, C. Luxey, W. Whittow, and J. Pinto, "O n-Body Measurements of Embroidered Spiral Antenna," in *Loughborough Antennas and Propagation Conference*, 2015, pp. 1-5.
- [137] L. Ukkonen, L. Sydänheimo, and Y. Rahmat-samii, "Sewed Textile RFID Tag and Sensor Antennas for On-Body Use," *6th Eur. Conf. Antennas Propag.*, pp. 3450-3454, 2011.
- [138] Y. P. Huang, "Effect of Sewing Types on Flexible Embroidery Antennas in UHF Band," in *Proceeding of the 43rd European Microwave Conference*, 2013, pp. 88-91.
- [139] T. Acti, A. Chauraya, S. Zhang, W. G. Whittow, R. Seager, J. C. Vardaxoglou, and T. Dias, "Embroidered Wire Dipole Antennas Using Novel Copper Yarns," *IEEE Antennas Propag. Lett.*, vol. 14, pp. 638-641, 2015.
- [140] A. Kiourti and J. L. Volakis, "Stretchable and Flexible E-Fiber Antennas with High Geometrical Accuracy," in *9th European Conference on Antennas and Propagationt (EuCAP)*, 2015, pp. 4-5.
- [141] M. S. Mahmud and S. Dey, "Design, performance and implementation of UWB wearable logo textile antenna," *2012 15th Int. Symp. Antenna Technol. Appl. Electromagn. ANTEM 2012*, pp. 1-4, 2012.
- [142] M. A. A. Majid, M. K. A. Rahim, N. A. Murad, N. A. Samsuri, N. F. A. Elias, and M. H. Mokhtar, "Fully Textile Slot Linear Array Antenna with Curvature and Crumple Analysis," in *International Symposium on Antennas and Propagation Conference Proceedings*,

2014, pp. 263-264.

- [143] F. Gemperle, C. Kasabach, J. Stivoric, M. Bauer, and R. Martin, "Design for Wearability," in *Digest of Papers. Second International Symposium on Wearable Computers*, 1998, pp. 116-122.
- [144] T. Blecha, R. Linhart, and J. Reboun, "Screen-printed Antennas on Textile Substrate," in *2014 Electronics System-Integration Conference*, 2014, pp. 1-4.
- [145] S. J. Boyes, P. J. Soh, Y. Huang, G. E. Vandenbosch, and N. Khiabani, "Measurement and Performance of Textile Antenna Efficiency on a Human Body in a Reverberation Chamber," *IEEE Trans. Antennas Propag.*, vol. 61, no. 2, pp. 871-881, 2013.
- [146] H. Giddens, D. L. Paul, G. S. Hilton, and J. P. Mcgeehan, "Influence of Body Proximity on the Efficiency of a Wearable Textile Patch Antenna," pp. 1353-1357, 2011.
- [147] D. L. Paul, H. Giddens, M. G. Paterson, G. S. Hilton, and J. P. Mcgeehan, "Impact of Body and Clothing on a Wearable Textile Dual Band Antenna at Digital Television and Wireless Communications Bands," *IEEE Trans. Antennas Propag.*, vol. 61, no. 4, pp. 2188-2194, 2013.
- [148] J. Hayward, G. Chansin, and H. Zervos, "Wearable Technology 2017-2027: Markets, Players and Forecasts," 2017.
- [149] C. Du and F. Yang, "Robust Planar Textile Antenna Integrated in Three Dimensional Orthogonal Woven Fabrics," in *3rd Asia-Pacific Conference on Antennas and Propagation*, 2014, pp. 372-374.
- [150] L. Yao, M. Jiang, D. Zhou, F. Xu, D. Zhao, W. Zhang, N. Zhou, Q. Jiang, and Y. Qiu, "Fabrication and Characterization of Microstrip Array Antennas Integrated in the Three Dimensional Orthogonal Woven Composite," *Compos. Part B*, vol. 42, no. 4, pp. 885-890, 2011.
- [151] USA Patent, "Patent US 6.779.369 B2 - Weft Knitted Spacer Fabrics," 2004.
- [152] C. Lopes, C. Loss, R. Salvado, P. Pinho, S. Agneessens, and H. Rogier, "Development of Substrate Integrated Waveguides with Textile Materials by Manual Manufacturing Techniques," in *Proceedings of the 2nd Int. Electron. Conf. Sens. Appl*, 2014, p. S3004.
- [153] K. Wu and E. Polytechnique, "Towards System-on-Substrate Approach For Future Millimeter-Wave and Photonic Wireless Applications," in *Proceedings of Asia-Pacific Microwave Conference*, 2006, pp. 1-6.
- [154] IEEE, "IEEE Standard for Definitions of Terms for Antennas," *IEEE Std 145-2013 (Revision IEEE Std 145-1993)*, pp. 1-50, 2014.
- [155] R. Moro, S. Agneessens, H. Rogier, A. Dierck, and M. Bozzi, "Textile Microwave Components in Substrate Integrated Waveguide Technology," *IEEE Trans. Microw. Theory Tech.*, vol. 63, no. 2, pp. 422-432, 2015.

Appendix A

Fundamental Parameters of Antennas

In this PhD Thesis some fundamental parameters of the antennas will be discussed, in order to relate the performance of the textile antennas to the textile materials and manufacturing techniques. The fundamental parameters of antennas are summarily described in this appendix, to support the reading of the thesis. All descriptions of the parameters are based on the IEEE Standard Definitions of Terms for Antennas. A more in-depth information and description is given in [8], [154].

A.1 Evaluation of Antennas

Along this PhD Thesis, the performance of the antennas will be evaluated through their S_{11} parameter and radiation pattern. The S_{11} parameter is one of the Scattering parameters (S-) that describes the input-output relationship between ports, or terminals, in an electrical system. The S_{11} defines the relationship between the injected signal into the antenna and the reflected signal, hence is known as the return loss. The reflection of the injected signal occurs due to the mismatch of impedances. A minimum return loss is reached when there is a perfect adaptation of the impedance of the antenna. The S_{11} is measured using a Vector Analyser Network (VNA), which is an instrument that measures the network parameters of electrical networks. The VNA measures both amplitude and phase properties of networks. Figure A-1 presents an example of a VNA measuring the return loss of a textile antenna, at the Department of Technology Information at Ghent University, in Belgium.

The radiation pattern is the spatial distribution of a quantity that characterizes the electromagnetic field generated by an antenna. This distribution can be expressed as a mathematical function or as a graphical representation. The quantities that are most often used to characterize the radiation from an antenna are proportional to or equal to power flux density, radiation intensity, directivity, phase, polarization, and field strength.

Also, the radiation pattern is measured at the anechoic chamber. It is a room designed to completely absorb reflections of either sound or electromagnetic waves. It is also often isolated from waves entering from its surroundings. Figure A-2 shows an example of an anechoic chamber at Instituto de Telecomunicações - Aveiro.

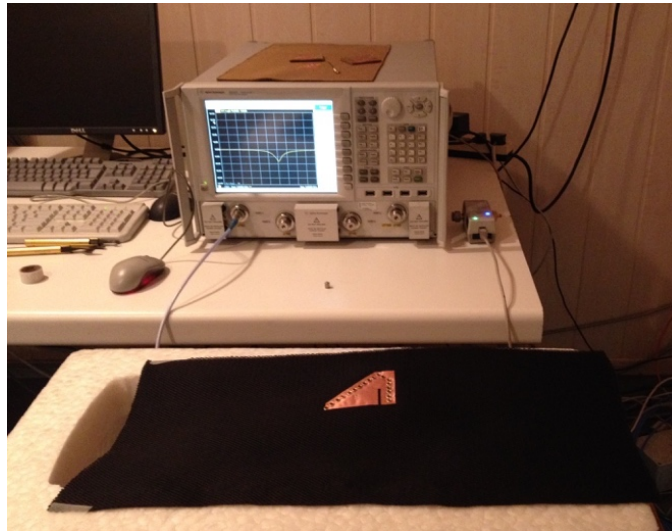


Figure A-1 Vector Network Analyser - Department of Technology Information at Ghent University



Figure A-2 Anechoic chamber at Instituto de Telecomunicações - Aveiro

A.2 Parameters of antennas

Input Impedance - The input impedance of an antenna is presented by an antenna at its terminals. The input impedance is the ratio between the voltage and the input current. Usually, has a real part associated with the radiated power and the dissipated power in the antenna, and an imaginary part constituted by the reactive power stored around the antenna. This parameter is defined by the geometry and the way to feed the antenna. Typically, the antennas and RF circuits are designed to have an input impedance of 50Ω . Also, the impedance mismatch

factor is associated with the Scattering parameters (S-) explained in A.1, and is defined by the ratio of the power accepted by an antenna to the power incident at the antenna's terminals from the transmitter.

Bandwidth - Is the range of frequencies within which the performance of the antenna conforms to a specified standard with respect to some characteristic. In the case of planar antennas, such as the ones presented in this thesis, the typical bandwidth can be defined as the range of frequencies which return loss is less than one tenth of the injected signal into the antenna. That is, all frequencies whose value of the S_{11} parameter is below -10dB.

Resonance Frequency - A frequency at which the input impedance of an antenna is nonreactive.

Directivity - The ratio of the radiation intensity in a given direction from the antenna to the radiation intensity averaged over all directions. If the direction is not specified, the direction of maximum radiation intensity is implied.

Gain - Although the gain of the antenna is closely related to the directivity, it is a measure that takes into account the efficiency of the antenna as well as its directional capabilities. Gain of the antenna is defined by the ratio of the radiation intensity in a given direction to the radiation intensity that would be produced if the power accepted by the antenna were isotropically radiated. Also, If the direction is not specified, the direction of maximum radiation intensity is implied.

Appendix B

Measurements of the Permittivity of Textiles

Table A-1 presents all permittivity measured values. In the column named ‘measurement file’, it is possible to see the date of the measurement, name of the material, number of sample, side in contact with the resonator board (S1 - face side and S2 reverse side), and which direction of the sample was aligned with the feed point on antenna, following the scheme presented in Figure 4-4.

Table B-1 Compilation of permittivity measurements

Material	ϵ_r	$\tan\delta$	Measurement file
Fake Leather I	1.66	0.005	2014_10_29_2GHz_patch_FLbrown_SAMPLE1_S1_D1
	1.66	0.011	2014_10_29_2GHz_patch_FLbrown_SAMPLE1_S1_D2
	1.66	0.004	2014_10_29_2GHz_patch_FLbrown_SAMPLE1_S1_D3
	1.66	0.008	2014_10_29_2GHz_patch_FLbrown_SAMPLE1_S1_D4
	1.25	0.011	2014_10_29_2GHz_patch_FLbrown_SAMPLE1_S2_fleeceside_D1
	1.24	0.010	2014_10_29_2GHz_patch_FLbrown_SAMPLE1_S2_fleeceside_D2
	1.24	0.007	2014_10_29_2GHz_patch_FLbrown_SAMPLE1_S2_fleeceside_D3
	1.24	0.006	2014_10_29_2GHz_patch_FLbrown_SAMPLE1_S2_fleeceside_D4
	1.66	0.009	2014_10_29_2GHz_patch_FLbrown_SAMPLE2_S1_D1
	1.66	0.012	2014_10_29_2GHz_patch_FLbrown_SAMPLE2_S1_D2
	1.66	0.005	2014_10_29_2GHz_patch_FLbrown_SAMPLE2_S1_D3
	1.67	0.001	2014_10_29_2GHz_patch_FLbrown_SAMPLE2_S1_D4
	1.25	0.007	2014_10_29_2GHz_patch_FLbrown_SAMPLE2_S2_fleeceside_D1
	1.24	0.006	2014_10_29_2GHz_patch_FLbrown_SAMPLE2_S2_fleeceside_D2
	1.24	0.004	2014_10_29_2GHz_patch_FLbrown_SAMPLE2_S2_fleeceside_D3
	1.23	0.004	2014_10_29_2GHz_patch_FLbrown_SAMPLE2_S2_fleeceside_D4
Fake Leather II	1.63	0.016	2014_10_28_2GHz_FLblack_SAMPLE1_S1_D1
	1.64	0.016	2014_10_28_2GHz_FLblack_SAMPLE1_S1_D2
	1.63	0.015	2014_10_28_2GHz_FLblack_SAMPLE1_S1_D3
	1.64	0.015	2014_10_28_2GHz_FLblack_SAMPLE1_S1_D4
	1.22	0.019	2014_10_28_2GHz_FLblack_SAMPLE1_S2_fleeceside_D1
	1.21	0.016	2014_10_28_2GHz_FLblack_SAMPLE1_S2_fleeceside_D2
	1.22	0.015	2014_10_28_2GHz_FLblack_SAMPLE1_S2_fleeceside_D3
	1.21	0.018	2014_10_28_2GHz_FLblack_SAMPLE1_S2_fleeceside_D4
	1.63	0.020	2014_10_28_2GHz_FLblack_SAMPLE2_S1_D1
	1.65	0.017	2014_10_28_2GHz_FLblack_SAMPLE2_S1_D2
	1.65	0.017	2014_10_28_2GHz_FLblack_SAMPLE2_S1_D3
	1.65	0.016	2014_10_28_2GHz_FLblack_SAMPLE2_S1_D4
	1.23	0.017	2014_10_28_2GHz_FLblack_SAMPLE2_S2_fleeceside_D1
	1.24	0.020	2014_10_28_2GHz_FLblack_SAMPLE2_S2_fleeceside_D2
	1.22	0.017	2014_10_28_2GHz_FLblack_SAMPLE2_S2_fleeceside_D3
	1.21	0.019	2014_10_28_2GHz_FLblack_SAMPLE2_S2_fleeceside_D4

Material	ϵ_r	$\tan\delta$	Measurement file
3D Fabric I	1.06	0.006	2014_10_28_2GHz_3Dblack_SAMPLE1_S2_D1
	1.07	0.005	2014_10_28_2GHz_3Dblack_SAMPLE1_S2_D2
	1.07	0.005	2014_10_28_2GHz_3Dblack_SAMPLE1_S2_D3
	1.08	0.011	2014_10_28_2GHz_3Dblack_SAMPLE1_S2_D4
	1.11	0.003	2014_10_28_2GHz_3Dblack_SAMPLE1_S1_D1
	1.13	0.005	2014_10_28_2GHz_3Dblack_SAMPLE1_S1_D2
	1.12	0.004	2014_10_28_2GHz_3Dblack_SAMPLE1_S1_D3
	1.12	0.006	2014_10_28_2GHz_3Dblack_SAMPLE1_S1_D4
	1.12	0.010	2014_10_28_2GHz_3Dblack_SAMPLE2_S2_D1
	1.13	0.006	2014_10_28_2GHz_3Dblack_SAMPLE2_S2_D2
	1.12	0.007	2014_10_28_2GHz_3Dblack_SAMPLE2_S2_D3
	1.13	0.004	2014_10_28_2GHz_3Dblack_SAMPLE2_S2_D4
	1.07	0.004	2014_10_28_2GHz_3Dblack_SAMPLE2_S1_D1
	1.08	0.001	2014_10_28_2GHz_3Dblack_SAMPLE2_S1_D2
	1.08	0.004	2014_10_28_2GHz_3Dblack_SAMPLE2_S1_D3
	1.08	0.002	2014_10_28_2GHz_3Dblack_SAMPLE2_S1_D4
3D Fabric II	1.09	0.011	2014_10_28_2GHz_3Dgold_SAMPLE1_S1_D1
	1.11	0.004	2014_10_28_2GHz_3Dgold_SAMPLE1_S1_D2
	1.10	0.006	2014_10_28_2GHz_3Dgold_SAMPLE1_S1_D3
	1.11	0.007	2014_10_28_2GHz_3Dgold_SAMPLE1_S1_D4
	1.08	0.010	2014_10_28_2GHz_3Dgold_SAMPLE1_S2_D1
	1.06	0.006	2014_10_28_2GHz_3Dgold_SAMPLE1_S2_D2
	1.08	0.010	2014_10_28_2GHz_3Dgold_SAMPLE1_S2_D3
	1.08	0.001	2014_10_28_2GHz_3Dgold_SAMPLE1_S2_D4
	1.11	0.011	2014_10_28_2GHz_3Dgold_SAMPLE2_S1_D1
	1.12	0.008	2014_10_28_2GHz_3Dgold_SAMPLE2_S1_D2
	1.12	0.004	2014_10_28_2GHz_3Dgold_SAMPLE2_S1_D3
	1.11	0.004	2014_10_28_2GHz_3Dgold_SAMPLE2_S1_D4
	1.08	0.002	2014_10_28_2GHz_3Dgold_SAMPLE2_S2_D1
	1.08	0.008	2014_10_28_2GHz_3Dgold_SAMPLE2_S2_D2
	1.07	0.002	2014_10_28_2GHz_3Dgold_SAMPLE2_S2_D3
	1.08	0.003	2014_10_28_2GHz_3Dgold_SAMPLE2_S2_D4
3D Fabric III	1.11	0.016	2014_10_28_2GHz_3Ddarkgreen_SAMPLE1_S1_D1
	1.11	0.019	2014_10_28_2GHz_3Ddarkgreen_SAMPLE1_S1_D2
	1.12	0.016	2014_10_28_2GHz_3Ddarkgreen_SAMPLE1_S1_D3
	1.12	0.018	2014_10_28_2GHz_3Ddarkgreen_SAMPLE1_S1_D4
	1.12	0.018	2014_10_28_2GHz_3Ddarkgreen_SAMPLE1_S2_D1
	1.12	0.017	2014_10_28_2GHz_3Ddarkgreen_SAMPLE1_S2_D2
	1.12	0.015	2014_10_28_2GHz_3Ddarkgreen_SAMPLE1_S2_D3
	1.13	0.018	2014_10_28_2GHz_3Ddarkgreen_SAMPLE1_S2_D4
	1.10	0.015	2014_10_28_2GHz_3Ddarkgreen_SAMPLE2_S1_D1
	1.10	0.018	2014_10_28_2GHz_3Ddarkgreen_SAMPLE2_S1_D2
	1.11	0.020	2014_10_28_2GHz_3Ddarkgreen_SAMPLE2_S1_D3
	1.11	0.016	2014_10_28_2GHz_3Ddarkgreen_SAMPLE2_S1_D4
	1.12	0.020	2014_10_28_2GHz_3Ddarkgreen_SAMPLE2_S2_D1
	1.12	0.020	2014_10_28_2GHz_3Ddarkgreen_SAMPLE2_S2_D2
	1.12	0.016	2014_10_28_2GHz_3Ddarkgreen_SAMPLE2_S2_D3
	1.12	0.018	2014_10_28_2GHz_3Ddarkgreen_SAMPLE2_S2_D4
3D Fabric IV	1.12	0.017	2014_10_28_2GHz_3Dgreen_SAMPLE1_S1_D1
	1.14	0.017	2014_10_28_2GHz_3Dgreen_SAMPLE1_S1_D2
	1.13	0.019	2014_10_28_2GHz_3Dgreen_SAMPLE1_S1_D3
	1.14	0.020	2014_10_28_2GHz_3Dgreen_SAMPLE1_S1_D4
	1.09	0.016	2014_10_28_2GHz_3Dgreen_SAMPLE1_S2_D1
	1.14	0.017	2014_10_28_2GHz_3Dgreen_SAMPLE1_S2_D2

Material	ϵ_r	$\tan\delta$	Measurement file
3D Fabric IV	1.11	0.017	2014_10_28_2GHz_3Dgreen_SAMPLE1_S2_D3
	1.11	0.019	2014_10_28_2GHz_3Dgreen_SAMPLE1_S2_D4
	1.11	0.015	2014_10_28_2GHz_3Dgreen_SAMPLE2_S1_D1
	1.15	0.019	2014_10_28_2GHz_3Dgreen_SAMPLE2_S1_D2
	1.13	0.016	2014_10_28_2GHz_3Dgreen_SAMPLE2_S1_D3
	1.13	0.019	2014_10_28_2GHz_3Dgreen_SAMPLE2_S1_D4
	1.13	0.018	2014_10_28_2GHz_3Dgreen_SAMPLE2_S2_D1
	1.14	0.019	2014_10_28_2GHz_3Dgreen_SAMPLE2_S2_D2
	1.13	0.019	2014_10_28_2GHz_3Dgreen_SAMPLE2_S2_D3
	1.15	0.017	2014_10_28_2GHz_3Dgreen_SAMPLE2_S2_D4
3D Fabric V	1.12	0.006	2014_10_29_2GHz_patch_3Dwhite_SAMPLE1_S1_D1
	1.11	0.003	2014_10_29_2GHz_patch_3Dwhite_SAMPLE1_S1_D2
	1.10	0.003	2014_10_29_2GHz_patch_3Dwhite_SAMPLE1_S1_D3
	1.12	0.002	2014_10_29_2GHz_patch_3Dwhite_SAMPLE1_S1_D4
	1.11	0.003	2014_10_29_2GHz_patch_3Dwhite_SAMPLE1_S2_D1
	1.11	0.003	2014_10_29_2GHz_patch_3Dwhite_SAMPLE1_S2_D2
	1.11	0.004	2014_10_29_2GHz_patch_3Dwhite_SAMPLE1_S2_D3
	1.11	0.002	2014_10_29_2GHz_patch_3Dwhite_SAMPLE1_S2_D4
	1.12	0.003	2014_10_29_2GHz_patch_3Dwhite_SAMPLE2_S1_D1
	1.11	0.003	2014_10_29_2GHz_patch_3Dwhite_SAMPLE2_S1_D2
	1.12	0.004	2014_10_29_2GHz_patch_3Dwhite_SAMPLE2_S1_D3
	1.12	0.001	2014_10_29_2GHz_patch_3Dwhite_SAMPLE2_S1_D4
	1.11	0.002	2014_10_29_2GHz_patch_3Dwhite_SAMPLE2_S2_D1
	1.11	0.011	2014_10_29_2GHz_patch_3Dwhite_SAMPLE2_S2_D2
	1.10	0.001	2014_10_29_2GHz_patch_3Dwhite_SAMPLE2_S2_D3
	1.10	0.010	2014_10_29_2GHz_patch_3Dwhite_SAMPLE2_S2_D4
Cordura I	1.65	0.008	2014_10_29_2GHz_patch_CORDURA_PU_SAMPLE1_S1_D1
	1.66	0.009	2014_10_29_2GHz_patch_CORDURA_PU_SAMPLE1_S1_D2
	1.63	0.001	2014_10_29_2GHz_patch_CORDURA_PU_SAMPLE1_S1_D3
	1.62	0.010	2014_10_29_2GHz_patch_CORDURA_PU_SAMPLE1_S1_D4
	1.50	0.001	2014_10_29_2GHz_patch_CORDURA_PU_SAMPLE1_S2_D1
	1.49	0.005	2014_10_29_2GHz_patch_CORDURA_PU_SAMPLE1_S2_D2
	1.51	0.005	2014_10_29_2GHz_patch_CORDURA_PU_SAMPLE1_S2_D3
	1.48	0.005	2014_10_29_2GHz_patch_CORDURA_PU_SAMPLE1_S2_D4
	1.65	0.008	2014_10_29_2GHz_patch_CORDURA_PU_SAMPLE2_S1_D1
	1.66	0.012	2014_10_29_2GHz_patch_CORDURA_PU_SAMPLE2_S1_D2
	1.63	0.010	2014_10_29_2GHz_patch_CORDURA_PU_SAMPLE2_S1_D3
	1.64	0.011	2014_10_29_2GHz_patch_CORDURA_PU_SAMPLE2_S1_D4
	1.50	0.013	2014_10_29_2GHz_patch_CORDURA_PU_SAMPLE2_S2_D1
	1.65	0.008	2014_10_29_2GHz_patch_CORDURA_PU_SAMPLE2_S2_D2
	1.65	0.008	2014_10_29_2GHz_patch_CORDURA_PU_SAMPLE2_S2_D3
	1.49	0.013	2014_10_29_2GHz_patch_CORDURA_PU_SAMPLE2_S2_D4
Cordura II	1.57	0.000	2014_10_29_2GHz_patch_CORDURA_TF_SAMPLE1_S1_D1
	1.59	0.001	2014_10_29_2GHz_patch_CORDURA_TF_SAMPLE1_S1_D2
	1.59	0.014	2014_10_29_2GHz_patch_CORDURA_TF_SAMPLE1_S1_D3
	1.59	0.013	2014_10_29_2GHz_patch_CORDURA_TF_SAMPLE1_S1_D4
	1.53	0.003	2014_10_29_2GHz_patch_CORDURA_TF_SAMPLE1_S2_D1
	1.53	0.007	2014_10_29_2GHz_patch_CORDURA_TF_SAMPLE1_S2_D2
	1.54	0.009	2014_10_29_2GHz_patch_CORDURA_TF_SAMPLE1_S2_D3
	1.54	0.008	2014_10_29_2GHz_patch_CORDURA_TF_SAMPLE1_S2_D4
	1.60	0.008	2014_10_29_2GHz_patch_CORDURA_TF_SAMPLE2_S1_D1
	1.60	0.013	2014_10_29_2GHz_patch_CORDURA_TF_SAMPLE2_S1_D2
	1.59	0.012	2014_10_29_2GHz_patch_CORDURA_TF_SAMPLE2_S1_D3
	1.59	0.004	2014_10_29_2GHz_patch_CORDURA_TF_SAMPLE2_S1_D4

Material	ϵ_r	$\tan\delta$	Measurement file
Cordura II	1.54	0.004	2014_10_29_2GHz_patch_CORDURA_TF_SAMPLE2_S2_D1
	1.55	0.011	2014_10_29_2GHz_patch_CORDURA_TF_SAMPLE2_S2_D2
	1.54	0.010	2014_10_29_2GHz_patch_CORDURA_TF_SAMPLE2_S2_D3
	1.55	0.013	2014_10_29_2GHz_patch_CORDURA_TF_SAMPLE2_S2_D4
Neoprene II	1.31	0.001	2014_07_01_2gh_patch_neo2_s2_d1
	1.33	0.001	2014_07_01_2gh_patch_neo2_s2_d2
	1.34	0.001	2014_07_01_2gh_patch_neo2_s2_d3
	1.35	0.001	2014_07_01_2gh_patch_neo2_s2_d4
	1.29	0.001	2014_07_01_2gh_patch_neo2_s1_d1
	1.24	0.001	2014_07_01_2gh_patch_neo2_s1_d2
	1.24	0.001	2014_07_01_2gh_patch_neo2_s1_d3
	1.30	0.001	2014_07_01_2gh_patch_neo2_s1_d4
Neoprene I	1.36	0.001	2014_07_01_2gh_patch_neo1_s2_d1
	1.36	0.001	2014_07_01_2gh_patch_neo1_s2_d2
	1.35	0.001	2014_07_01_2gh_patch_neo1_s2_d3
	1.34	0.001	2014_07_01_2gh_patch_neo1_s2_d4
	1.38	0.001	2014_07_01_2gh_patch_neo1_s1_d1
	1.38	0.001	2014_07_01_2gh_patch_neo1_s1_d2
	1.37	0.001	2014_07_01_2gh_patch_neo1_s1_d3
	1.37	0.001	2014_07_01_2gh_patch_neo1_s1_d4

Appendix C

Experiments with Cork

C.1 Dielectric Characterization

During the Short Term Scientific Mission (STSM), in the framework of the European Cooperation in Science and Technology (COST) - Project IC 1301 - Wireless Power Transmission for Sustainable Electronics (WIPE), realized in the Department of Information Technology at Ghent University (Belgium), besides the textile materials, several cork materials were also characterized.

Cork was chosen due to their intrinsic characteristics, such as flexibility, non permeability to liquids and gases, thermal and electrical insulating. Also, cork is an emblematic material of Portugal, being this STSM a great opportunity to explore other applications for it. Further, on the past decade, several fashion products were emerged using cork materials.

Five cork sheet materials were characterized using the Resonator-Based Experimental Method, following the procedure presented on Chapter 4, at 2.25 GHz. Table B-1 presents the average values of measured permittivity and the characteristics of the tested corks. Thickness was characterized using Kawabata's Evaluation System for Fabrics, KES - 3 Compressional Tester, at UBI.

Table C-1 Description of cork materials characterized at 2.25 GHz

Sample	Material	Manufacturer	Manufacturer reference	Composition	Thickness (mm)	ϵ_r	$\tan\delta$
Cork 1	Cork composite	Corticeira Amorim	8822	100% cork	3	1.30	0.005
Cork 2	Cork composite			100% cork	2.5	1.26	0.009
Cork 3	Cork composite			100% cork	1.5	1.17	0.005
Corktex	Synthetic leather		8245 L	100% cork	1	1.29	0.006
Corktex PES	Cork fabric		8245 T	100% cork, one side laminated with plain weave 100% PES	1.1	1.35	0.006

C.2 Validation

In order to validate the results, a coaxial antenna to resonate at 2.45 GHz, using cork 3 as dielectric substrate, was designed. For the conductive parts, Pure copper taffeta fabric (Less EMF Inc., Latham, USA), with sheet resistance = $0.05 \Omega/\square$ and thickness equal to 0.080 mm, was used. The antenna was assembled using the Adhesive Sheet II (see Table 6-4). Figure C-1

presents the design and dimensions of the coaxial cork antenna, and Figure C-2 shows the measured return loss.

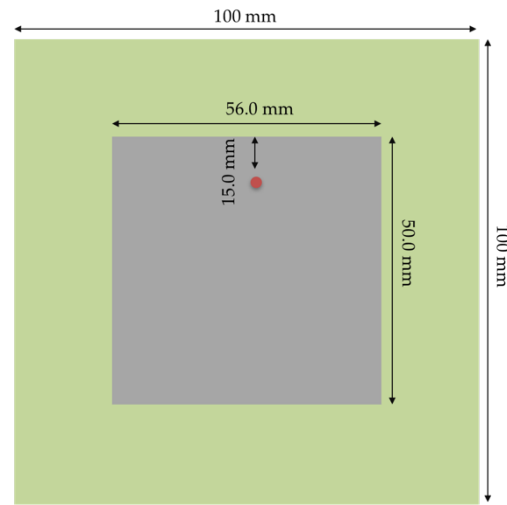


Figure C-1 Design and dimensions of coaxial cork antenna for 2.45 GHz

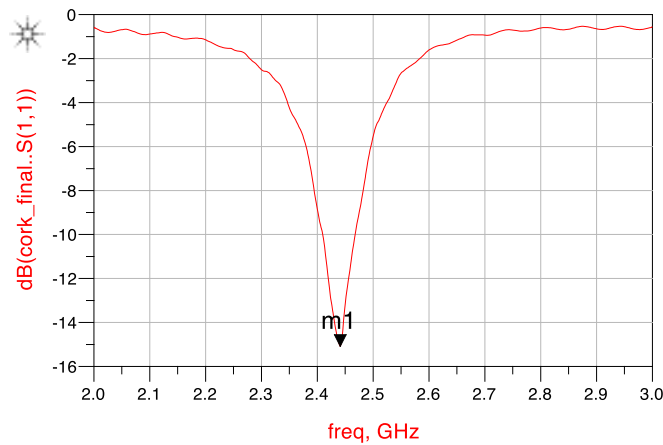


Figure C-2 Measured S_{11} of coaxial cork antenna

Based on the return loss parameter presented in Figure B-2, one may observe the measured coaxial cork antenna works well at 2.44 GHz, that is in agreement with the simulated resonance frequency (2.45 GHz). Further, one may conclude that the Resonator-Based Experimental Technique is also suitable to characterize the permittivity of other planar materials, at 2.25 GHz, such as cork composites.

C.3 Experiments at 5 GHz

During the STSM, cork 3 was also characterized, using the Resonator-Based Experimental Technique, at 5 GHz. The obtained average values were $\epsilon_r = 1,3571$ and $\tan\sigma = 0,0089$.

In order to validate these results, two coaxial antennas, with the same dimensions (see Figure B-3) were manufactured using the Copper taffeta fabric for the conductive parts, feed by a SMA connector. The antennas were designed to resonate at 5 GHz and Figure B-4 shows the measured S_{11} .

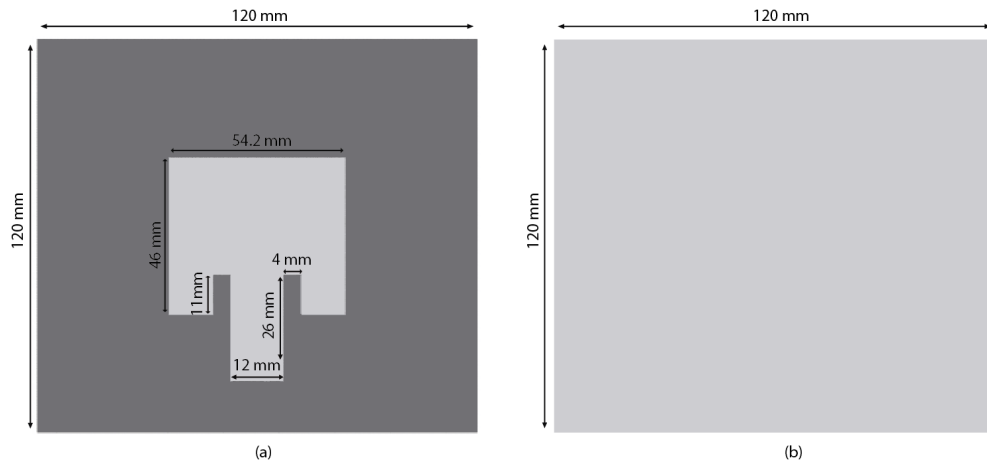


Figure C-3 Design and dimensions of coaxial cork antenna for 5 GHz (a) front (b) rear

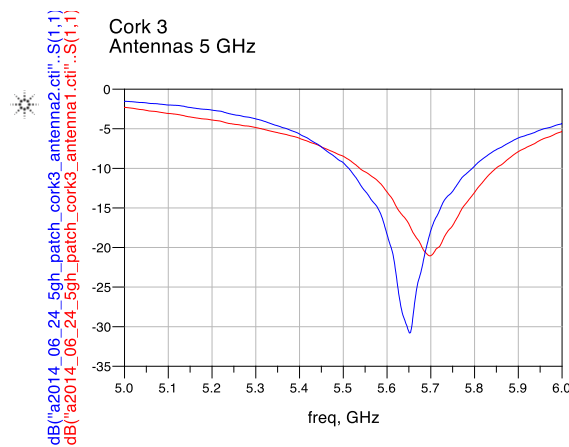


Figure C-4 Measured return loss of coaxial cork antennas (prototype 1 - red line and prototype 2, blue line)

As one can see on Figure B-4, the manufactured antennas presented very different results, and thus the obtained ϵ_r values do not well characterize the material. At this frequency, 5 GHz, the cork composite has shown an instable electromagnetic behaviour, and due to the naturally high superficial porosity of cork, it is not compatible to the Resonator-Based Experimental Technique.

Further, cork 3 was characterize at 5 GHz, using the method explained on [155] and the an antenna combining cork substrate and conductive fabric was designed and published in [70].

Appendix D

Preliminary Tests of Integration of Textile Antenna on Cloth

The first experiment to integrate a textile antenna on cloth was performed at Ghent University, during the STSM reference IC1301-18709. A miniaturised textile antenna was made using the Substrate Integrated Waveguide (SIW) technique. This Quarter-Mode wearable antenna has a compact dimension, and has been excellent for off-body communications. Also, this antenna is an adaptation of the wearable antenna presented in [67], using protective foam as dielectric substrate.

In this version, 3D fabric II is used for the substrate and Pure copper taffeta fabric is used for the conductive parts. The antenna was assembled using the Adhesive Sheet II. The waveguides were hand made using manual embroidering technique [152], with Silverpam conductive yarn (see Table 6-7) . The antenna was designed for 2.4 GHz ISM band. Figure D-1 shows the Quarter-Mode SIW textile antenna.

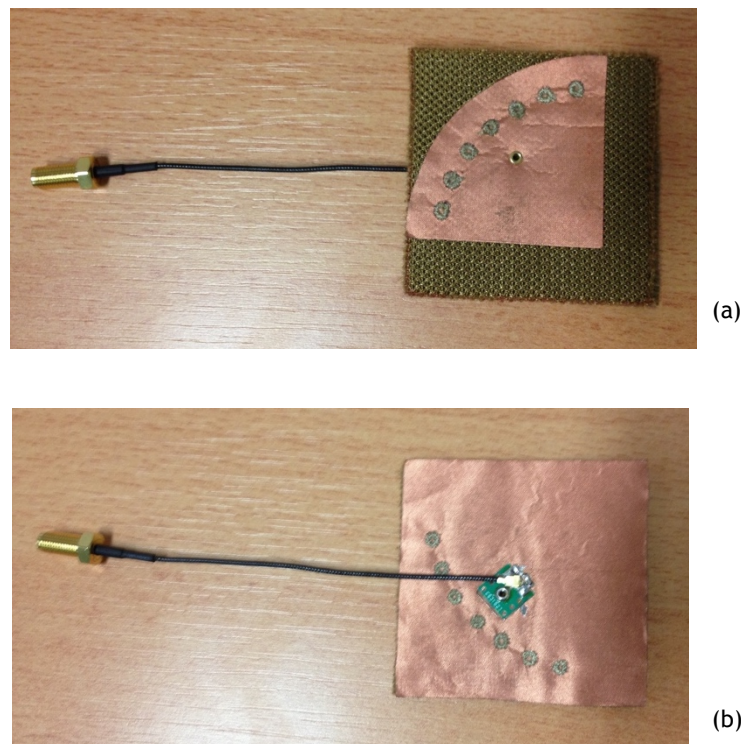


Figure D-1 Quarter-Mode SIW textile antenna

Due to the small size of the antenna, a glove was designed to integrate this antenna. In order to facilitate the measurements, a front pocket was created to place the antenna. Also, a structure using Styrofoam was made to stabilise the glove during the measurements, as one can see on Figure D-2.

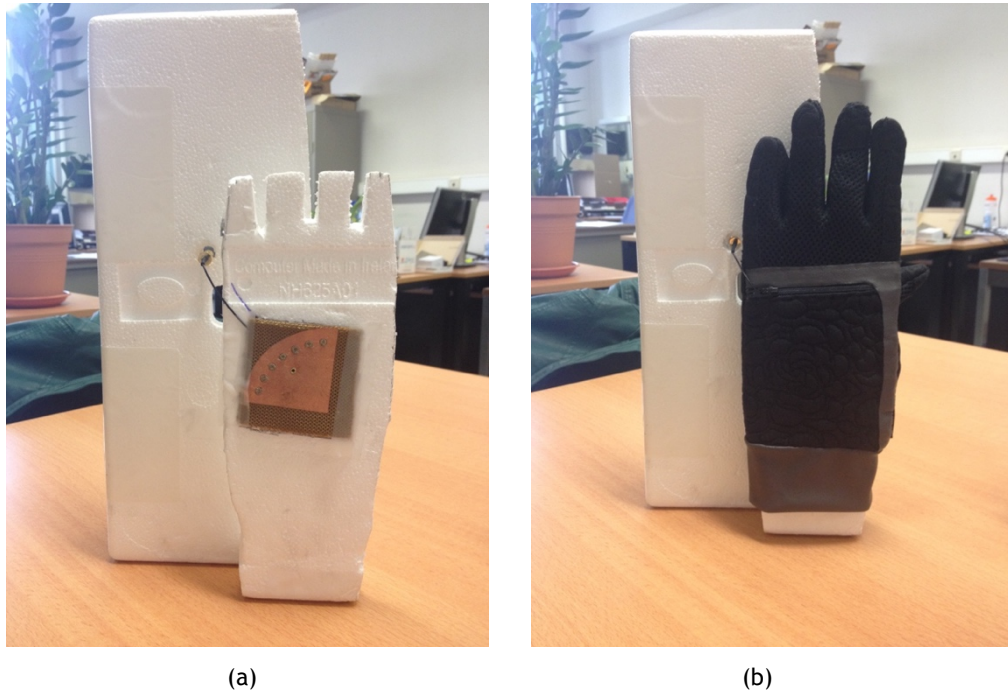


Figure D-2 Styrofoam support to stabilise the glove during the measurements. In (a) antenna stand-alone (b) on the glove

For the first time, the results between a stand-alone and integrated antenna were compared. Figure D-3 presents the measured return loss and Figure D-4 shows the 3D radiation pattern. Both measurements were performed in the anechoic chamber on Department of Technology Information at Ghent University.

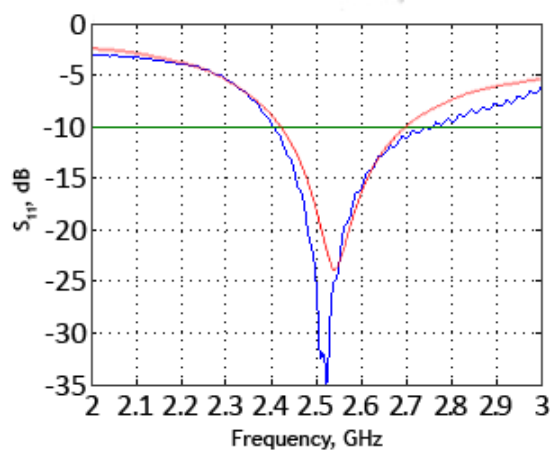


Figure D-3 Measured S_{11} of Quarter-Mode SIW textile antenna (a) stand-alone - red line, and (b) on glove - blue line

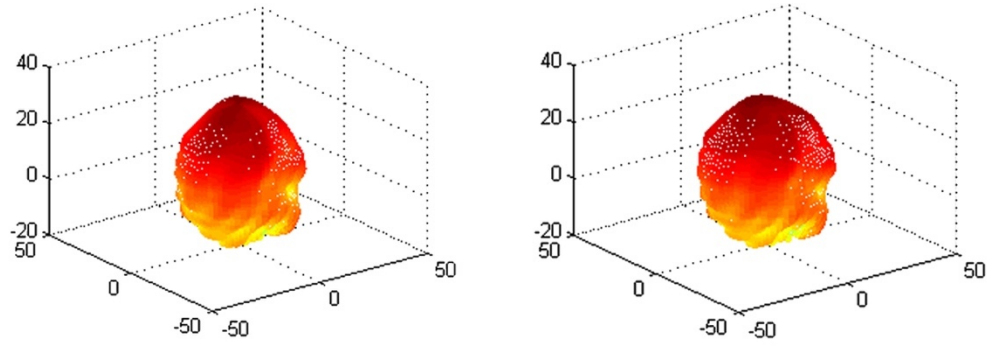


Figure D-4 3D radiation pattern of Quarter-Mode SIW textile antenna (a) stand-alone and (b) on glove

As one can see in Figures D-3 the integration process does not influence the performance of the antenna. In fact, both measurements gave similar results, both antennas work at 2.52 GHz, covering the ISM band, and the efficiency of the antenna is 0.5026 for the stand-alone, and 0.5056 for the integrated antenna. Also, observing Figure D-4, is possible see that the radiation pattern still being clearly omnidirectional even after the integration on the glove.

Appendix E

E-Caption on Television Show

E-Caption coat was presented in the television show called “*Há Volta on RTP TV*”, during the “*Volta a Portugal de Ciclismo*” (Cycling Tour of Portugal), in 02 of August of 2016. This program was part of the program of “*Volta ao Conhecimento*”, with the aim to disseminate the science and culture around the country. The “*Volta ao Conhecimento*” was an initiative of the Ministry of Science, Technology and Higher Education. On the sequence of an award and prize won by Caroline Loss in the UBI internal competition named “*3 minutos, 1 slide, a tua tese*” the E-Caption Coat was chosen by the Research Coordinating Institute (Instituto Coordenador da Investigação - ICI) of UBI to represent the scientific work developed at Universidade da Beira Interior.



Figure E-1 The RTP TV presenter, Mário Augusto, using the E-Caption Coat during the TV show *Há Volta* (Courtesy RTP TV)

Appendix F

E-Caption 2.0 - A Smart and Safety Coat

Ongoing research. The E-Caption 2.0 - Smart and Safety Coat, is a Personal Protective Equipment (PPE) developed to warning the tower climbers to the radiation level exposure. As the first version of E-Caption, this coat will be a proof-of-concept of the textile antennas used for energy harvesting.



Figure F-1 Logotype of E-Caption 2.0



(a)



(b)

Figure F-2 E-Caption 2.0 under construction (a) front and (b) rear

Appendix G

Awards & Honours

- **The Fiber Society Student Paper Competition**

3rd place in the international The Fiber Society Student Paper Competition with the paper “Influence of Some Structural Parameters of Textiles on Their Dielectric Behaviour”. One of the three worldwide finalists that have presented the paper during the fall The Fiber Society meeting, held in Athens (GA - USA), November 2017.

- **IEEE MTT-S Student Paper Award**

Honourable mention in the Student Paper Award at the IEEE MTT-S International Microwave Workshop Series on Advanced Materials and Processes (IMWS-AMP) 2017 Conference, with the paper “Influence of the Laminating Manufacturing Technique on the S_{11} Parameter of Printed Textile Antennas”. Conference promoted by IEEE Microwave Theory and Techniques Society (MTT-S) and the European Microwave Association (EuMA), held in Pavia (IT), September 2017.

- **3 Minutes, 1 Slide... Your Thesis Challenge**

3rd Place at the 3M Thesis Challenge promoted by the Instituto Coordenador de Investigação (ICI - UBI) and Santander Totta, in November 2015.

- **STS ITALIA 10 Best Papers of Young Researchers**

One of the the best papers of young researchers on 5th STS Italia Conference - A Matter of Design: Making Society through Science and Technology, with the paper “Developing Sustainable Communication Interfaces Through Fashion Design”. Merit fellowship to participate on the conference, held in Milan (IT), May 2014.